The Gravity Loading Countermeasure Skinsuit: A Passive Countermeasure Garment for Preventing Musculoskeletal Deconditioning During Long-duration Spaceflight

by

Dustin Paul Kendrick

S.B., Aeronautics and Astronautics (2010)
Massachusetts Institute of Technology

Submitted to the Department of Health Sciences and Technology
in partial fulfillment of the requirements for the degree of

Doctor of Philosophy

at the

MASSACHUSETTS INSTITUTE OF TECHNOLOGY

June 2016

Author ..... Signature redacted .....
Department of Health Sciences and Technology
May 16, 2016

Certified by ..... Signature redacted .....
Lera Stirling, PhD
Assistant Professor
Charles Stark Draper Professor of Aeronautics and Astronautics
Thesis Supervisor

Accepted by .... Signature redacted .....
Emery N. Brown, MD, PhD
Director, Harvard-MIT Program in Health Sciences and Technology
Professor of Computational Neuroscience and Health Sciences and Technology

The Gravity Loading Countermeasure Skinsuit: A Passive Countermeasure Garment for Preventing Musculoskeletal Deconditioning During Long-duration Spaceflight

by

Dustin Paul Kendrick

Submitted to the Department of Health Sciences and Technology
on May 16, 2016, in partial fulfillment of the
requirements for the degree of
Doctor of Philosophy

Abstract

One of the hallmarks of long-duration spaceflight is physiological deconditioning seen in the absence of gravity. Negative changes in bone, muscle, and other physiological systems occur rapidly in space, and have the potential to severely limit the human space exploration program. The deficits in bone are mostly seen in the weight-bearing areas of the skeleton, highlighting the influence of gravity. Current countermeasures employed on the International Space Station are vastly improved over previous countermeasures equipment, however, with long duration exploration missions, there is a need to optimize countermeasures to adequately combat these physiological changes. One countermeasure concept that may aid in helping prevent deconditioning is the Gravity Loading Countermeasure Skinsuit, which uses elastic materials to provide bodyweight loading similar to that seen in the presence of gravity via compression along the cephalocaudal (head to toe) axis of the body. Preliminary work performed in our lab produced prototype garments that were characterized for comfort and wearability, but had design deficiencies that prevented them from providing full bodyweight loading to the subjects. In order to create an effective countermeasure garment we first developed a model of suit-body interactions through computational simulations to inform suit design. We then built and characterized prototype suits, and evaluated the potential of the suit for efficacy in ameliorating musculoskeletal deconditioning in earth-based analogs of unloading. Modeling efforts showed that the GLCS could provide bodyweight-like loading to the subjects in simulated microgravity, and in some cases provided higher loads to the muscles and joints than those seen during unsuited movements in Earth gravity. Prototype suits were constructed that provided 76-84%

bodyweight loading to the subjects. During exercise testing on a vertical treadmill, the subjects were able to run and walk normally, and the suit was shown to increase physiological workload, as well as joint and muscle loading, during running in simulated microgravity.

Thesis Supervisor: Leia Stirling, PhD
Title: Assistant Professor
Charles Stark Draper Professor of Aeronautics and Astronautics

Acknowledgments

It's amazing to look back on my time at MIT, and realize that 10 whole years have passed since I entered "The Institute" as a wide-eyed freshman. Attending MIT was a dream of mine since junior high, and I was fortunate to not only attain my undergraduate degree from MIT, but to continue my studies here on the long road to obtaining my PhD. In my decade here, I've made lifelong friendships, worked with incredible faculty members, and been exposed to the incredible diversity of the institute, in both people and activities. MIT has had an intimate role in forging who I am today, and I am fortunate to have called the institute home for this period of my life.

There are many people who deserve acknowledgment for supporting me on this journey. I would first like to thank my original advisor, Professor Dava Newman, who NASA was fortunate enough to lure away from MIT for short while to be their Deputy Director. Your expertise and advice helped set this project up for success, and your connections and tireless work opened up so many unique and interesting opportunities for me as I went through my time in grad school. Your commitment to your students' development, both personally and professionally, is incredible, and I am grateful for our time working together.

I would like to thank Professor Leia Stirling, who originally helped guide my research as a member of my thesis committee, and then took over as my thesis advisor after Professor Newman's departure. Your calm and expert guidance in shepherding this project through its final stages, even in the face of some pretty extreme time constraints, helped me to produce work that I will always be proud of. The Man-Vehicle lab is in excellent hands for the future.

I want to acknowledge the other members of my Thesis Committee, whose advice and suggestions were invaluable in formulating and executing this project. Professor Jeff Hoffman, thank you for stepping in to helm my thesis committee and contributing your unique perspectives to help me think critically about how my project might actually be used in spaceflight. Dr. Mary Bouxsein, thank you for making sure the physiological background of the project was always firmly rooted in the literature, and for all your advice about maintaining sanity within the PhD student life. Last, but not least, thank you to Professor Brad Holschuh for your help and advice, specifically in getting the suits from the design stage to actual prototypes. It's an honor to call you my friend, and I wish you the best in your endeavors back in God's Country (AKA the great state of Minnesota).

I have been fortunate to be supported by many institutions during my graduate work. First, to my NASA Space Technology Research Fellowship (NSTRF) sponsors in the NASA Office of the Chief Technologist, thank you for the financial support that made my graduate education possible, as well as the incredible opportunities for collaboration provided by the fellowship. Through your support, I was able to use the unique resources of three different NASA centers to enhance my research, and was able to collect thesis data using NASA experimental labs, which was a dream come true. Thank you as well to the MIT-Skolkovo initiative, which, apart from offering financial support, afforded me the opportunity to collaborate with colleagues in Russia, which was a one-in-a-lifetime experience.

A special thank you to the Bioastronautics program, housed within the Medical Engineering and Medical Physics (MEMP) program in the Harvard-MIT Division of Health Sciences and Technology. The program introduced me to all facets of the space life sciences community, and the multi-disciplinary approach needed to perform the complex work required to help humans thrive in space. Specific thanks to Professor Larry Young for founding and championing this unique program, and to Dr. Alan Natapoff and Dr. Julie Greenberg for helping everything to run smoothly on

the administrative side, even when dealing with the bureaucratic behemoth that is NASA.

So many others have been involved with this project on the technical side. To Dr. James Waldie, whose vision for the GLCS made all of this work possible, thank you for allowing me to run with your idea and contribute in my own, small way. Your advice and enthusiasm pushed this project to the heights (literally!) that it has achieved. To the teams at King's College (Dave Green, Phil Carvil and Julia Attias) and ESA (Simon Evetts, Jon Scott, and Alexandre Frechette, among others), thank you for allowing me to collaborate with you all on pushing Skinsuit forward. Seeing the skinsuit flying on ISS, and knowing I had a small part in developing something that flew in space was a dream come true, and completely the result of your tireless work. The opportunities to travel to London, Cologne, and Bordeaux to meet with you all and conduct experiments were some of the highlights of my graduate experience (excepting the second half of the parabolic flight!).

I had the unique opportunity to collaborate with many people at different NASA centers during my time in grad school. To my NSTRF mentor, Gail Perusek, it was a pleasure getting to know you, both personally and professionally. Thank you so much for all that you did for me over the course of my fellowship. You offered sage advice on the research, opened so many doors for me and smoothed the path for this project to become what it was. To Kelly Gilkey, who had the monumental task of helping me get these human studies approved, and helped coordinate all the research efforts at NASA Glenn, this project would never have been completed without your advice, patience and prodding off the various regulatory mechanisms. To Bill Thompson, thank you for all your help and advice with the always finicky OpenSim and motion capture systems. To the rest of the qualified operators who helped with testing on-site, including Beth Lewandowski, Chris Gallo, Chris Sheehan, Sarah Czerwien and Evan Markley, thank you for sacrificing your time and energy to help me get the data that I needed. To my hosts at NASA Ames and NASA Johnson Space Center, Jessica

Marquez and Smith Johnston, thank you for allowing me the opportunity to work with you and for your enthusiasm in helping this project along.

Over the lifetime of this project, many hands have been involved in constructing the prototype suits. Thank you to Liz Perlman at CostumeWorks for stepping outside your usual customer base, and indulging us engineers trying our hand at garment design. Your suggestions helped make the GLCS what it is today. To all the people at Dainese, thank you for leveraging your considerable expertise to help us make something that flew in space! To the folks at Terrazign, thank you for volunteering your expertise and materials to allow me to convert my design ideas into actual, physical suits. Finally, thank you to Heidi Woelfle at the University of Minnesota for sacrificing your time and energy to help me make these newest prototypes a reality. Without your design suggestions and tireless work this thesis would not exist.

I have been so fortunate to be a part of the Man-Vehicle Lab during my time in grad school. To all the professors and students too numerous to name who make the lab what it is, thank you for fostering a fun, creative research environment that allows us all to do our best work. A special thanks is owed to Liz Zotos, Quentin Alexander and Sally Chapman, administrative extraordinaires. Without them, the lab would fall apart.

I have an incredibly supportive group of friends that kept me sane throughout this process, who are too numerous to thank individually. To the members of Titehouse (Angela, David, Gabe, Jess, Michael, and Sam), living with you all will always be some of my best memories. To Kent and Lindsay, thanks for your friendship, hospitality, life advice, shared nerdy interests (Kent), and tolerance of those interests (Lindsay). Abe, thanks for all of our conversations, ranging from the silliest, to most serious, conversations I've had. To the Burton Conner House team, and to my students on B1, my time as a GRT has been incredibly rewarding, and you've helped make my grad school experience that much better. To my church community at CCFC, thanks for

all of your support and prayers as I've gone on this journey. Finally, thank you to my wonderful girlfriend, Aimee. Your patient support and enthusiastic encouragement helped get me over the finish line.

To my incredible family - Mom, Dad, Cody and Charise - thank you for everything. I couldn't have completed this endeavor without your support. Thanks for keeping me grounded, and for your love and encouragement as I've pursued my academic goals.

Contents

1 Introduction **21**

1.1 Bone Response to Loading 22

1.2 Physiological Deconditioning During Long-Duration Spaceflight . . . 23

1.3 Current Countermeasures 27

1.4 Current Countermeasure Limitations 28

1.5 Loading Suit History 29

1.5.1 Penguin Suit 29

1.5.2 Gravity Loading Countermeasure Skinsuit Concept 30

1.5.3 Loading Suit Limitations 37

1.6 Project Goal 38

1.7 Specific Aims 38

1.8 Thesis Overview 40

2 GLCS Suit-Body Modeling **43**

2.1 Suit Requirements 44

2.2 Model Development 44

2.2.1 OpenSim 44

2.2.2 Base Model 46

2.2.3 Suit Model 47

2.3 Model Assumptions and Limitations 50

2.4 Modeling Simulations 51

2.4.1 Static Upright Pose 51

2.4.2 Maximally Smooth Knee-Hip Bend 52
2.5 Model Validation and Verification 54
2.6 Modeling Results 56
2.7 Summary of Modeling Results 63

3 Suit Design and Characterization **65**
3.1 Design Considerations 65
3.1.1 Loading Material 65
3.1.2 New Loading Element Integration 73
3.1.3 Suit Anchoring 74
3.1.4 Subject Comfort 75
3.2 Final Design and Construction 75
3.2.1 Final Design 75
3.2.2 Subject Measurements 78
3.2.3 Suit Sizing 80
3.3 Suit Construction 83

4 Suit Testing **85**
4.1 Bed Rest Study 85
4.1.1 Testing Protocol and Data Collection 86
4.1.2 Suit Loading Characterization Results 89
4.1.3 Suit Stretch Characterization Results 91
4.1.4 Subjective Comfort During Long Term Wear 94
4.1.5 Spinal Elongation Study Results 95
4.2 Vertical Treadmill Testing 97
4.2.1 Testing Protocol 97
4.2.2 Data Collection 99
4.2.3 Data Analysis 102
4.2.4 Vertical Treadmill Testing Results 103
4.3 Summary of Suit Testing Results 120

5 Conclusion **125**

5.1 Discussion of Key Findings 125

5.1.1 Summary of Modeling Findings 126

5.1.2 Summary of Suit Design and Characterization 126

5.1.3 Summary of Suit Testing Results 127

5.2 Recommendations for Suit Design and Use 128

5.2.1 Suit Design Recommendations 128

5.2.2 Recommendations for Use 130

5.2.3 Earth-based Applications 131

5.3 Summary of Contributions 131

5.4 Limitations 132

5.5 Future Work 133

A Subjective Comfort Survey **135**

B Ground Reaction Force Analysis Code **137**

C Institutional Review Board Approvals **147**

Bibliography **151**

List of Figures

1-1 Advanced Resistive Exercise Device (ARED) 28
1-2 GLCS loading and anchor stage representation 31
1-3 GLCS Mark I prototype 32
1-4 GLCS Mark III suit 34
1-5 GLCS Mark IV suit: (L-R) Back Zip, Side Zip, and Side Zip Lacing . 35
1-6 GLCS Mark V suit: (L-R) Suit during parabolic flight and stirrup design 36
1-7 GLCS Mark VI suit: (L-R) Astronaut exercising in suit, Mark VI suit 37

2-1 Front and Side view of Gait2392 Model 46
2-2 Anthropometric Measurements from NASA-STD-3000 47
2-3 CLose up of GLCS model 48
2-4 Leg segment representation used to calculate leg segment mass 50
2-5 GLCS Model during knee-hip bend 53
2-6 Knee suit spring forces during knee-hip bend 55
2-7 Hip suit spring forces during knee-hip bend 56
2-8 Knee flexor forces during knee-hip bend 57
2-9 Hip flexor forces during knee-hip bend 58
2-10 Knee joint forces during knee-hip bend 59
2-11 Hip joint forces during knee-hip bend 59
2-12 Knee flexor forces during knee-hip bend for different suit loading levels 60
2-13 Hip flexor forces during knee-hip bend for different suit loading levels 61
2-14 Knee joint forces during knee-hip bend for different suit loading levels 62
2-15 Hip joint forces during knee-hip bend for different suit loading levels . 62

3-1 Zwick tensile testing machine 67
3-2 Force production over time at fixed length for suit spandex 68
3-3 Spandex force production over multiple cycles 68
3-4 Narrow Elastic 69
3-5 Resistive Exercise Bands 70
3-6 Force-length relationship for Narrow Elastics 70
3-7 Force-length relationship for Resistive Exercise Bands 71
3-8 Force generation of narrow elastics over multiple loading cycles 73
3-9 Top view of circumferential loading band 77
3-10 Final GLCS prototype design 78
3-11 Hand measurements taken for GLCS construction 79
3-12 NatickMSR software with subject body scan and measurements . . . 80
3-13 Final suit design with loading stages 81
3-14 Representation of unworn and stretched loading segment 82

4-1 Novel Pliance system with pressure sensing insoles 87
4-2 GLCS with markers to measure loading segment lengths 88
4-3 GLCS foot loading 89
4-4 GLCS foot loading distribution 90
4-5 GLCS shoulder loading 91
4-6 Subjective discomfort over long term wear 95
4-7 Subject height during bed rest ('x' are unsuited measurements and 'o' are suited measurements) 96
4-8 eZLS and suspended subject 98
4-9 Motion capture marker placements 99
4-10 Suit testing subject with marker placements 100
4-11 Marker placement on static pose 102
4-12 Subject heart rate during walking 103
4-13 Subject heart rate during running 104

4-14 Subjective discomfort and mobility hindrance rating during treadmill testing 105
4-15 Normalized ground readction forces for one subject for (l) walking and (r) running 106
4-16 Average GRF profiles for all subjects for walking 107
4-17 Average GRF profiles for all subjects for running 108
4-18 Box plots for Ground Reaction Force data for all subjects 109
4-19 Box plots for Step Time data for all subjects 109
4-20 Maximum force data from novel sensors for all subjects 111
4-21 Subject-scaled model with virtual and experimental markers 113
4-22 Inverse Kinematics results for the knee for one subject 113
4-23 Knee torque profile during running 116
4-24 Hip torque profile during running 117
4-25 Muscle forces during running 118
4-26 Knee joint forces during running 118
4-27 Hip joint forces during running 119

List of Tables

2.1 Anthropometric Measurements from NASA-STD-3000 47
2.2 Body Segment Mass Proportions 49
2.3 Suit spring force generation 54
2.4 Joint and muscle forces during static upright pose 57

3.1 GLCS loading stages 81
3.2 GLCS suit testing subject characteristics 83

4.1 Testing order for spinal elongation study 86
4.2 Suit loading segment resting length errors 92
4.3 Suit loading segment stretched lengths as a percent of loading stage resting length. Cells highlighted red indicate a segment that is over-stretched, while cells highlighted yellow indicate a segment that is under-stretched 92
4.4 Leg loading stage slip analysis 93
4.5 Hip loading stage slip analysis 94
4.6 Testing order for vertical treamill testing 101
4.7 Variables of mixed hierarchical regression model for max ground reaction force data 110
4.8 Variables of mixed hierarchical regression model for step time data . . 110
4.9 Knee range of motion and minimum and maximum angles during running 114
4.10 Hip range of motion and minimum and maximum angles during running 114

Chapter 1

Introduction

The dream of spaceflight has long captured the human imagination, and the extreme environment of space provides a unique scientific platform that has led to numerous breakthroughs in research. However, spaceflight is not without risks. The microgravity environment of space is hostile to humans, adapted as we are to living in the presence of gravity, and has myriad effects on the human body. Some of the most profound effects observed are those on the musculoskeletal system. The skeleton is a dynamic organ, and bone responds to the mechanical loading placed upon it. In the absence of gravity, unloaded bones lose mineral density; in weight-bearing bones these losses can approach 1-2% per month [44]. Similarly, significant decreases in both muscle size and strength occur after prolonged microgravity exposure [24]. Spinal elongation occurs due to chronic unloading, and this leads to back pain in astronauts, and an increased risk of herniated disks [35]. These changes occur even in the presence of current exercise countermeasures [67]. The physiological deconditioning will negatively affect astronaut health and performance, especially on proposed long-term missions to the moon and Mars, by decreasing their capacity to do work and increasing their risk of injury.

One proposed concept to combat musculoskeletal deconditioning is to replace gravitational loading using a Gravity Loading Countermeasure Skinsuit (GLCS) [78]. The

GLCS uses elastic materials to create a vertical loading regime similar to the weight-bearing regime normally experienced on earth by providing 1-G bodyweight loading to the soles of the feet. This type of suit has the potential to mitigate musculoskeletal deconditioning caused by static unloading.

In this thesis, we describe work done to design, build and characterize prototype countermeasure suits. This chapter outlines the need for a loading suit countermeasure, describes the history of loading suit development, and outlines the research aims undertaken to develop an effective countermeasure suit.

1.1 Bone Response to Loading

It is well known that bone is a dynamic organ. According to Wolff's Law, bone adapts to the loads it is placed under [81]. As the loading profile on a bone changes, it will remodel itself to better resist the new loads. This remodeling process is primarily carried out by three cells: osteoblasts, osteocytes, and osteoclasts. Osteoblasts are responsible for bone formation, osteoclasts are responsible for bone resorption, and osteocytes are responsible for sensing the mechanical forces on the bone and translating those forces into biologic activity. All three cell types work together in tightly coupled processes of resorption and remodeling to regulate bone homeostasis and maintain bone strength [17]. Various forms of stimuli can tip the balance to increase either bone formation or bone loss.

Mechanical loading greatly influences bone loss and formation. Frost proposed a "mechanostat" hypothesis in which the bone, plus other mechanisms, sense loads and translate those loads into biologic activity through the process of mechanotransduction [21]. Bone optimizes its structure to take on the routine daily stimuli it encounters [22]. Studies of athletes show that weightlifters have higher bone mass than swimmers, and gymnasts have a higher bone mass than the normal population, due to the

higher loads under which their skeletons are placed [56]. Terrestrial studies involving gymnasts suggest that peak loading may be just as important as frequency of loading in maintaining bone density, as gymnasts have higher bone mineral density than the general population [71]. Dynamic loads to the skeleton have been shown to be more effective in preventing bone loss than static loading [46], however, there is some evidence that static loading can attenuate bone loss. Studies have determined that periods of standing can significantly reduce calcium loss during long term bed rest [33, 76]. Additionally, spinal cord injury patients who are confined to a wheelchair show significant losses in bone mineral content (BMC) in their lower extremities, however, there are no losses of BMC in the lumbar spine, which is still under the influence of gravity while sitting [9]. Additionally, it has been shown that loading signals to bone eventually saturate, and become less effective in preserving bone, so periods of rest are required for effective prevention of bone loss [26, 43]. Effective countermeasures to bone loss will provide a variety of different loads to the skeleton.

Loading provided by gravity is an important source of mechanical loading on the skeleton. In older men and women, body mass is a significant predictor of bone mass, with heavier people having higher bone mass [8]. Ground reaction forces during human locomotion caused by gravitational acceleration are also a large source of bone loading. In the hip, these forces can be as high as 3-4 times normal body weight while walking, or 5.5 times normal body weight while running [12]. The absence of gravitational loading in space has significant consequences for musculoskeletal health.

1.2 Physiological Deconditioning During Long-Duration Spaceflight

Before the first man was launched into space, scientists speculated about the negative effects space would have on the human body. Experiments to determine the magni-

tude of bone loss were performed during spaceflight as early as the Gemini, Apollo, and Skylab missions, and were the first studies to show a negative calcium balance during the flight, as well as disparities in bone loss between the upper and lower extremities [15, 51, 10, 68]. The first use of modern imaging techniques occurred when dual-energy x-ray absorptiometry (DXA) was used to study Russian cosmonauts and American astronauts on the MIR space station and the International Space Station. These studies showed losses of 1-2% per month in weight bearing areas such as the spine, pelvis, and proximal femur, but no loss in the upper extremities [44, 51]. The ISS studies also utilized quantitative computerized tomography (QCT) that could differentiate between losses in cortical and trabecular bone. They found that the rate of loss of trabecular bone was nearly twice that of the rate of loss of cortical bone in the proximal femur [44]. As trabecular bone aids in force transfer within the bone structure, these losses and the subsequent changes in bone geometry may compromise bone strength over time, and increase their risk of fractures [13, 31]. While astronauts lose bone at a rapid rate, they are slow to recover it when they return to earth, with astronauts showing only partial recovery during the first year after their mission [45], and it is unknown whether they ever fully recover. A follow up study on Skylab astronauts showed that not all bone lost during the mission had been recovered even five years after flight [10].

Evidence from studies of bone markers suggests that bone loss in space is due to an increase in bone resorption and a decrease in bone formation [69, 47], and is concentrated in the lower spine and lower extremities, which are the areas of highest gravitational loading on earth. These results are similar to those seen due to immobilization or spinal cord injury, which suggests that research into physiological deconditioning seen in space could have terrestrial applications [12].

A major concern with bone loss in space is the increased risk of fracture. This risk would arise during activities that put high strains on the skeleton, such as surface activities on the moon and Mars, during liftoff or aerobraking, or during extravehicular activities in microgravity [78]. Finite element analysis performed using DXA scans of

the proximal femur of ISS astronauts pre and post flight showed that the percentage losses of strength during the 4-6 month flights matched the estimated lifetime loss of caucasian women [38]. Additionally, the increase in serum calcium levels due to bone resorption increases the risk of developing kidney stones [62].

Unloading due to microgravity also has significant effects on human musculature. Similar to what has been reported in bone, protein synthesis and breakdown in muscle responds to loading. The major effect of microgravity is muscle atrophy with an accompanying loss of peak force and power. Biopsies taken from astronauts who flew on the ISS for extended missions showed substantial loss of muscle fiber mass, force and power, with the effects having different magnitudes based on fiber type [19]. At the whole-muscle level, the maximum power of the lower limbs was reduced to 67% of the preflight levels in astronauts after 31 days in space, and to 45% after 180 days [24]. This problem is coupled with skeletal deconditioning, because muscle contractions are also a major source of bone loading [42, 63], with peak loads that meet or exceed those experienced during the impace phase of gait [70]. In space, the muscle forces required to move the limbs are reduced due to the absence of gravity, and muscle atrophy would only decrease the muscle forces generated, which could exacerbate bone loss. A countermeasure that provides resistive force to the muscles addresses both of these issues.

Astronauts experience significant spinal elongation due to unloading in space, most likely due to the swelling of intervertebral discs, which leads to height changes of 4-6 cm during the initial exposure to microgravity [61]. Over half of all astronauts experience back pain, ranging from mild to severe, with varying duration [37]. This pain can affect astronaut productivity by interfering with restful sleep and decreasing concentration [79]. This spinal elongation can also affect the fit of custom-made components, such as the launch and re-entry seats made for the Russian Soyuz vehicle, or the current Extravehicular Activity (EVA) spacesuit, the Extravehicular Mobility Unit (EMU) [83]. NASA design standards state that changes in the spine can be up to 3% of preflight baseline height during flight [53]. This unloading also leads to

an increased risk of herniated disks for astronauts, which is up to 4.3 times that of the general population [35]. These changes could compromise astronaut safety and comfort. A countermeasure providing axial loading to the spine could prevent this elongation from happening, or at least reduce the effects before the astronauts return to earth [61].

Another phenomenon that occurs in astronauts during spaceflight is a pronounced cephalad fluid shift. This fluid shift causes many physiological alterations, such as facial edema ("puffy face"). One consequence of this fluid shift is increased intracranial pressure (ICP), which is proposed as one of the main causes of vision changes recently discovered in astronauts returning from long-duration missions aboard the ISS [52]. Custom thigh cuffs, currently in use on the ISS, have been shown to subjectively reduce some of the negative effects of the fluid shift, using pressures of around 20mmHg [27]. This type of thigh-cuff works by sequestering blood in the legs, and could be easily integrated into the GLCS. However, studies have also shown that ICP and intraocular pressure (IOP) increase during exercise due to the use of the valsalva maneuver and weight-lifting belts [77], so the potential of the suit to negatively effect ICP and IOP would need to be determined before integrating this functionality into the suit.

Head-down-tilt bed rest studies provide a terrestrial analog of unloading experienced during spaceflight. Given the high cost, technical problems, and size limitations of space flight studies, having this model of spaceflight allows further testing of the effects of unloading on the body, and a way to test countermeasure protocols. It produces effects in fluid shift, changes in bone mineral density, calcium excretion, and urinary bone markers that are qualitatively similar to what is seen in spaceflight [51]. The changes seen during the bed rest studies are less severe than those seen in actual spaceflight [15]. During a 17 week bed rest study, changes in bone mineral density were observed in the lumbar spine (-1.3%), hip (-3.4%), and proximal femur (-3.6%) [65]. Bed rest studies have also demonstrated increases in intervertebral disc height [50], and height changes [74, 80] after periods of unloading.

1.3 Current Countermeasures

Currently, the main countermeasure consistently used to combat physiological deconditioning in space is physical exercise. Crewmembers on the ISS currently use three different types of exercise machines. The machines are the Advanced Resistive Exercise Device (ARED), which allows the astronauts to perform resistive exercise and can be seen in figure 1-1, a cycle ergometer, and a treadmill [15]. A possible reason for the ineffectiveness of the current exercise programs in preventing bone loss is the loading that is placed on the bones during exercise. Force sensors placed in the shoes of astronauts showed that there was a 26% reduction in the loads experienced while walking on the treadmill as opposed to walking on earth, and a 45% reduction compared to running [15]. More recent data show that resistive exercise afforded by the ARED (which has a 600 lbf capacity) coupled with adequate nutrition has been more effective in maintaining bone mass of ISS crewmembers [67], however, it has not been successful in completely preventing bone loss and muscle atrophy.

Current exercise protocols for the ISS call for a period of 2.5 hours per day, six days per week to be set aside for exercise activities. However, a substantial portion of this time is allotted for set-up, stowage, and personal hygiene. When taking these activities into account, only 90 minutes remain for actual exercise, including 60 minutes for resistive exercise, and 30 minutes of aerobic or anaerobic training [12]. This distribution of exercise emphasizes resistive exercise, which provides higher loads to the muscles and skeleton due to muscular contractions, while also promoting cardiovascular health.

Beyond exercise, NASA is attempting to improve astronaut nutrition to prevent musculuskeletal deconditioning [67]. Additionally, pharmacological measures, such as bisphosponates, are currently being investigated [48, 14]. Bisphosponates have been shown to be effective in preventing bone loss during bed rest studies, by preventing bone resorption [49].

Figure 1-1: Advanced Resistive Exercise Device (ARED)

1.4 Current Countermeasure Limitations

All of the data presented on bone loss in space is collected in the presence of an active exercise countermeasure program, which shows that the current exercise protocols are not sufficient to completely prevent bone loss and muscle wasting in space. Additionally, the current exercise countermeasures only provide loads to astronauts during periods of exercise, so astronauts are unloaded for the majority of the day, apart from small (<60N) interaction forces produced as astronauts push off to move around the station [55]. The large mass and power requirements of these exercise devices make them less than ideal for use in the confined environment of an interplanetary mission, where volume will be more restricted than on the ISS. Given these limitations, other countermeasure paradigms should be investigated to increase the effectiveness of the

overall countermeasure program, especially as NASA looks ahead to future planetary missions.

1.5 Loading Suit History

1.5.1 Penguin Suit

The idea of a passive countermeasure suit has existed for nearly as long as human spaceflight. The Russian Pingvin (Penguin) suit uses elastic bands attached to non-stretch anchors at the shoulders, waist, knees and feet to impose three stages of loading on the body. It was not designed to mimic gravity, but induces weight-bearing stresses on the skeleton, and resistive exercise to the muscles. Reports from the Russian Institute for Biomedical Problems (IBMP) state that the Penguin suit can provide up to 70% bodyweight loading axially during treadmill running, and up to 40kg of static and dynamic loading during working hours [41]. Some Russian Cosmonauts who used the suit in conjunction with treadmill running on the International Space Station showed slightly reduced bone mineral density losses in the lumbar vertebra [41]. Multiple studies have shown that wearing the Penguin suit preserves soleus muscle function during long-term bed rest [82, 59]. However, to date, no studies have been done either on the ground to test its efficacy in preventing bone loss, and the in-flight studies involve the suit being used in conjunction with other countermeasures [78]. Additionally, Russian Cosmonauts have reported the suit to be difficult to wear for the recommended 8 hours a day because it is hot and uncomfortable. The Penguin suit concept has already been leveraged to aid in the rehabilitation of patients with various forms of cerebral palsy in Europe. A modified version of the suit, called the Adeli suit, has been implemented and tested in rehabilitation programs. The suit uses its elastic capabilities to provide external stabilization to the patient. Various

studies utilizing these loading suits to treat cerebral palsy patients showed marked improvement in gross motor function compared to traditional therapies, as the suit provided stability to the patients as a soft exoskeleton, which enforced normalized movements that gradually improved patient performance [64, 4].

1.5.2 Gravity Loading Countermeasure Skinsuit Concept

The Gravity Loading Countermeasure Skinsuit (GLCS) was first described by Waldie and Newman [78]. The GLCS seeks to replace gravitational bodyweight loading to the wearer during periods of musculoskeletal unloading, such as that experienced by astronauts in microgravity during long-duration spaceflight. The GLCS is a mechanical loading garment, whose construction uses the same principal as the Penguin suit - horizontal belts to anchor vertical bands that impose tension in the axial direction. Instead of a three-stage loading garment, the GLCS seeks to more closely replicate gravitational bodyweight loading by increasing the number of loading stages. The weight-bearing loading profile of the design is imposed by gradually increasing the force generated by each subsequent loading stage moving from the head to the feet, with the force generated by each loading stage equal to the weight of the body segments superior to the loading stage. In order to produce this graded loading, horizontal anchoring bands between the loading stages anchor the suit to the body and prevent suit slip. Without this anchoring, the various loading stages would pull each other into equilibrium, resulting in a single level of loading throughout the body. The anchoring force needed between two loading stages is equal to the difference in loading between the two adjacent stages. A representation of this can be seen in figure 1-2. Therefore, increasing the number of stages not only improves the resolution of the loading gradient, making it closer to gravitational loading, it also causes the force differential between stages to decrease, which decreases the necessary anchoring force. The load produced by the suit is transferred to the body at the soles of the feet, though stirrups, and at the shoulders. The graded loading of the suit allows for

full bodyweight loading at the feet, while decreasing the load at the shoulders, which will improve subject comfort. The Gravity Loading suit has manifested in a series of prototypes, each offering incremental improvements over previous generations. The work described herein outlines efforts to build upon these previous efforts and produce a loading garment that can be effective as a countermeasure to musculoskeletal deconditioning.

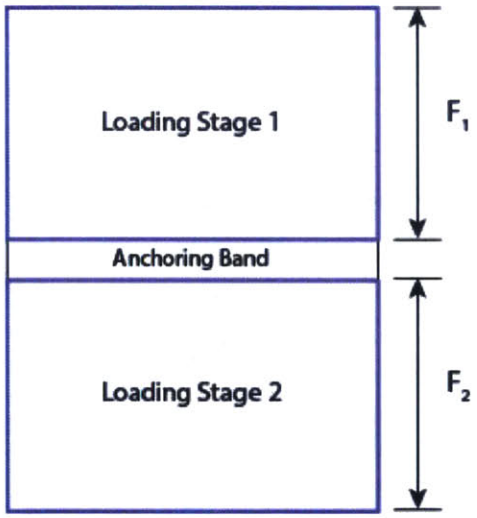

Figure 1-2: GLCS loading and anchor stage representation

Mark I

The first GLCS prototype was developed for a parabolic research flight. The suit uses a lycra material with a bidirectional elastic weave: meaning that the tension in the vertical fibers differs from that in the horizontal direction. This allows the material to provide high loading potential in the vertical direction, while the less stiff horizontal fibers offer circumferential anchoring pressure. The reduced stiffness in the horizontal fibers allow the suit to be robust to changes in body circumference caused by breathing, fluid shifts or body movements, as the circumferential suit tension will be less sensitive to changes in body circumference. Non-stretch canvas was used for the region of the suit above the armpits, to ensure accurate and consistent placement

of the elastic weave on the body. Because the arms are not weight-bearing and suffer little, if any, bone loss in microgravity, the suits are sleeveless. The loading material begins below the armpits, as this is the first area where a full circumference around the body is achievable without hindering the arms. Non-stretch nylon stirrups transfer the load to the soles of the feet. Stretch arrestor ribbons were added along each neutral side axis of the body to prevent the spandex from overstretching. Two subjects wearing the suits can be seen in figure 1-3. The results from the parabolic flight showed that the suit was stretching to around 60% of its design strain at the lower leg, based on in-flight measurements, although no loading measurements were taken. Comfort and mobility were assessed using subjective feedback, and the suits were shown to be comfortable enough for eight hours of wear with minimal mobility hindrance [78].

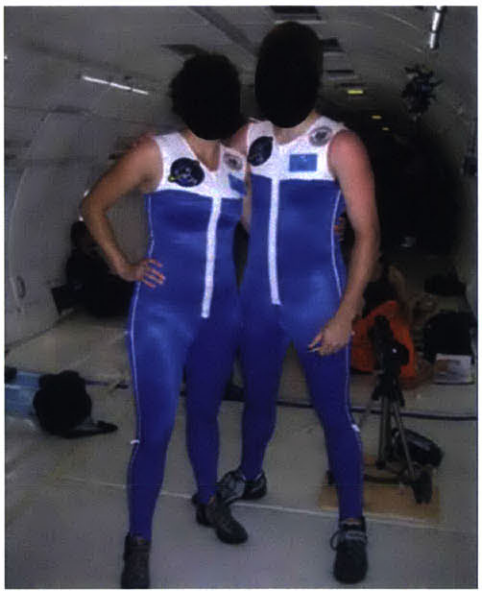

Figure 1-3: GLCS Mark I prototype

Mark II

The second generation of prototypes were developed for a sleep study. The main design change was an increased number of stretch arrestor ribbons on the suit to

ensure the suit was stretching to the desired lengths, as the single arrestor ribbon on each side of the Mark I suit had been shown to be insufficient to ensure accurate suit stretch. The results of the sleep study are not yet available.

Mark III

These prototypes were constructed for exercise testing at King's College London. Major design changes included a zipper at the ankle to allow the foot to pass through for easier donning, modifications to the shoulder yoke sizing to improve comfort under the arms, and changes to the stretch arrestor ribbons around the shoulder yoke to better integrate with the modified design. The suit can be seen in figure 1-4. Exercise testing performed with the suits found that they provided tolerable axial loading, and did not significantly impede exercise, although it decreased subject range of motion at the knee and in shoulder flexion/extension [1].

Mark IV

These prototypes were developed to investigate new designs for donning and doffing. Previous iterations of the suit utilized a zipper on the front of the suit to allow the suit to open and be donned. However, subjects often had difficulty donning the suit due to the difficulty of stretching the suit and fitting their arms through the shoulder holes simultaneously, which lead to some shoulder discomfort. Two different versions of the suit were produced, one with a back zipper inspired by wetsuit design, and the other with an additional zipper on the side of the body in combination with a front zipper. After numerous design iterations, it was determined that, for the side zip system to work, a lacing system would be necessary to bring the suit panels together so that the zipper could close. User donning and doffing testing led to the back zipper design being adopted for future designs. The different designs can be seen in figure 1-5

Figure 1-4: GLCS Mark III suit

Mark V

This phase of prototypes were developed for another parabolic flight campaign, which was used to evaluate the suit in preparation for a potential ISS flight. Heavier, more durable spandex was used in this iteration, to attempt to achieve higher loading than had been previously achieved. The shoulder yoke was redesigned, with integrated padding and improved stitching around the edges of the yoke to improve shoulder comfort. Wider straps were used for the stirrups, which, in combination with custom fitted carbon fiber insoles, were used to disperse the load more evenly over the sole of the foot. Finally, the stirrups were redesigned to be tightened by the subject pulling up, which made solo donning and doffing of the suit to its full loading potential possible. The suit and the stirrup design can be seen in figure 1-6. The suits effects

Figure 1-5: GLCS Mark IV suit: (L-R) Back Zip, Side Zip, and Side Zip Lacing

on comfort and mobility were assessed, and the suit was found to be comfortable to wear with minimal movement restrictions. Additionally, suit loading was assessed using pressure sensing equipment, and found to load the subjects to between 15 and 40% of their bodyweight. These were the first accurate measurements of suit loading that were acquired.

Mark VI

Modified versions of the Mark V suit were produced for use in testing on the International Space Station, as well as ground testing. The only major change for this iteration was to include a zipper near the crotch of the suit to allow for male urination. During ground testing subjects wearing the suit were unloaded by having them lie on a modified water bed for a period of 8 hours. Despite this version of the suit only providing around 15-20% of bodyweight loading to the soles of the foot, the suit was able to decrease the height change during unloading, which suggests that the suit

Figure 1-6: GLCS Mark V suit: (L-R) Suit during parabolic flight and stirrup design

may be effective in ameliorating the spinal elongation seen during spaceflight [32]. Additionally, European Space Agency Astronaut Andreas Morgensen wore the suit during his mission to the International Space Station. Data from the mission is still being analyzed, and includes heart rate and subjective data taken during exercise with and without the suit, pre- and post-wear height measurements, and subjective comfort measures. An image of Andreas Morgensen exercising in the suit, and an image of the suit can be seen in figure 1-7

Figure 1-7: GLCS Mark VI suit: (L-R) Astronaut exercising in suit, Mark VI suit

1.5.3 Loading Suit Limitations

Previous loading suits, including the Russian Penguin Suit and the GLCS, have had various deficiencies that would limit their effectiveness as a countermeasure. The first of these is the loading provided by the suits. The Penguin suit provides around 40 kg of static loading, which for a 50^{th} percentile male astronaut would provide around 50% bodyweight loading. The GLCS has only been able to produce a maximum of 40% bodyweight loading, with loading magnitudes of 15-25% bodyweight being the most common. Previous GLCS prototypes also had insufficient suit anchoring, leading to considerable suit slip and essentially a single stage loading garment. Additionally, these suits have also had comfort and mobility issues that made it difficult for subjects to use the suit. The loading provided by the suits and the effects of the suit on the body during unloading and exercise have not been sufficiently characterized. New GLCS prototypes will attempt to improve upon previous loading suits to address

these issues.

1.6 Project Goal

The goal of this project is to develop, produce, and characterize a comfortable countermeasure garment that can be used to provide axial body loading similar to 1-g loading on earth, in order to augment existing countermeasures, with the goal of preventing musculoskeletal deconditioning during long-duration spaceflight.

The GLCS was originally envisioned solely as a bone countermeasure. However, the loads produced by the GLCS may be effective in preventing other forms of physiological deconditioning. The axial loading provided by the suit may reduce spinal elongation and improve spine health over the duration of unloading, and the elastic properties of the suit can provide resistive exercise to the muscles, making the GLCS a more complete countermeasure.

1.7 Specific Aims

In order to create a more effective GLCS, the following research aims have been developed.

Aim 1: To produce a comprehensive model of suit-body interactions. Developing a model of suit-body interactions based on proposed suit characteristics will allow us to better understand the forces the suit will put on the body, how the suit affects the biomechanics of motion, and the joint torques it provides while performing these motions in zero gravity. This model was used to inform suit design by allowing investigation into various suit parameters, such as material stiffness, and seeing how these changing these parameters affect the forces the suit is putting on the body. The

GLCS model has been developed in OpenSim musculoskeletal modeling software, and integrated with existing musculoskeletal models.

Aim 2: To design, build, and characterize prototype countermeasure suits. Using knowledge gained from Aim 1 and lessons learned from previous suit prototypes, new suit prototypes were designed and constructed. The major design elements that were focused on include: i) identifying and testing candidate elastic materials, ii) improving suit anchoring, iii) improving suit comfort, and iv) improving the patterning process . Suit loading properties were characterized using pressure-sensing technology, material stretch properties were determined using motion capture, and suit comfort was ascertained using subjective measurements.

Design goals: 1) Suit provides 100% Bodyweight loading at the sole of the foot; 2) material stretch is within 5% of design stretch; 3) the suit is comfortable enough to be worn for 4 hours at a time and; 4) loading doesn't decrease more than 10% over the course of 4 hours.

Aim 3: To examine the potential efficacy of the countermeasure suit in mitigating the effects of microgravity on muscle and bone loss. In preliminary studies of the GLCS, the suit's ability to reduce the effects of microgravity on muscle and bone loss was not explored. To test the potential efficacy of the GLCS in reducing the physiological deconditioning seen in spaceflight, we tested the suit using ground-based analogs. The following tests were performed:

Short-term Bed Rest: The suit's effects on spinal elongation were assessed. Subjects laid down supine for four hours, and the difference in height between suited and unsuited conditions were assessed and compared to standing height. Long-term wearability and comfort were assessed during the test.

Hypothesis: Subject height in the supine, suited condition will not be significantly different from standing height, while subject height in the supine, unsuited condition will be greater.

Simulated Zero-g Exercise Testing: We plan to use the enhanced Zero-g Locomotion Simulator at NASA Glenn Research Center, which provides a high-fidelity simulation of the cephalocaudal unloading seen in spaceflight, by suspending the human test subject horizontally, while allowing for locomotor exercise, movements in simulated zero-g, or the use of other exercise modalities. Subject performed walking and running in both suited and unsuited conditions to ascertain the suits effects on exercise. Gait parameters were measured using motion capture and ground reaction force data taken from force plates in the treadmill. Pressure sensing insoles recorded the loading at the sole of the foot to determine the suit's contribution to loading. Heart rate and subjective workload measures were taken to determine how the suit affects the physiologic costs of exercise.

1.8 Thesis Overview

This thesis is organized into 5 chapters that follow the stated research aims:

Chapter 2: Outlines the development of the suit-body model in order to gain insight into suit loading capabilities and inform suit design to complete research aim 1. A model was developed in OpenSim musculoskeletal modeling software, and simulations were run to determine the joint and muscle forces during movement for a variety of suit loading conditions and compared to unsuited movement in earth gravity. The simulations showed that the suit could provide forces to the muscles similar to those provided by unsuited bodyweight motion, and that the suit also provided high dynamic loads to the joints.

Chapter 3: Describes the suit design and construction process, including selection and integration of new loading materials, suit anchoring improvements, subject measurements and suit patterning. In order to provide higher loading than previously achieved, the loading elements were integrated into a soft exoskeleton comprised of

the loading elements and non-stretch nylon webbing that was worn over a spandex bodysuit that provided an interface between the loading exoskeleton and the body. This chapter addresses the design aspects of research aim 2.

Chapter 4: The constructed prototype suits had their loading capability and comfort characterized, and were then tested in analogs of unloading. Specifically, they were tested during a 4 hour bed rest study to determine the suit's effects on spinal elongation and long term comfort, as well as on a vertical treadmill to determine how the suit affected exercise in a simulated ISS environment. The suits were found to achieve much higher loading capabilities than any loading achieved through the previous suits, although there were comfort issues in the long term wear of the suit, due to design and construction inadequacies. Additionally, the suit was shown to increase physiological workload in the subjects during exercise, and increased loading to the muscles and joints. This chapter addressed suit characterization aspect of research aim 2, and the entirety of aim 3.

Chapter 5: A summary of the thesis is presented, including the major findings and contributions, limitations, suit design recommendations and future work.

Chapter 2

GLCS Suit-Body Modeling

Measuring the forces that the GLCS puts on the body is difficult to do *in vivo*. Additionally, suit materials with different stiffness properties will affect how the suit loads the body during dynamic movements, and it is unknown what the ideal material properties would be for the suit loading material. Developing a model of the GLCS will allow investigation into how changing suit loading properties affect the static loads the suit puts on the body, as well as the loads it imposes during dynamic movement. The specific questions we seek to answer with the model are:

1. How does changing the stiffness of the suit loading material affect loads to the musculoskeletal system?

2. How does changing the static loading level of the suit loading material affect loads to the musculoskeletal system?

This chapter describes the development of the suit-body model used to investigate these questions, the simulations developed to verify the model implementation and determine the dynamic joint and muscle forces imposed by the suit during movement, the results of the simulations, and the implications these findings have for suit design.

2.1 Suit Requirements

In order to develop a suit-body model that can be useful in determining the forces that the suit imposes on the body and also be useful in informing suit design, the requirements for the GLCS must be made explicit. The requirements for the suit that determined the model development process are as follows:

- The GLCS will provide 100% bodyweight loading to the soles of the feet in upright posture in the nominal case (i.e. the load experienced at the sole of each foot will be 50% bodyweight).
- The loading elements of the GLCS will provide graded loading, with each loading stage providing force equal to the weight of the body above the loading stage to replicate the loading seen in gravity.
- The suit will be skin-tight and follow the contours of the body.

2.2 Model Development

2.2.1 OpenSim

To develop a suit-body model for the GLCS, we used OpenSim, an open-source musculoskeletal modeling program developed at Stanford University [18]. It is built on SimBody, an open source multibody dynamics engine. OpenSim models consist of rigid bodies that are connected by joints and moved by actuators. There are many different varieties of bodies, joints, and actuators. For musculoskeletal models, the bodies are bones, and the actuators are muscles, the properties of which have been determined through anthropometric studies or empirical data. OpenSim is highly

versatile, and has a variety of built-in analyses that can be used to analyze dynamic simulations of movement. OpenSim has been used to simulate a variety of movements and exercises, including walking [6, 66], running [29], jumping [5] and squatting [23]. OpenSim is also being used by NASA's Digital Astronaut Project to analyze novel exercise countermeasures [73]. To date, no one has utilized OpenSim to model soft suits and their effects on body loading.

The OpenSim capabilities that will be used in GLCS modeling include:

Model Scaling: Scales musculoskeletal models to match measured subject anthropometry.

Inverse Kinematics: Takes in marker motion history data from motion capture studies, and steps through each time point to position the model in a pose that best matches the experimental marker data. This allows analysis of subject kinematics, and is used as an input to other tools to determine muscle and joint forces during motion.

Inverse Dynamics: Determines the generalized joint torques required to produce a given movement.

Static Optimization: Extends Inverse Dynamics by computing the individual muscle forces required to produce a given movement. Static Optimization takes the body's state at each discrete time point over a given motion, and solves for the muscle forces necessary to produce the kinematics and dynamics of the motion, while minimizing muscle activation.

Joint Reaction Analysis: Takes the muscle forces computed in Static Optimization, subject kinematics, and any external forces, and calculates the resulting forces and moments in each joint, which correspond to the internal loads carried by the joint structure, which represents the loading being applied to the skeleton at the joints.

With these analyses, we can begin to understand the relative forces the suit is applying

to the bones and muscles for various loading properties during movements.

2.2.2 Base Model

The base model chosen was the Gait2392 model, a 23 degree-of-freedom model developed by Darryl Thelen (University of Wisconsin-Madison) and Ajay Seth, Frank C. Anderson, and Scott L. Delp (Stanford University). The model consists of a highly detailed lower body and torso, with 76 individual muscles represented by 92 muscle actuators. Muscle geometry and the inertial properties of the body segments were defined using empirical data from human subject testing and cadaver studies. The arms are not represented in this model. As the GLCS does not cover the arms, this was appropriate and removed some unnecessary complexity. The default version of the model represents a subject that is 1.8m tall, and has a mass of approximately 75kg. This model can be seen in figure 2-1 .

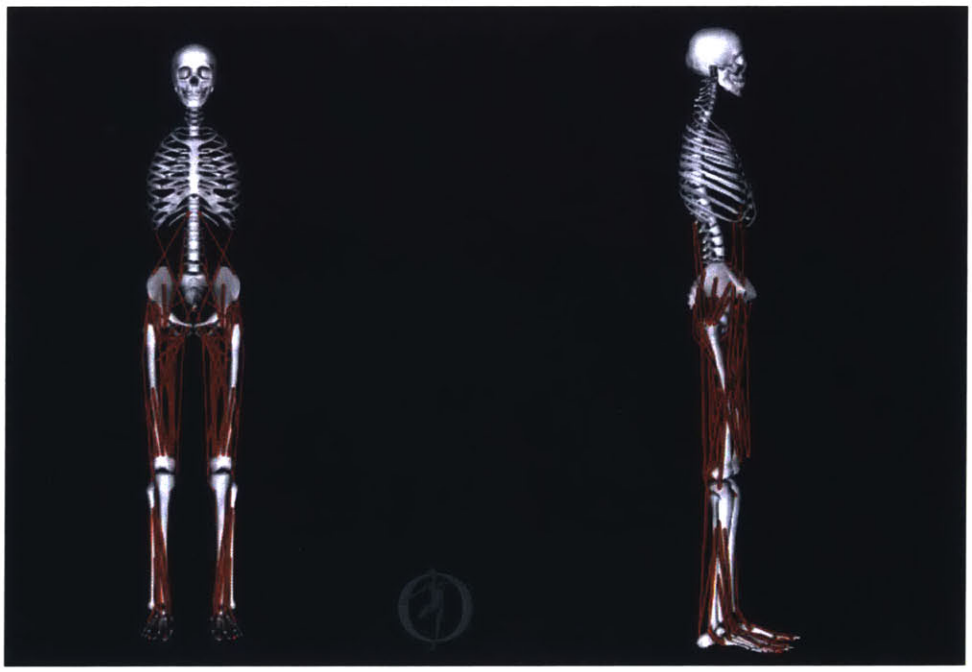

Figure 2-1: Front and Side view of Gait2392 Model

In order to scale the model to represent the astronaut population, anthropometric

data was taken from the NASA Standard 3000 - Man-Systems Integration Standards [53]. Scaling factors were determined using the body measurements representing the 50^{th} percentile male astronaut. An example of measurements taken for the anthropometric database are shown in figure 2-2. Measurements for the 5^{th}, 50^{th} and 95^{th} percentile males are included in table 2.1 below.

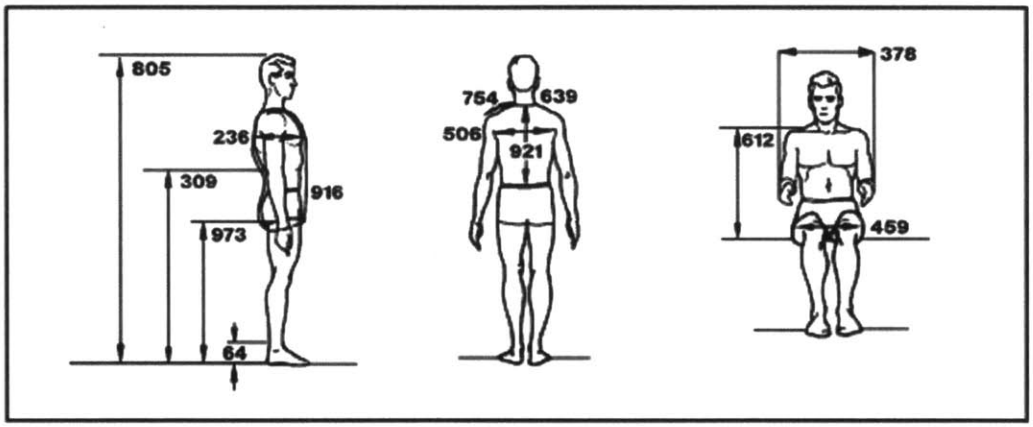

Figure 2-2: Anthropometric Measurements from NASA-STD-3000

Table 2.1: Anthropometric Measurements from NASA-STD-3000

Measurement	5th (cm)	50th (cm)	95th (cm)
Stature	169.7	179.9	190.1
Waist Height	100.4	108.3	116.2
Crotch Height	79.4	86.4	93.3
Trochanteric Height	88.3	95.8	102.9
Tibiale Height	44.9	47.8	50.7
Ankle Height	12	13.9	15.8
Chest Circumference	89.4	100	110.6
Waist Circumference	77.1	89.5	101.9
Thigh Circumference	52.5	60	67.4
Knee Circumference	35.9	39.4	42.9
Calf Circumference	33.9	37.6	41.4

2.2.3 Suit Model

When implementing the GLCS into the musculoskeletal model, the suit model was developed to be as simple as possible, while still retaining sufficient complexity to

provide useful insights. The suit loading elements were modeled using OpenSim's predefined spring actuators. The model uses Path Spring actuators, which are a spring class that follow a path prescribed by the user. This allows the lines of action of the spring to change during movement, and follow the contours of the body. To create an interface between the suit springs and the body model, anchor bodies were created, representing thin discs whose circumferences are determined using the circumference of the body segment at the point of attachment. The anchoring bodies are rigidly attached to the corresponding body segment, and offer an attachment point for the path springs. The anchoring bodies were given a negligible, non-zero mass, in order to allow the various OpenSim analyses to run properly. Finally, wrapping elements, whose dimensions were determined using the anthropometric data, were added at the knee and hip joints to ensure the suit springs would wrap around the joint in the manner of a skin-tight suit. The model can be seen in figure 2-3.

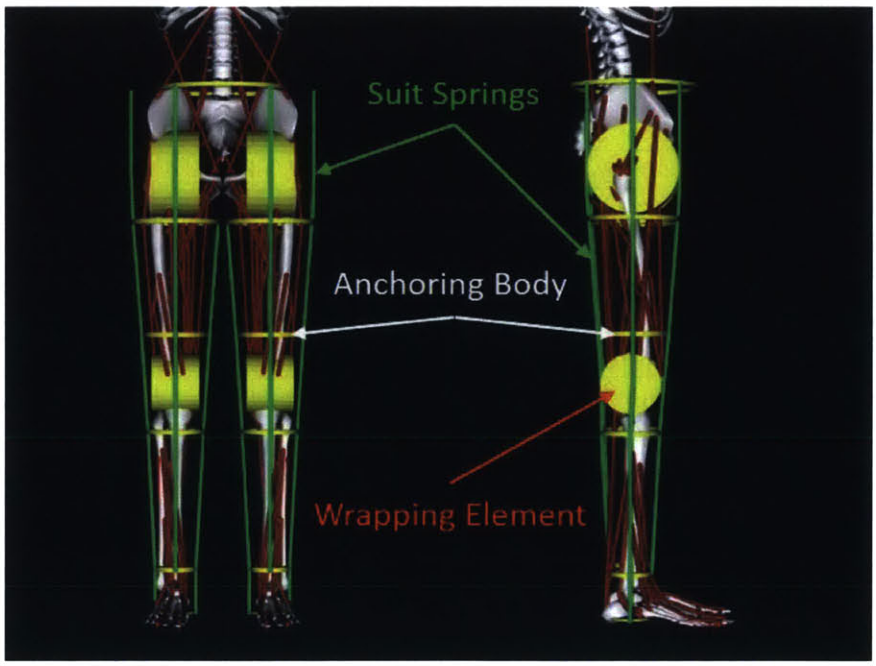

Figure 2-3: CLose up of GLCS model

The suit model has five loading stages: Torso/hip, thigh, knee, shank, and ankle. This loading stage allocation allowed for differential loading over the joints, where most of the stretch and movement of the suit would be occurring, while minimizing the

number of loading stages to reduce model complexity, as additional loading stages over the rigid bodies of the model would not affect the results. For each loading stage on the leg, 4 path springs were used per stage, and placed on the front, back, medial and lateral sides of the stage. The force produced by the springs at each loading stage was determined by calculating the mass of the body segment covered by the loading stage, and adding the mass of the body segments superior to the loading stage. For instance, the knee stage springs force is equal to half the mass of the upper body segment (as each leg supports half the weight of the upper body), plus the mass of the thigh, plus the mass of the segment of the shank that the knee segment overlays. Body segment masses were calculated using established segment mass data from anthropometric literature [60, 16]. The percent of total body mass values for each segment can be seen in table 2.2. For the purposes of body segment mass calculations, the thigh and shank body segments were assumed to have uniform density and a circular cross-section with a circumference that decreased linearly from the upper thigh to the knee in the case of the thigh, or from the knee to the ankle in the case of the shank. This can be seen in figure 2-4.

Table 2.2: Body Segment Mass Proportions

Body Segment	% Total Body Mass
Upper Body	66.64
Thigh	10.5
Shank	4.75
Foot	1.43

The force generated by each suit spring is equal to:

$$\frac{F}{n} = k\,(x - x_o) \tag{2.1}$$

where F is the required segment load force, n is the number of springs used in the loading segment, k is the spring stiffness coefficient, x is the length of the loading segment, and x_o is the resting length of the spring. F and x are known from subject anthropometry, and k is based on previously performed tensile tests on commercially available loading materials. The number of segment springs, n, can be set to allow

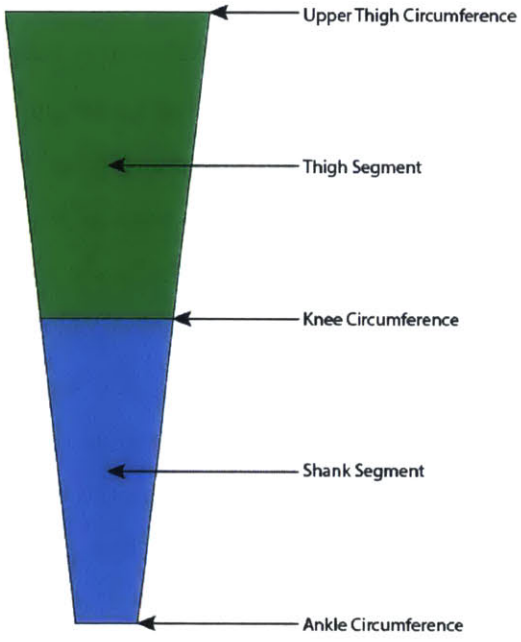

Figure 2-4: Leg segment representation used to calculate leg segment mass

the desired range of k, as the loading segment length x creates an upper bound on how far the suit spring can stretch, and fewer suit springs at a lower stiffness level may not achieve the necessary segment loading force. Four loading springs per stage on the suit leg segments were found to be sufficient to allow the use of the full range of previous measured suit material stiffness levels. The spring resting length x_o can be calculated from equation 2.1. As the suit springs stretch during motion, the tension in the spring increases, and they will provide resistive loading to the musculature.

2.3 Model Assumptions and Limitations

There were a few important assumptions made during the development of this model. The first is that the suit loading elements would exhibit linear stiffness. As will be shown in chapter 3, this is a reasonable assumption to make. Many loading materials used in the suit have regions of linearity in their force-length relationship. The second

major assumption is that the suit will be perfectly anchored to the body, giving distinct loading stages. This means that the suit stretch over different loading stages on the body are independent of all the other loading stages for these analyses. In actuality, as shown in chapter 4, suit anchoring is not perfect and there may be some interaction between loading stages. However, it is assumed that these interaction effects will be much smaller in magnitude than the contributions from the suit stiffness and loading properties, as suit slip would not change the material stiffness properties of the suit and the length changes of the loading material would still be the same, resulting in similar forces being applied by the suit to the body. Finally, there are some limitations associated with the Gait2392 model, specifically, that its predictions may be inaccurate for high degrees of knee flexion. However, the motions analyzed in this chapter do not approach the maximum knee angle allowed in OpenSim.

2.4 Modeling Simulations

In order to examine the forces the GLCS can impose upon the body, two separate simulations were developed and executed. These simulations, a static upright pose and a knee-hip bend motion, are outlined in the following sections.

2.4.1 Static Upright Pose

The first simulation was the model maintaining a static, upright pose to determine the body forces in the baseline, nominal suit design case. For this simulation, three different suited cases with varying levels of suit material stiffness were analyzed. The three stiffness levels chosen were 500 N/m, 1000 N/m, and 2000 N/m, and were based on previous material testing performed on commercially available materials that were being considered for suit design and construction. The three suited conditions were

analyzed with gravity removed, to simulate the suit's performance in microgravity. Static optimization and Joint Reaction Force Analyses were completed, along with a Force Reporter analysis that tracks the forces imposed by the suit springs in the model. The results of these analyses were used to verify the implementation of the GLCS model.

2.4.2 Maximally Smooth Knee-Hip Bend

In order to determine the forces the suit provides to the body during dynamic movement, a second simulation was performed using a multi-joint movement encompassing the knee and hip, to determine suit loading over the range of motion of these joints, as the hip and knee are major regions of bone loss during spaceflight. A maximally smooth motion, as described by Flash and Hogan [20], minimizes the mean-squared jerk, which is the time derivative of acceleration. For a "rest to rest" motion of amplitude θ_α, and duration D starting at a joint angle of zero, this results in an equation of the position with respect to time of

$$\theta(t) = \theta_\alpha \left[10\left(\frac{t}{D}\right)^3 - 15\left(\frac{t}{D}\right)^4 + 6\left(\frac{t}{D}\right)^5 \right] \tag{2.2}$$

For this analysis, a motion where the hip and knee simultaneously move from 0 (straight leg) to 90 degrees of flexion was simulated. The range of motion for the knee and hip during this motion covers most of the range of motion the astronauts will experience during exercises on the ISS, such as squats or treadmill running [39, 58, 57], while also not exceeding the limitations of the Gait2392 model, as the model results start to become inaccurate as the joint angles exceed 90 degrees of flexion. A motion file was created with this maximally smooth motion. Images of the model at different time points in the motion can be seen in figure 2-5.

Two sets of simulations were performed, looking at two separate independent vari-

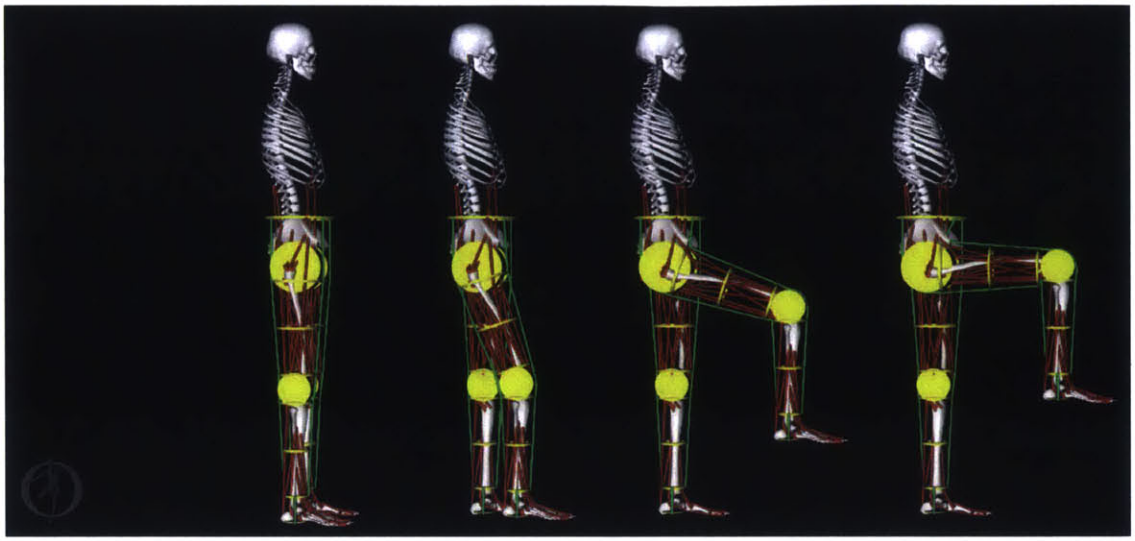

Figure 2-5: GLCS Model during knee-hip bend

ables.

1. **Varying Material Stiffness:** The first set of simulations tested how changing suit material stiffness affects suit loading during movement. For these simulations, three suited cases, with gravity removed, were analyzed with material stiffness values of 500 N/m, 1000 N/m, and 2000 N/m (the same cases analyzed in the static upright pose). For each case, Static Optimization, Joint Reaction, and Force Reporter analyses were run, and compared to simulation results from an unsuited model in earth gravity in order to compare how the suit matched normal bodyweight forces during movement.

2. **Varying Static Loading Level:** The second set of simulations varied the static loading level provided by the suit in the baseline upright pose, to see how loading during movement changes if the suit is unable to provide full bodyweight loading. Static loading levels of 25%, 50%, 75%, and 100% achieved using suit springs with a stiffness coefficient of 2000 N/m were simulated without gravity, and compared to the unsuited case in earth gravity.

2.5 Model Validation and Verification

In order to ensure accurate results, models need to be validated and verified. The validation process involves determining "the degree to which a model is an accurate representation of the real world" or "are we solving the correct equations?" Verification is the "process of determining that a computational model accurately represents the underlying mathematical model and its solution" or "are we solving the equations correctly?" [72, 30]. The OpenSim Software package was extensively tested before release. The Gait2392 model, upon which the GLCS model was built, has been comprehensively validated. Variations on the model have been used in many simulations of walking [34, 66] and running [29, 28]. In all cases the simulated values of muscle activation matched measured EMG patterns, and other predictions matched values contained in the literature.

As the musculoskeletal portion of the model has been verified and validated, the contributions from the loading suit elements that were added to the model need to be examined. Table 2.3 outlines the desired loading stage force, and the actual force provided by the loading springs for each of the suited cases. In every case the loads provided by the suit springs almost exactly matched the desired design loads. This shows that the suit spring resting lengths and displacement were implemented correctly in the model.

Table 2.3: Suit spring force generation

		Suit Stiffness Level (N/m)		
Loading Stage	Design (N)	500 (N)	1000 (N)	2000 (N)
Torso	294.88	294.88	294.88	294.88
Thigh	340.02	340.02	340.02	340.02
Knee	362.85	363.64	364.44	366.02
Shank	387.77	387.77	387.77	387.77
Ankle	403.55	403.55	403.55	403.55

In order to further verify the implementation of the suit springs, the results of the Force Reporter Analyses performed during the maximally smooth knee-hip bend mo-

tion were examined. Figure 2-6 shows the loading for the four knee stage springs for one of the suited cases during the knee bend motion. As expected, the front spring tension increases as it is stretched around the knee as the knee bends. The lateral and medial spring tension remains relatively constant, as their length remains mostly unchanged during motion. The back spring tension decreases during the motion, as its length decreases. These patterns are what would be expected during actual suit motion, and furthers our confidence that the suit springs were implemented correctly. Similar patterns can be seen in the hip springs in figure 2-7.

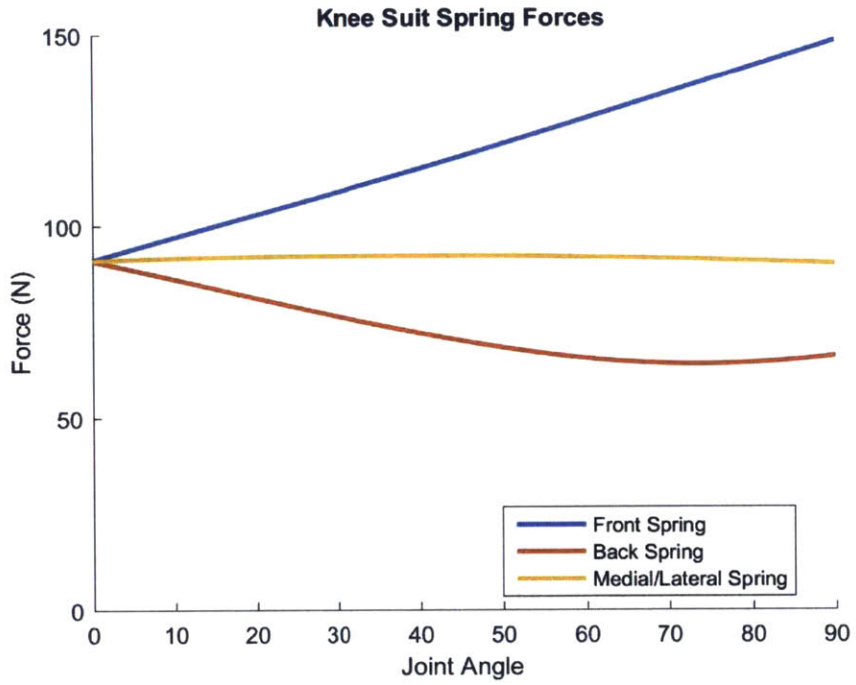

Figure 2-6: Knee suit spring forces during knee-hip bend

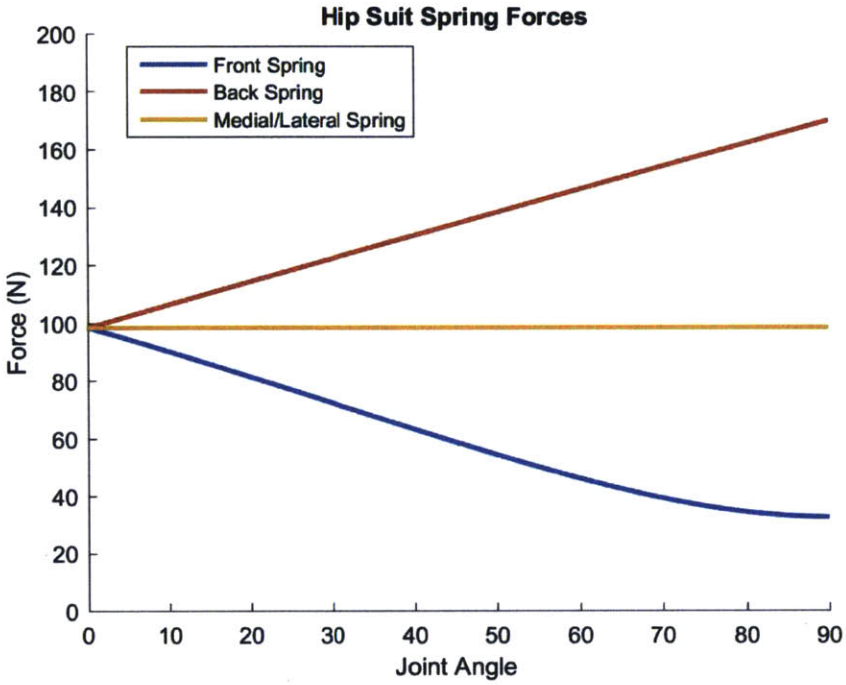

Figure 2-7: Hip suit spring forces during knee-hip bend

2.6 Modeling Results

Table 2.4 shows the Joint Reaction Forces in the individual knee and hip joints during static, upright posture in simulated microgravity for the three suited cases with varying levels of material stiffness. In all three suited cases, the joint loading was similar, which is to be expected, as the suit springs were calculated to give identical loading in the baseline standing pose. The small differences between the three suited cases can be explained by the small differences in the muscle forces required to maintain the static upright pose, examples of which are also listed in table 2.4. These differences in muscle forces are most likely caused by the small differences seen in the force produced by the knee segment suit springs, as seen in table 2.3, as those differences would change the muscle forces calculated by the optimization to maintain the upright posture.

Table 2.4: Joint and muscle forces during static upright pose

	Joint Loading				Muscle Forces	
Suit Stiffness (N/m)	Hip Force (N)	% Bodyweight	Knee Force (N)	% Bodyweight	Knee Flexors (N)	Hip Flexors (N)
500	489.97	60.71	472.68	58.56	109.97	140.27
1000	490.46	60.77	474.27	58.76	110.79	140.62
2000	491.50	60.90	477.48	59.16	112.44	141.35

Figures 2-8 and 2-9 show the sum of the knee flexor and hip flexor muscle forces, respectively, for the suited and unsuited cases during the maximally smooth knee-hip bend for varying levels of suit material stiffness.

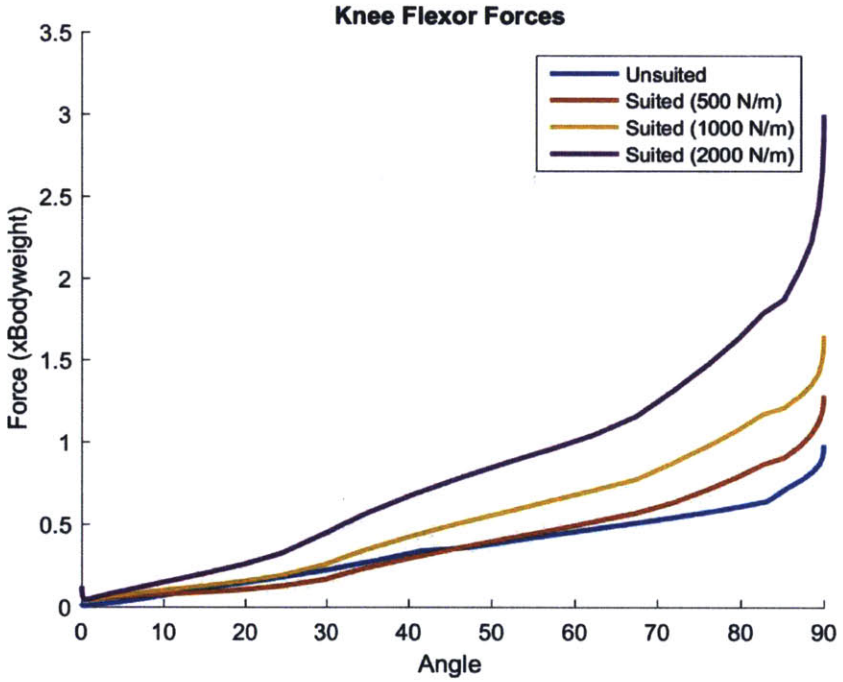

Figure 2-8: Knee flexor forces during knee-hip bend

As can be seen in the figures, the muscle force patterns for both the suited and unsuited cases have a similar shape, which shows that the GLCS can replicate bodyweight forces for the user. Additionally, for the knee flexor muscle forces, the unsuited case tracks well with the suited case with 500 N/m material stiffness, while for the hip flexor muscle forces, on the other hand, the unsuited case tracks closely with the 2000 N/m suited case. This suggests that different levels of suit loading material stiffness can better recreate bodyweight forces for different joints.

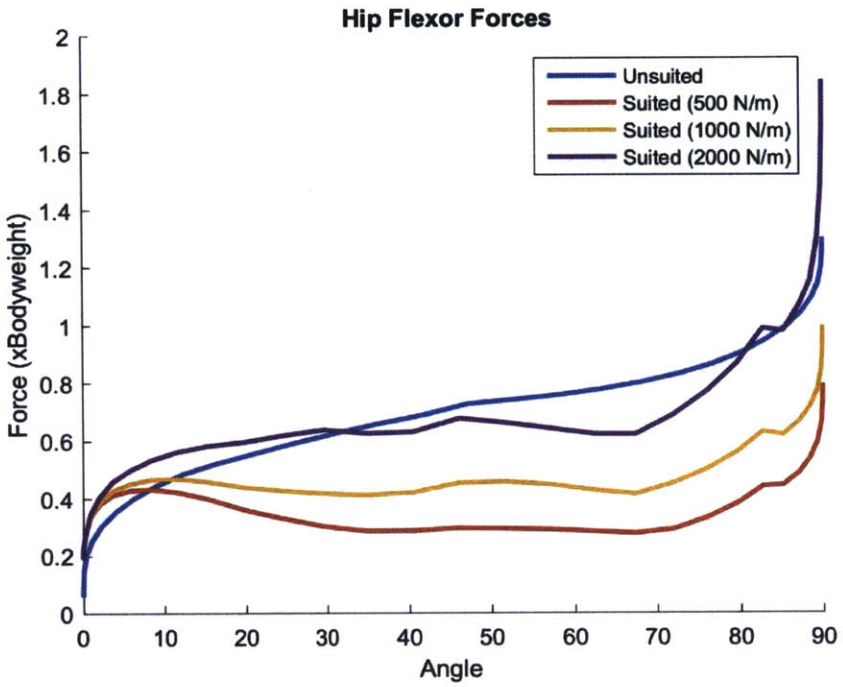

Figure 2-9: Hip flexor forces during knee-hip bend

The results of the joint reaction analysis for varying levels of material stiffness can be seen in figures 4-26 and 4-27, for the knee, and hip, respectively.

At the beginning of the motion, there is an offset in the joint loading, as the suit provides static loading to the body in the suited cases, while the unsuited case was simulated without an initial ground reaction force, so the unsuited model was initially unloaded. This only affects the initial time point, because as soon as the motion starts, the foot would lift off the ground causing the ground reaction force to disappear. In all of the suited cases, the joint forces in both the knee and the hip were higher than the unsuited bodyweight case. This was most likely due to the combination of suit loading and resultant muscle forces, as the joint loading in the unsuited case would be solely the result of the muscle forces generated during the movement. These analyses show that the suit is capable of producing high loads in the joints during movement.

In order to examine how these forces change if the suit is not providing full body-weight loads to the subject, further simulations of the maximally smooth motion were

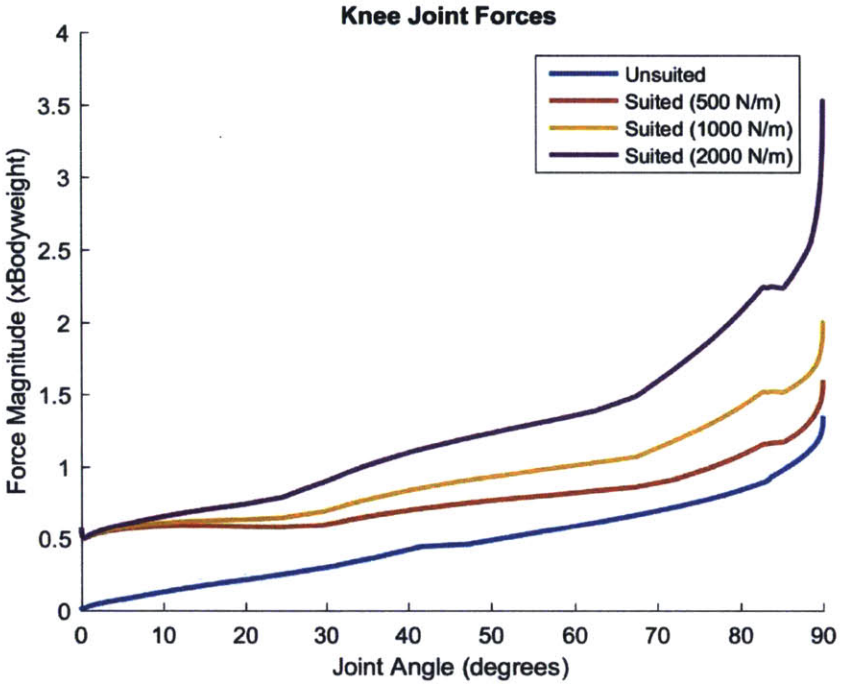

Figure 2-10: Knee joint forces during knee-hip bend

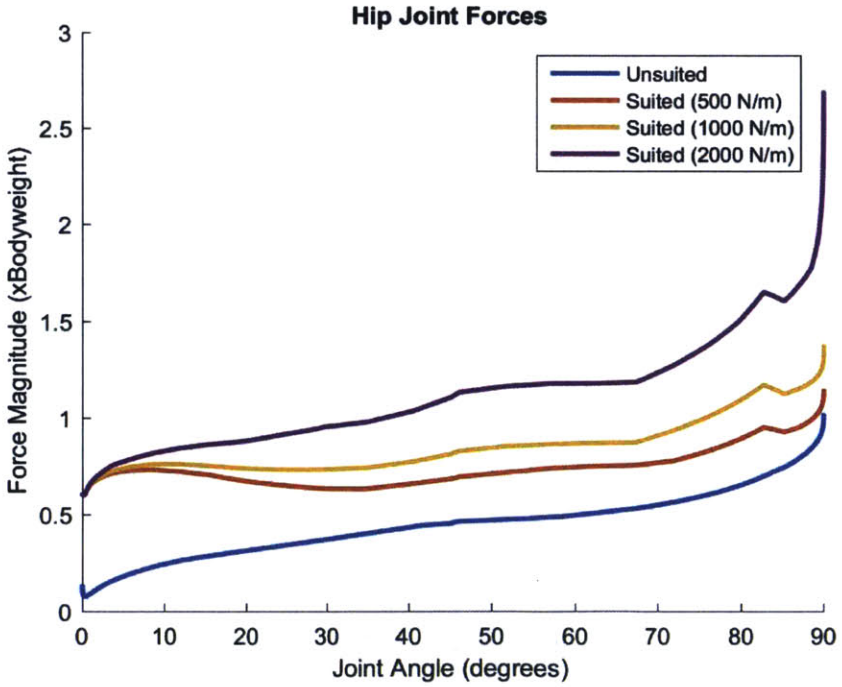

Figure 2-11: Hip joint forces during knee-hip bend

performed using suit models that provided 25%, 50%, 75%, and 100% bodyweight loading, using the 2000 N/m suit stiffness level. Figures 2-12 and 2-13 show the knee and hip flexor muscle forces required to perform the motion in all cases.

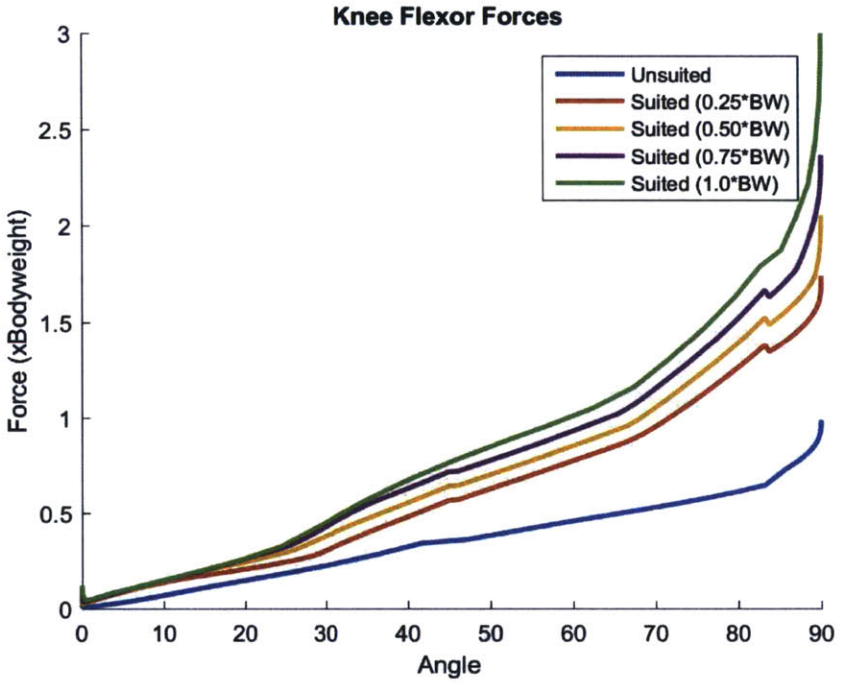

Figure 2-12: Knee flexor forces during knee-hip bend for different suit loading levels

For both the knee and the hip, the muscle forces go down as the static loading level is reduced, because the total force produced by the loading springs during the movement is reduced. The magnitude of the change in muscle loading is smaller than the changes seen when varying the loading material stiffness, which suggests that the material stiffness has a larger effect on the resistive load applied to the muscles than the static loading level achieved by the suit.

Similarly, the joint forces in the suited cases decrease as static loading magnitude decreases, due to both the reduction in static loading level and the dynamic loads applied to the joints via muscle contractions. In all cases, the joint loading was still higher than the unsuited case, which shows that the GLCS can provide high loads to the joints during dynamic movement, even if the suit is not providing full bodyweight

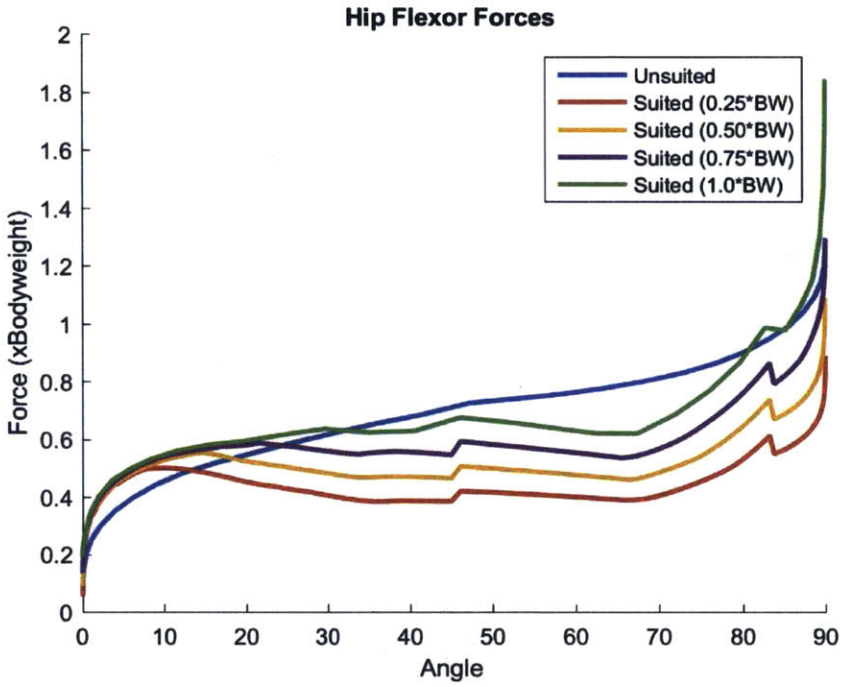

Figure 2-13: Hip flexor forces during knee-hip bend for different suit loading levels

loading to the subjects. These results can be seen in figures 2-14 and 2-15.

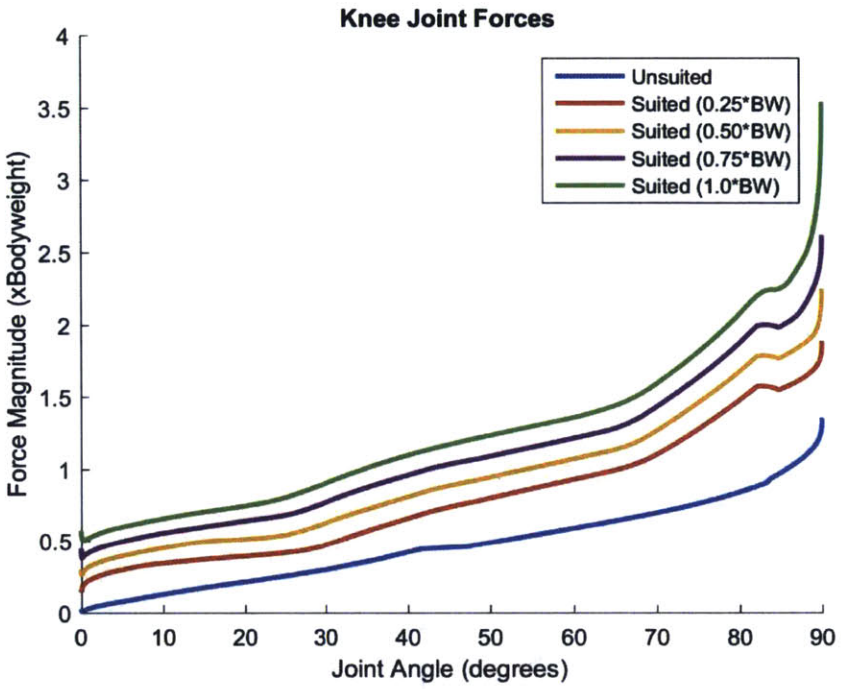

Figure 2-14: Knee joint forces during knee-hip bend for different suit loading levels

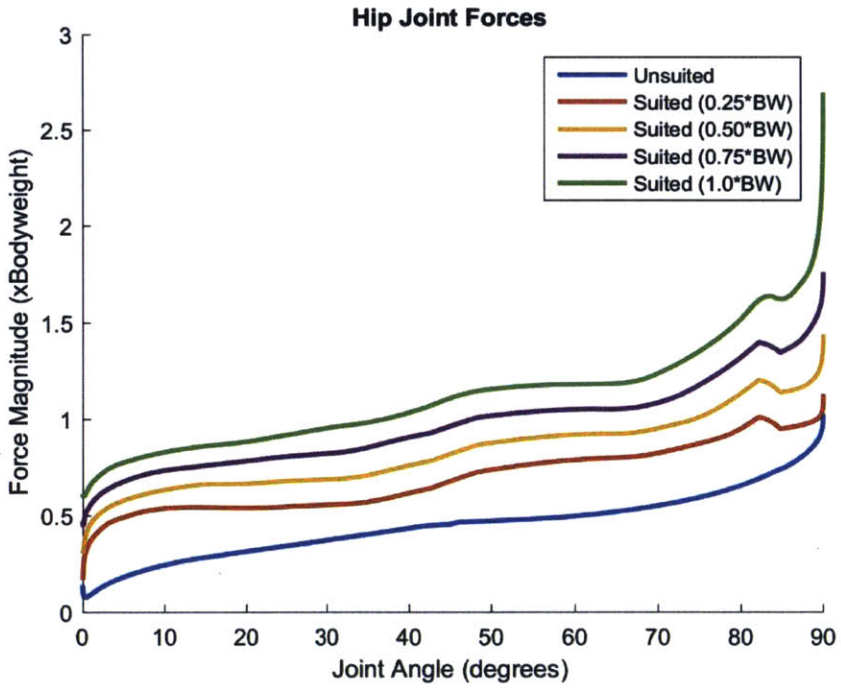

Figure 2-15: Hip joint forces during knee-hip bend for different suit loading levels

2.7 Summary of Modeling Results

A suit-body model was developed using an existing musculoskeletal model, and OpenSim's existing actuator and body classes to create a model of the suit. Anthropometry for a 50^{th} percentile male subject was used to scale the model and compute the necessary suit model parameters to replicate predicted real-world suit performance. The musculoskeletal model has been previously verified and validated, and tests were performed to verify the implementation of the suit model, and these tests showed that the implementation of suit springs and other suit elements was successful.

Simulations run on the forces generated by the suit in its baseline configuration, the static standing pose, showed that the suit provided slightly above 50% bodyweight loads to each leg at the hip and knee joints, which is expected given that each leg is supporting half of the bodyweight in the static standing pose.

Further simulations were run using a maximally smooth knee-hip bend motion to analyze forces over the range of motion of the knee and hip joints. The basic patterns of muscle forces were similar between the suited and unsuited cases. However, the knee flexor forces in the unsuited case were most similar to the knee flexor forces in the suited case with 500 N/m stiffness, while the hip flexor forces in the unsuited case were most similar to the hip flexor forces generated in the suited case with 2000 N/m stiffness. This suggests that, for the suit to achieve bodyweight loading during motion, different levels of material stiffness are desirable for different joints. It also suggests that the material stiffness range represented by the suit models is appropriate for suit design and construction, as the muscle forces generated by the suit tracked well with the unsuited case in earth gravity. Joint loading was higher in all suited cases than the unsuited case, which is unsurprising given the external loads imposed on the body by the suit, above and beyond the muscle forces required to perform the motion. While the suit increases joint loading, the magnitude of these increases are much less than those seen during locomotion [75], which suggests that the increased

loading levels imposed by the suit would not increase the users chance of injury.

An additional analysis was performed to determine the effect of lower suit baseline loading levels on the muscle and joint reaction forces elicited during the maximally smooth motions. The lower baseline loading led to lower joint and muscle forces as the baseline load decreased. However, the joint reaction forces for all suited cases were still higher than the unsuited joint reaction loads. All of these results taken together suggest that the suit is capable of providing physiologically relevant loading to the body.

Now that the model has been developed, it can be used to analyze a variety of motions for a range of different material properties.

Chapter 3

Suit Design and Characterization

Using lessons learned from previous suit prototypes, as well as insights from modeling, new Gravity Loading Countermeasure Skinsuit prototypes were designed and constructed. This chapter describes the selection of loading materials for the new prototypes, the integration of the new loading materials into the suit, improved suit anchoring techniques, and the final suit design, patterning and construction.

3.1 Design Considerations

3.1.1 Loading Material

One of the most important elements in the design of the GLCS is the selection of the loading material. In all previous iterations of the GLCS, the suit loading was provided entirely by Lycra (Spandex) fabrics. Spandex is an elastic material that is widely used in many types of clothing. The advantages of spandex are numerous. It is readily available commercially, its porous nature allows for regulation of body temperature, and it is used in many types of performance apparel, making its integration

into a loading suit straightforward. However, in evaluating previous suit prototypes, various limitations in using Spandex as a loading material have arisen. Spandex is not nominally designed as a loading material. While its elastic nature allows it to produce force when stretched, it is not generally put under the kind of loads necessary to reproduce bodyweight loading for the subjects. Because of this, there are limitations on its durability, repeatability and accuracy as a loading material.

For each suit prototype, material testing was performed on the Spandex to be used as the loading material, in order to characterize its stiffness properties to be used in creating suit patterns that would produce suits that gave accurate, bodyweight loading. For suit prototypes Mark I-Mark IV, the spandex used was Jumbo Spandex (90% lycra, 10% nylon), sourced from Costumeworks, Inc (Sommerville, MA), while the Mark V and Mark VI prototypes used Elastot 200 spandex sourced from Dainese (Molvena, Italy). Additional testing was performed on the Jumbo Spandex to determine how the Spandex loading changed over time, and with repeated stretch cycles. All tests were performed at the Institute for Soldier Nanotechnologies at MIT, on a Zwick Mechanical Testing machine [Zwick/Roell, Ulm, Germany]. The testing setup can be viewed in figure 3-1.

Figure 3-2 shows the results of a test where a 75 mm long sample of Spandex was stretched to a desired force, then held at a constant length to measure the force production over time. As seen in the figure, the force produced by the spandex decays over time, eventually reaching an asymptote just above 75% of its initial value. This would result in the GLCS under-loading the subject as the suit is worn.

Additionally, the spandex was cycle-tested to see how loading might change over repeated uses. In this test, another 75 mm long Spandex sample was stretched at a rate of 5 mm/second to a desired force output, returned to its initial length, then stretched again to the desired force output. This process was repeated to produce six total cycles. The results are shown in figure 3-3. For each successive cycle, the material has to stretch incrementally further to produce the same force. This means

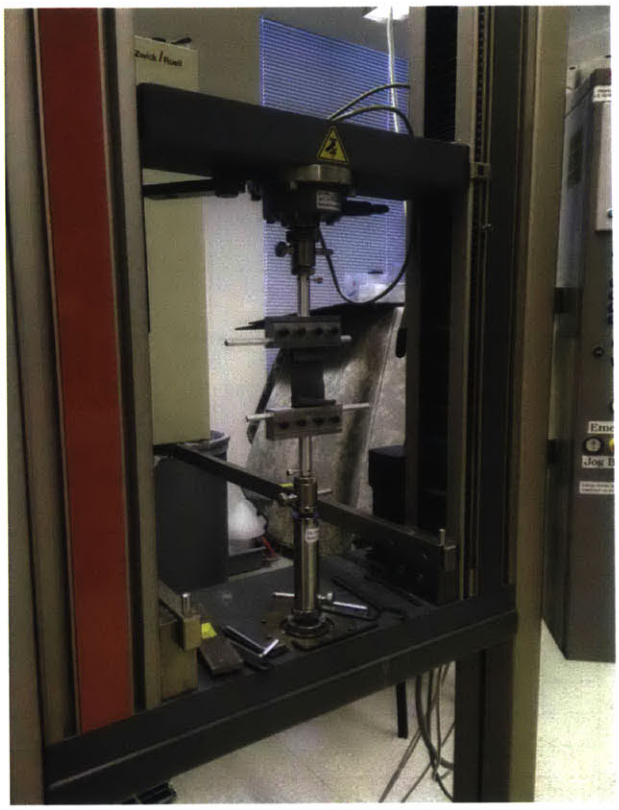

Figure 3-1: Zwick tensile testing machine

that as the suit is used repeatedly, the loading to the wearer will decrease with each successive use. The rate of stretching during testing was much slower than would be experienced when the suit stretches over the joints when walking or running in the suit, due to limitations imposed by the machine used to perform the tensile testing.

Because of these limitations, it was necessary to find other materials that can be used to as loading elements in the suit. After researching commercially available options, and discussing the issue with industry experts, two different loading materials were investigated and characterized for use in suit construction: **narrow elastics** (EL196, Lowy Enterprises, Inc., Rancho Domingo, CA) and **resistive exercise bands** (Rogue Fitness, Columbus, OH). An image of a narrow elastic sample in the Zwick testing machine can be seen in figure 3-4, and an image of the resistive exercise bands can be seen in figure 3-5.

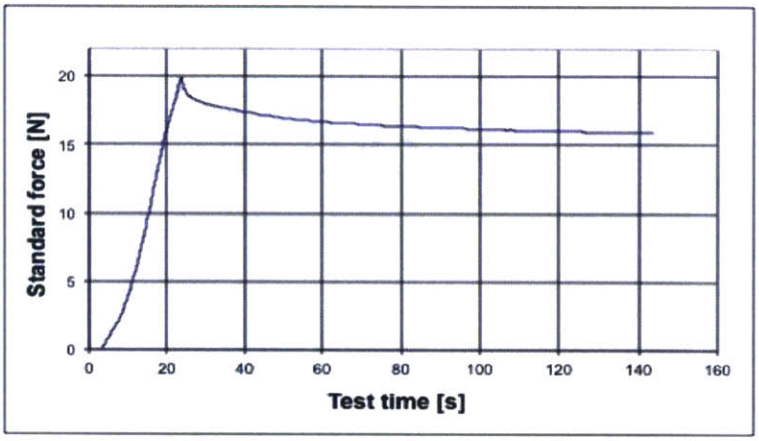

Figure 3-2: Force production over time at fixed length for suit spandex

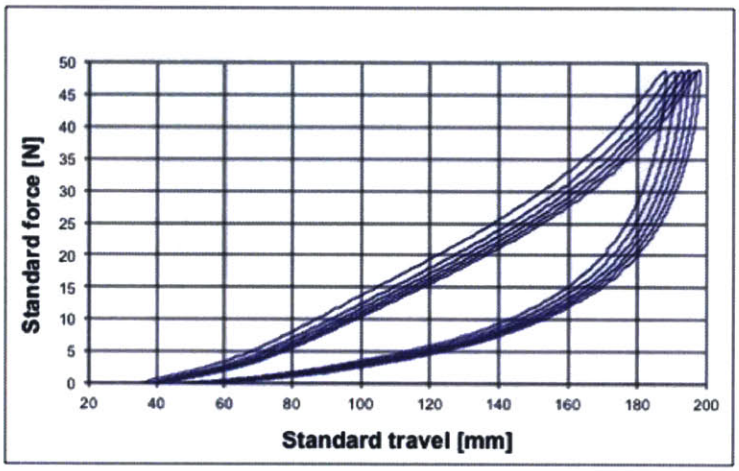

Figure 3-3: Spandex force production over multiple cycles

Narrow elastics are composed of polyester material interwoven with rubber elements to produce a flat band of elastic material. It has the advantages of a higher strength per width than the spandex materials used in previous suit prototypes, while also being easy to integrate into a soft goods suit. The resistive exercise bands are larger bands made of latex rubber and used in resistive exercise training. They are specifically designed to provide force when stretched. The main advantage of these bands is their high loading capacity. Once obtained, tensile testing was performed on multiple samples of both of the loading materials to obtain their material properties for use in manufacturing suits. The results of these tests can be seen in figures 3-6 and 3-7. As seen in the figures, the narrow elastics have nearly constant stiffness characteristics

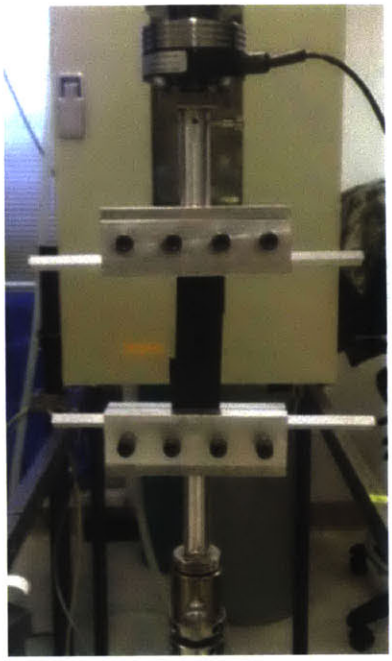

Figure 3-4: Narrow Elastic

over most of the range of stretch, while the resistive exercise bands can provide higher magnitude forces. While the force-length relationship of the resistive exercise bands is not perfectly linear, it does not deviate drastically from linearity, and will therefore provide consistent load increases as it is stretched.

Figure 3-5: Resistive Exercise Bands

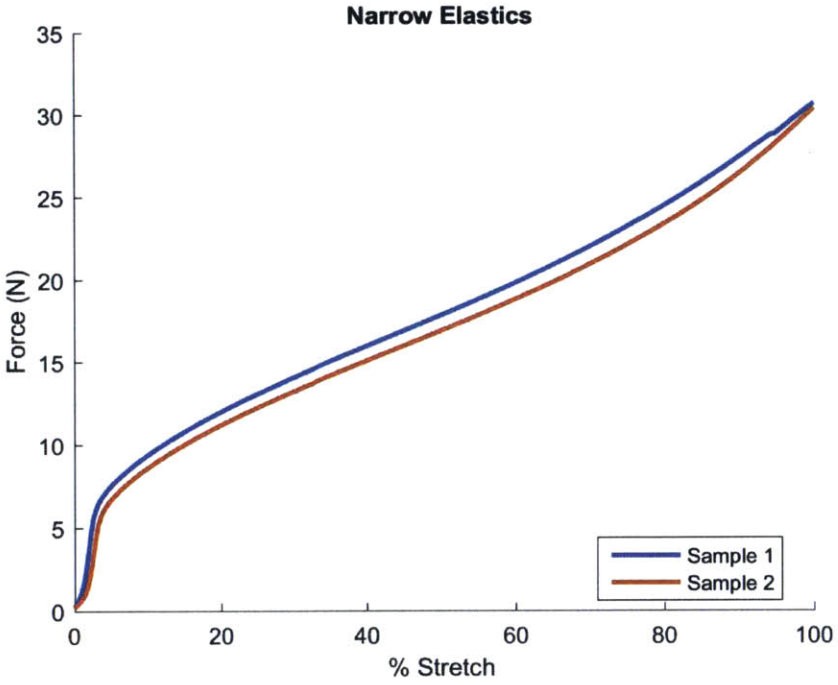

Figure 3-6: Force-length relationship for Narrow Elastics

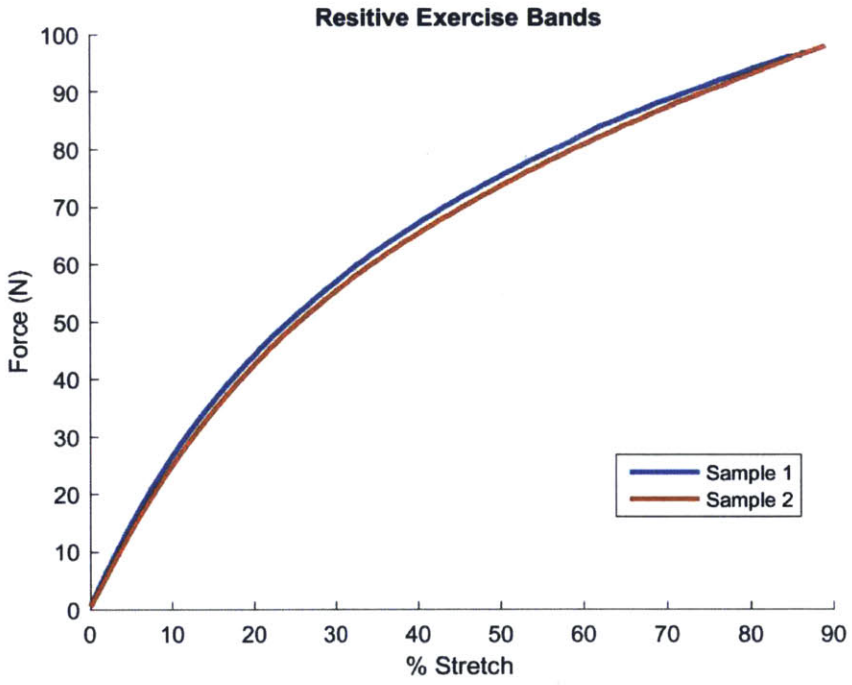

Figure 3-7: Force-length relationship for Resistive Exercise Bands

An additional test was performed to examine the durability of the narrow elastics in use as loading elements. Cycle testing was performed on a 75 mm long sample of narrow elastic that was stretched to 60% of its initial length at a rate of 5 mm/second, and then returned to its resting length, and then stretched again. This process was repeated for 50 total cycles, and the force generated by the stretching of the narrow elastic sample was recorded and can be seen in figure 3-8. While the force generated by the narrow elastic did decrease over the course of the testing, the magnitude of the losses were greatly reduced compared to the changes in loading seen when testing the spandex used in previous suit prototypes. The reduction in force generation over 50 cycles was under 2 N. The stretch to 60% strain was chosen because that is the maximum strain recommended by the manufacturer. In actuality, the deign strain achieved by the narrow elastics while wearing the prototype suits ranged from 25-50% in the final design, so the reductions in force generation over multiple wearing cycles would be reduced. The rate of stretching during testing was selected to match previous testing, based on the limitations of the tensile testing machine. The rate of stretching during running would be an order of magnitude faster than the testing speed, over 100 mm/second, based on calculations using the GLCS model. It is possible that velocity and magnitude of stretching during locomotion will wear out the force generation of the narrow elastics more quickly over the joint loading stages in the suit than was demonstrated in this cycle testing. However, despite its limitations, this testing was able to provide intuition into the durability of the narrow elastics, relative to the previously used spandex loading material.

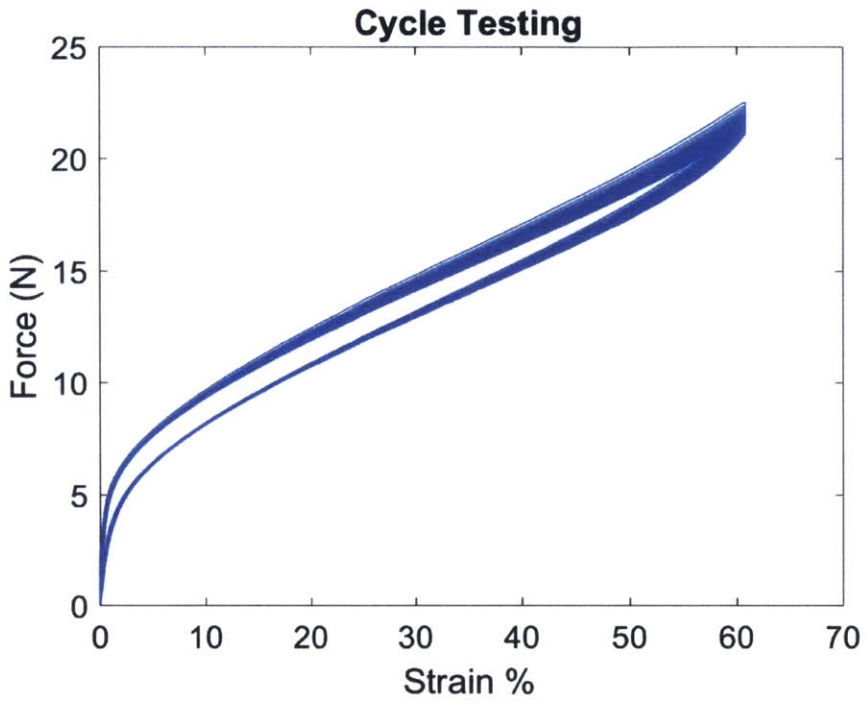

Figure 3-8: Force generation of narrow elastics over multiple loading cycles

3.1.2 New Loading Element Integration

When adding in these novel loading materials into the suit, consideration was given to how they would be integrated with the suit spandex. Initially, the designs for the new suit prototypes involved the loading being created by the spandex, narrow elastics, and resistive exercise bands working together. For each loading stage, the narrow elastics and resistive exercise bands would be attached to horizontal bands made of non-stretch nylon webbing, which would then be attached to the spandex. However, during the prototyping process, it was discovered that integrating the three different materials in this way was extremely difficult, and that the spandex often was unable to withstand the high loads being imposed on it by the other loading elements. Because of this, the decision was made to completely decouple the loading elements from the spandex. This resulted in the suit becoming two distinct pieces: a spandex skinsuit and a soft exoskeleton containing the loading elements. The skinsuit

provides an interface between the loading exoskeleton and the body, while the loading exoskeleton carries the heavy loads produced by the loading elements and transfers them to the subject.

3.1.3 Suit Anchoring

In past suit prototypes, the suit anchoring was provided by the horizontal fibers of the bidirectional Spandex weave. The circumferential tension of the material creates a normal force between the suit fabric and the subject's skin. This force creates a friction interaction between the suit and body that anchors the suit to the body at that point if the friction force is greater than the difference in force between the two loading stages. In all previous prototypes, the suit has been under-stretched in many areas, particularly the shank, which suggests that this anchoring was insufficient to hold the suit at the desired lengths, and was therefore under-loading the wearer. In order to increase the coefficient of friction between the subject and suit material, new materials were selected with input from soft goods manufacturing experts. For final suit construction, siliconized tape from Framis Italia was selected due to its elastic qualities, high coefficient of friction, and ease of application. One side of the tape is coated with silicon, which provides the increased friction, while the other side contains a heat activated adhesive for use in integrating the tape into the suit.

For integrating the loading exoskeleton to the skinsuit, 3M Dual $Lock^{TM}$ fasteners were selected. Dual Lock is similar in function to hook and loop fasteners, but has highly increased holding power over traditional hook and loop options.

3.1.4 Subject Comfort

Subject comfort is of paramount importance, as the suit needs to be tolerable to wear in various scenarios in order to be an effective countermeasure. In previous iterations of the suit, comfort issues arose around the shoulder yoke. Foam padding was added under the shoulder straps of the loading exoskeleton to disperse the load over the shoulder, and anchoring stages were added to the torso to decrease the load at the shoulder. The ankle stirrups were designed to be worn over shoes to disperse the load over the foot. The spandex bodysuit was implemented to act as an interface between the subjects and the loading exoskeleton and prevent any adverse interactions between the subject and loading exoskeleton, such as excessive rubbing.

3.2 Final Design and Construction

3.2.1 Final Design

Skinsuit: The skinsuit component of the suit was constructed using Spandura spandex fabric (Seattle Fabrics, Seattle, WA), which is a spandex fabric with nylon elements that help increase durability. The skinsuit is sized to be skin tight, offering some circumferential compression to the wearer. Siliconized tape was attached to the inside of the suit, to improve the suit-body interface. The tape runs in the head-to-toe direction, and was placed in areas where minimal skinsuit stretch is expected. This includes the torso, waist, mid-thigh, and shank. Areas such as the hip and knee are avoided, as there will be more movement of the fabric at those points due to joint movement. On the exterior of the suit, Dual Lock strips are attached in a similar manner, in order to provide attachment points for the loading exoskeleton.

Loading Exoskeleton: The loading exoskeleton is comprised of narrow elastics and resistive exercise bands in a skeleton of non-stretch nylon webbing. Previous suit prototypes were designed to have a loading stage every two centimeters, which theoretically resulted in over 50 stages of loading. In actuality, due to inadequacies in suit anchoring, the suits were most likely single-stage loading garments. In order to decrease construction complexity, as well as allow enough length for the loading stages to stretch and provide the required loading, the number of loading stages has been reduced. The exoskeleton has five total loading stages: a torso loading stage, and then stages over the hips, thigh, knee, and shank. This number of stages allowed for graded loading between the shoulders and feet, while not having any stage transitions over the joints, which would impede movement in the suit. This number of stages also allowed adequate length for each loading stage to stretch and achieve the desired loading stage force. The loading stages were separated by circumferential bands of non-stretch nylon. Each of these circumferential bands were straps that could be loosened for donning and doffing, and then tightened to anchor the exoskeleton to the skinsuit, using Dual Lock velcro to secure the straps in place. Dual Lock strips were attached to the side of the anchor strap facing the skinsuit, so that it would fasten to the equivalent Dual Lock strips on the skinsuit. An illustration of the circumferential strap can be seen in figure 3-9.

In order to provide the necessary loading, the loading stages contain a combination of narrow elastic and resistive exercise bands. For the four stages covering the legs (hips, thigh, knee, shank), the loading elements were grouped at the front and back of the leg to provide symmetrical loading. Each of these groups consisted of a resistive exercise band at the center, with groups of narrow elastic bands to either side. The number of narrow elastic bands varied by subject, based on their individual loading needs. On the three torso stages, the loading was provided solely by narrow elastic bands, as the narrow elastics were sufficient to fulfill the loading requirements over the torso and are easier to integrate into the suit than the resistive exercise bands. Stretch arrestor ribbons were included in this design, as in previous prototypes, to

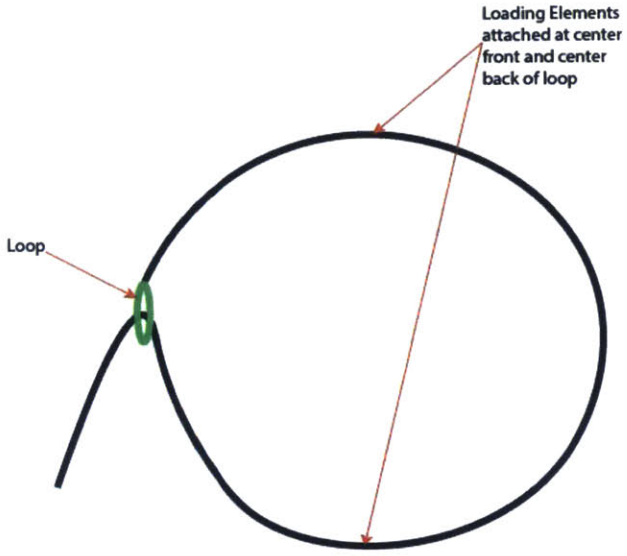

Figure 3-9: Top view of circumferential loading band

ensure that the suit does not overstretch. Over the shank and thigh stages, the ribbons were non-stretch nylon webbing, while over the knee and hip stages they consisted of narrow elastics. This was to allow additional stretch at the joints so as to not impede subject movement, while still providing a restoring force to ensure accurate suit stretch. Shoulder straps and ankle stirrups consisting of non-stretch nylon webbing were implemented to transfer the load to the subject's body. Foam padding was added under the shoulder straps to improve subject comfort. A diagram of the final suit design can be seen in figure 3-10.

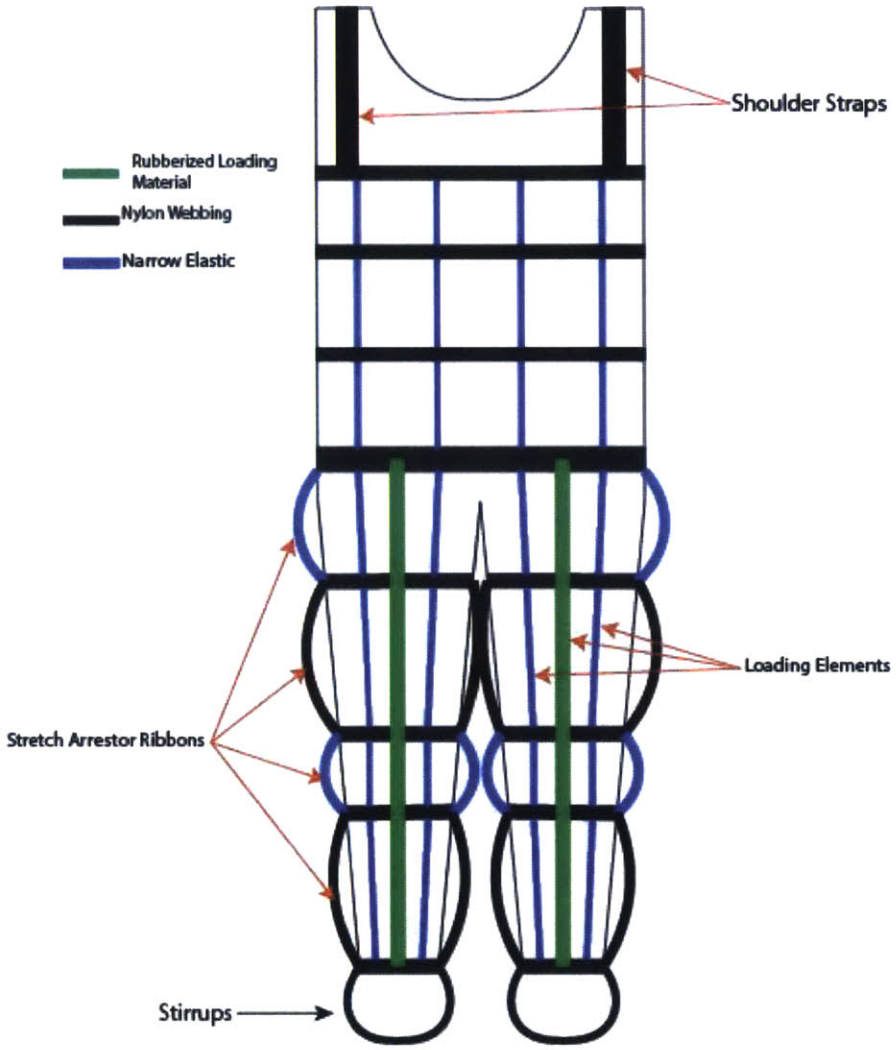

Figure 3-10: Final GLCS prototype design

3.2.2 Subject Measurements

In order to construct prototype suits, accurate measurements must be taken for each individual subject, to properly size the suits to ensure accurate loading and suit fit. For the previous suit prototypes, the measurements were taken by hand, using a standard tailoring measuring tape. Circumferential measurements were taken every two centimeters along the head to toe axis, along with other measurements between body landmarks. A representation of some example measurements are shown in figure

3-11.

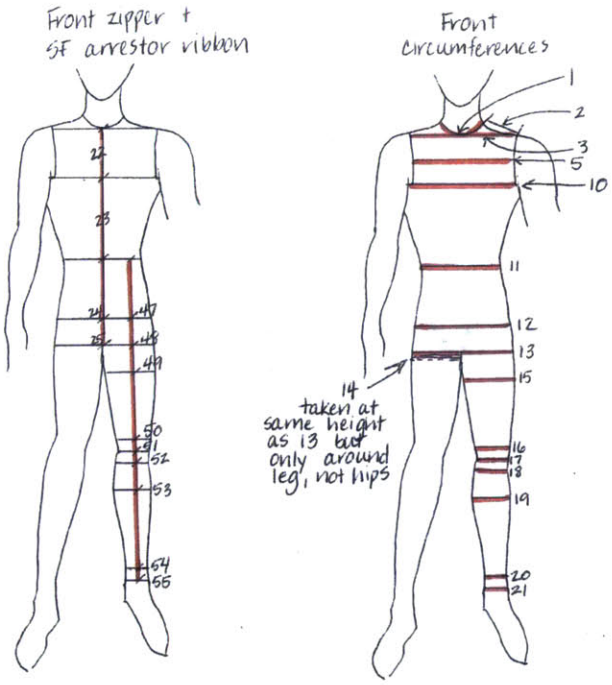

Figure 3-11: Hand measurements taken for GLCS construction

These measurements were converted to patterns used to size the spandex to provide the correct vertical and circumferential loading to each individual subject, based on the material properties of the spandex loading material used in the prototype. This system of body measurement was time-consuming, and introduced many opportunities for human error in producing inaccurate measurements, which could lead to inaccuracies in suit construction. In order to eliminate this source of error, a new sizing procedure was implemented to produce new prototypes suits. First, 3D body scans were taken for all subjects at the Natick Soldier Research Development and Engineering Center (NSRDEC, Natick, MA). These scans were then loaded into proprietary software developed at NSRDEC, called NatickMSR. This software has the ability to produce measurements based on the body scans. Circumferential measurements were taken at different landmarks along the vertical axis of the body, and the vertical distance between the landmarks was measured. A screenshot of a subject body scan in the NatickMSR software program can be seen in figure 3-12 with some

key measurements highlighted. The landmarks for the measurements taken for each subject, from head to toe, are: chest, waist, thickest part of the hips, upper thigh at the crotch, center knee, thickest part of the calf, and ankle. These measurements were used to size the suits for each individual subject, which is described in the next section.

Figure 3-12: NatickMSR software with subject body scan and measurements

3.2.3 Suit Sizing

Once the subject body measurements had been collected, the sizing of various suit elements could be determined. The stretched lengths of the loading stages, L_S, were determined using specific landmarks. The loading stages and their upper and lower landmarks are outlined in table 3.1.

The loading stages can be seen labeled on the final suit design in figure 3-13

Table 3.1: GLCS loading stages

Loading Stage	Upper Boundary	Lower Boundary
Torso	Chest	Waist
Hip	Waist	5 cm below Crotch
Thigh	5 cm below Crotch	10 cm above Center Knee
Knee	10 cm above Center Knee	Thickest part of the Calf
Shank	Thickest part of the Calf	Ankle

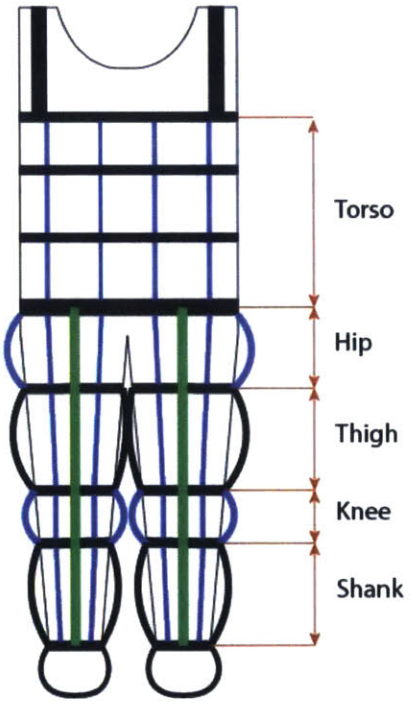

Figure 3-13: Final suit design with loading stages

Once the stretched lengths of the loading stages were determined from subject measurements, the resting lengths, L_o, of the loading stages could be computed. A representation of these lengths is shown in figure 3-14.

The first step in this process was to calculate the necessary force to be provided by each loading stage, F_S. Similar to how the suit spring parameters were calculated for the model in chapter 2, each loading stage was required to provide loading equal to the weight of the superior body segments, plus the weight of the segment encompassed by the loading stage. F_S was determined for each of the different loading stages for all subjects based on their individual anthropometry, and using the previously described

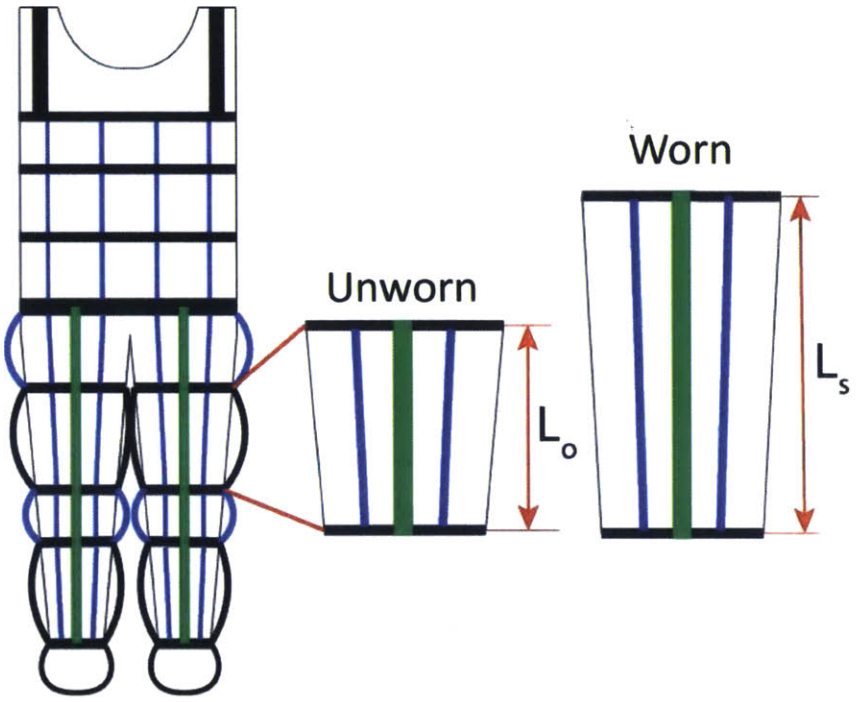

Figure 3-14: Representation of unworn and stretched loading segment

body segment mass data and assuming uniform density across each segment.

$$F_S = \text{(weight of superior body segments)} + \text{(weight of loading stage body)} \quad (3.1)$$

The resting length, L_o, of the loading stage is set so that when the loading stage is stretched and reaches its stretched length L_S, it provides force equal to F_S. To achieve F_S, the suit gets loading contributions from the narrow elastics (F_{NE}) and resistive exercise bands (F_R) contained in the loading stage.

$$F_s = F_{NE} + F_R \quad (3.2)$$

The loading contributions from the narrow elastics and resistive exercise bands are calculated using the following equations,

$$F_{NE} = k_{NE}\left(\frac{L_S - L_o}{L_o}\right) \tag{3.3}$$

$$F_R = k_R\left(\frac{L_S - L_o}{L_o}\right) \tag{3.4}$$

where k is the stiffness coefficient from the force-length relationships for the loading elements determined during tensile testing. Using these equations and the known variables, L_o was calculated for each suit loading stage for all subjects and used to size the suits for construction.

3.3 Suit Construction

In order to determine GLCS loading characteristics and its potential for efficacy in mitigating physiological deconditioning during long duration spaceflight, four suits were constructed by Heidi Woelfle and other students in the Wearable Technology Laboratory at the University of Minnesota for characterization and testing. The suits were constructed for four subjects, all fit, male graduate students in the Man-Vehicle Laboratory at MIT who were familiar with the GLCS project. These subjects were selected for their ability to complete all testing procedures. Subject characteristics are outlined in table 3.2

Table 3.2: GLCS suit testing subject characteristics

Subject	Age	Height (in)	Weight (lbs)
1	24	68.5	160
2	25	68	158
3	25	66	145
4	28	72	190

The subjects and suit underwent testing in two separate analogs of unloading. The first test, performed at MIT, was a 4 hour bed rest test to determine suit loading characteristics, as well as the suits effects on spinal elongation and long term comfort.

The second test, performed at NASA Glenn Research Center, involved the subjects exercising on a vertical treadmill to ascertain the suits effects on joint and muscle forces while exercising. The testing protocols for these tests were approved by both the NASA Institutional Review Board (IRB), as well as the MIT Committee on the Use of Humans as Experimental Subjects (COUHES). All subjects provided written consent to participate in the studies. The detailed study protocol, as well as the results of the tests, are presented in chapter 4.

Chapter 4

Suit Testing

After prototype suits were constructed, they were tested in analogs of unloading to determine their loading characteristics, wearability, and effects on the body during bed rest and exercise. This chapter describes the testing protocols carried out at MIT and NASA Glenn Research Center, and the results of the suit testing. Along with characterizing suit loading, the main research questions we wanted to answer during testing were:

1. How does the suit affect spinal elongation during unloading?
2. How does the suit affect the physiological cost of exercise?
3. How does the suit affect gait during exercise?
4. How does the suit affect joint and muscle loading during exercise?

4.1 Bed Rest Study

In order to characterize the suit's loading capabilities in a simulated unloading environment, as well as measure the suits' effects on spinal elongation during unloading,

a bed rest study was conducted at MIT.

4.1.1 Testing Protocol and Data Collection

Subjects participated in two sessions of supine rest for a period of four hours each, one session unsuited, the other while wearing the GLCS. The test sessions were completed on consecutive days, and testing began at the same time each day, to offset any effects caused by normal diurnal fluctuations in height. The order of testing either suited or unsuited was counterbalanced, and the order of testing for all subjects can be seen in table 4.1.

Table 4.1: Testing order for spinal elongation study

Subject	Test Session 1	Test Session 2
1	Suited	Unsuited
2	Unsuited	Suited
3	Unsuited	Suited
4	Suited	Unsuited

During the suited session of the bed rest study, suit characterization testing was performed to determine the loads the suit imposes on the body during unloading, and the accuracy of suit construction and suit stretch while the suit is being worn.

Suit Loading Characterization

Suit loading characteristics were measured using the Novel Pliance measurement system (novel inc., Munich, Germany), which uses state of the art capacitive sensors to measure pressure distributions and force production. For suit testing, two different sensors were used: pressure sensing insoles to measure foot forces, and a mat sensor to measure forces over the shoulder. The Pliance system can be seen in figure 4-1.

Before putting on the suit, subjects stood on the insole sensors to take a bodyweight

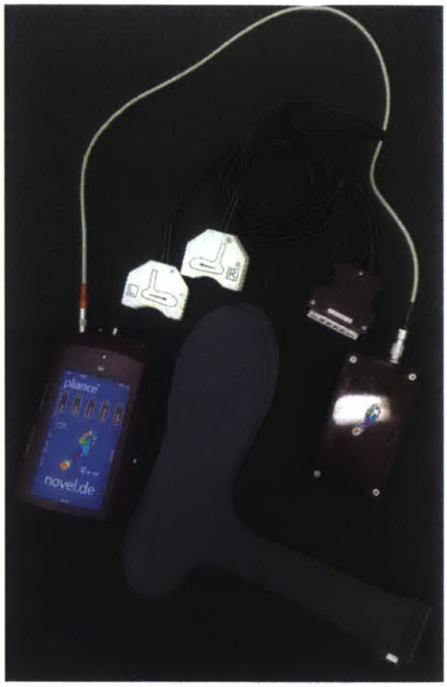

Figure 4-1: Novel Pliance system with pressure sensing insoles

reading for later comparison with suit loading readings. Suit loading was measured while the subject was lying supine. The insoles were placed in the subjects shoes, over which the suit stirrups were placed. To measure the suit loads at the shoulder, the mat sensor was placed between the shoulder straps and padding, and the subject's right shoulder. An additional reading of the suit loading at the feet was taken at the completion of the bed rest study to assess how suit loading changes over time.

Suit Stretch Characterization

Due to the stiffness characteristics of the loading elements used in the suit design, small inaccuracies in suit construction and suit stretch can lead to significant changes in the loading provided by the suit. In order to accurately measure the lengths of suit loading segments, the Vicon Motion Capture System (Vicon Motion Systems Ltd, United Kingdom) in the Man-Vehicle lab was utilized. This system uses cameras to track the 3D coordinates of reflective markers. One reflective marker was placed at the

center of each circumferential band separating the suit loading segments. Measurement readings were taken of the loading segment lengths while the suit was unworn, and then again while the subject was wearing the suit in a supine position. Stretched and resting lengths were determined by calculating the distance between the reflective markers. The unworn suit with markers can be seen in figure 4-2.

Figure 4-2: GLCS with markers to measure loading segment lengths

Spinal elongation testing

Subject height measurements were taken during both test sessions to determine the suit's effects on spinal elongation. Before starting the bed rest portion of the test, the subject's standing height was measured using the Vicon motion capture system and reflective markers placed on the floor and the top of their head. They then laid down on an air mattress and an initial supine height measurement was taken using markers placed on the head and soles of the feet. Supine height measurements were then taken every 15 minutes until the end of the test. For each supine height measurement, subjects were instructed to maintain the same pose for each measurement, to reduce uncertainty between measurements. The subjects then had their standing height taken immediately upon completion of the supine portion of the test.

The bed rest test also functioned as a long-term comfort and wearability test. The subjects filled out subjective comfort surveys every 15 minutes during the test, immediately following the supine height measurements. The form used in the test can be seen in Appendix A. This scale was previously used by Waldie and Newman in their initial suit tests [78].

4.1.2 Suit Loading Characterization Results

Suit loading results at the feet, both the initial reading and after the extended wear test, are presented in figure 4-3 as the percent of total bodyweight loading achieved.

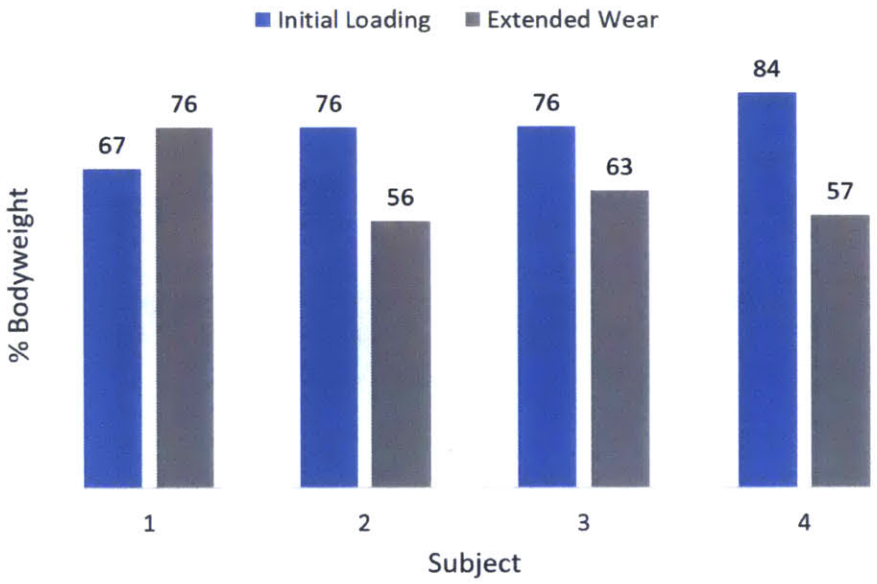

Figure 4-3: GLCS foot loading

Initial loading produced by the suit ranged from 67-84% of subject bodyweight. While this total did not achieve our goal of 100% bodyweight loading at the feet, this level of loading greatly exceeded any of the loads achieved by previous iterations of the GLCS. At the end of the bed rest test, this value had decreased for 3 of 4 subjects. The loading that subject 1 experienced increased after extended wear, but this was

most likely due to the loading measurement procedures. At the end of the extended wear test, the subject's stirrups were removed from the feet in order to place the Novel insoles inside their shoes. The stirrups were then reattached and the suit was re-tightened. The loading discrepancy was most likely caused by the fact that Subject 1's suit was not fully tightened before his initial loading, and was tightened further before the final loading measurement.

Additional analysis was performed to determine the load distribution over the sole of the foot. For the standing bodyweight measurement, as well as the suited measurement, the percentage of the total foot load carried by the front half and back half of the foot was calculated using Novel software. The results for the percentage of total foot load carried on the rear of the foot for both the bodyweight standing and suited measurements are shown in figure 4-4.

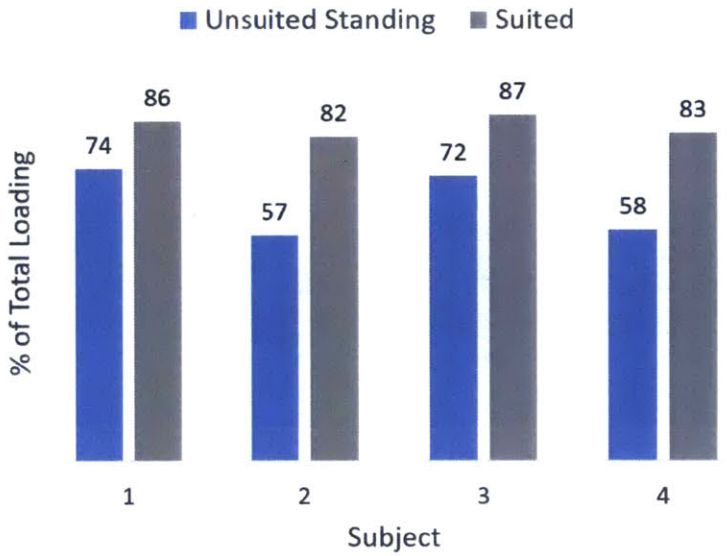

Figure 4-4: GLCS foot loading distribution

The loading distribution over the sole of the foot was different between the standing bodyweight reading and suited cases. In the standing case the load on the rear of the foot ranged from 56-73% of the total load. In the suited case, the load was distributed much more towards the back of the foot, with about 82-87% of the total load on the

back of the foot. This shows that the load was not being properly distributed over the sole of the foot by the stirrup sitting over the subject's shoes.

Loading measurements were also taken at the shoulder. These measured loads are presented in figure 4-5, and are compared to expected loads calculated from suit design parameters. For 3 of 4 subjects, the measured loads at the shoulder were significantly higher than design loads.

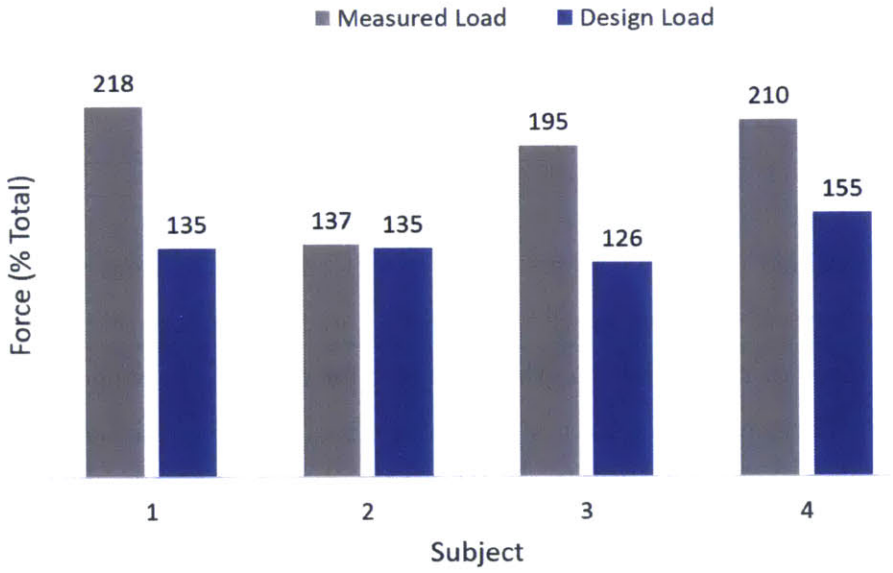

Figure 4-5: GLCS shoulder loading

In order to gain more insight into suit load production, and specifically why there was under-loading at the feet and overloading at the shoulders, the suit loading stage resting and stretched lengths were determined.

4.1.3 Suit Stretch Characterization Results

For each subject, measurements were taken of the suit segment lengths both when the suit was unworn and unstretched, and again while the subject was wearing the suit, and these values were compared to design values. Table 4.2 outlines the differ-

ences between the design values and actual values in the unstretched suit. Positive differences indicate that the segment was longer than designed, while negative differences show that the actual length was shorter than design length. Total error for each subject, as well as the average of the absolute value of the errors for each stage are also given.

Table 4.2: Suit loading segment resting length errors

	Subject				
Segment	1 (mm)	2 (mm)	3 (mm)	4 (mm)	Average (Absolute) Segment Error (mm)
Torso	-8.72	6.63	-6.16	1.73	5.81
Hip	-1.89	6.23	3.24	2.73	3.52
Thigh	-6.27	15.25	-5.44	-5.36	8.08
Knee	0.41	-2.63	-0.38	-4.63	2.01
Shank	-4.67	-13.21	-1.34	-6.74	6.49
Total Error	-21.14	12.27	-10.07	-12.27	

The errors outlined in table 4.2 were errors in suit construction, and were generally small. Only two segments among all the subjects had construction errors greater than 1 cm. The error in the overall length of the suit for all subjects ranged between 10 and 21 mm. There were no patterns of greater errors in any given loading segment. Overall, the suits were constructed very accurately, based on design specifications.

Similarly, the measured suit loading stage stretched lengths as a percentage of their resting length are presented in table 4.3, alongside the design stretch length percentages.

Table 4.3: Suit loading segment stretched lengths as a percent of loading stage resting length. Cells highlighted red indicate a segment that is overstretched, while cells highlighted yellow indicate a segment that is under-stretched

	Subject							
	1		2		3		4	
Loading Stage	Design	Measured	Design	Measured	Design	Measured	Design	Measured
Torso	45	70	45	48	40	79	40	—
Hip	45	31	40	33	40	28	50	50
Thigh	40	24	35	19	50	42	45	55
Knee	45	30	45	39	55	33	50	39
Shank	50	14	50	13	60	—	60	33

For all subjects for which the measurements were available, there was over-stretching of the torso loading stage. Subject 2 had minimal over-stretching, while subjects 1

and 3 had suits that exhibited significantly higher levels of stretch than the design stretch. This is the consistent with the high levels of loading measured at the shoulder for subjects 1 and 3, which greatly exceeded the design force. For the leg loading segments, almost all of the segments for each subject exhibited under-stretching, with the lone exception of Subject 4's thigh segment. This is consistent with the measurements of loading at the feet, which found that the suits did not provide full 100% bodyweight loading to the subjects. These errors in the suit stretch were most likely a result of a failure in the suit anchoring system. The Dual Lock strips on the bodysuit were not attached strongly enough to the Spandura, and were breaking off as the subject wore the suit. This meant there were not sufficient attachment points for the loading exoskeleton, which resulted in suit slip.

In order to test the hypothesis that suit slip contributed to the errors in suit stretch and loading that occurred for all subjects, analyses were conducted to relate the suit loading to the measured suit stretch. For the loading stages covering the leg, all loading segments (Hip, Thigh, Knee, and Shank) were considered to be a single loading stage covering the leg, without any anchoring points. The predicted loading level was calculated using equations 3.1-3.4, based on the total measured stretch of the leg loading segments and the material properties of the loading elements over the leg. This predicted loading was compared to actual suit loading at the foot for all subjects for which these loading segment length measurements were available. The results of this analysis are shown in table 4.4.

Table 4.4: Leg loading stage slip analysis

Subject	Predicted Foot Force	Measured Foot Force (N)	% Predicted
1	217.14	225.87	104.02
2	236.24	268.94	113.84
4	341.00	353.76	103.74

As seen in the table, the actual measured foot loading matches the predicted values of foot loading if the suit was behaving as a single loading stage garment over the leg.

A similar analysis was run on the shoulder loads. Again, predicted shoulder loading

was calculated based on the measured suit stretch and the material properties of the suit loading elements on the torso, and compared to the measured load. The results of this analysis are presented in table 4.5.

Table 4.5: Hip loading stage slip analysis

Subject	Predicted Shoulder Force	Measured Shoulder Force (N)	% Predicted
1	180.50	218.00	120.78
2	140.10	137.00	97.79
3	196.50	195.00	99.24

For two of the three subjects, the measured loads closely matched the predicted loads, while for subject 1, the measured load was higher than predicted, possibly due to insufficient padding over the shoulder. From the analysis of suit stretch, it has been shown that the suit was acting as a two-stage loading garment, with one loading stage over the torso, and the other over the lower body. This failure in creating graded loading on the body resulted in under-loading at the feet, with most of the load distributed on the back of the foot, and overloading at the shoulders. The suit loading characteristics had negative consequences on subject comfort while wearing the suit for an extended period of time.

4.1.4 Subjective Comfort During Long Term Wear

Subject comfort was also measured using subjective scales that the subjects filled out every 15 minutes during the trial. Two of the subjects were unable to complete the entire suited testing session due to discomfort brought on by wearing the suit. Subject 1 completed 2.5 hours of the 4 hour test, and subject 2 completed 2.75 hours out of 4. Subjects 3 and 4 were able to complete the entire 4 hours. The time course of subjective comfort is shown in figure 4-6, with the scale the subjects used to rate their discomfort level.

At the beginning of the test, the subjects felt they could wear the suit for 4-8 hours,

Rating	Discomfort
1	Nude Comfort
2	Pyjamas, casual clothes
3	Formal Attire
4	Minor discomfort if worn all day (16 hrs)
5	Too uncomfortable to wear all day
6	Too uncomfortable for 8 h
7	Too uncomfrtable for 4 h
8	Too uncomfortable for 2 h
9	Too uncomfortable for 1 h
10	Too uncomfortable for 10 min

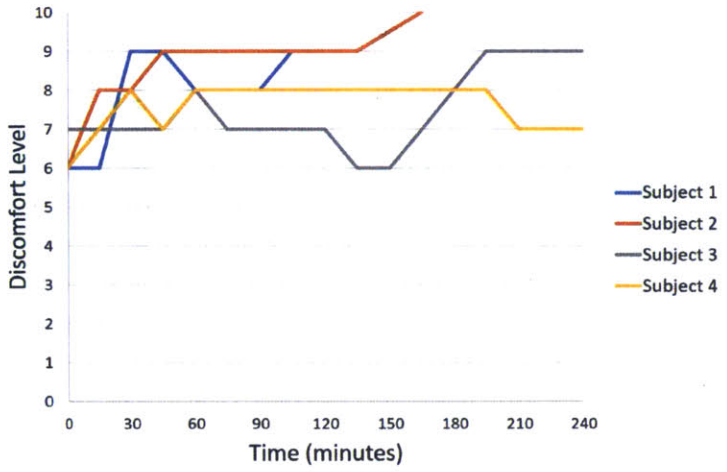

Figure 4-6: Subjective discomfort over long term wear

but that estimate quickly dropped as the tests went on. The main sources of subject discomfort were their feet and shoulders, at the points of load transference. This feedback was consistent with the loading profile measured for each subject, as the subjects experienced higher than expected loads at the shoulders, and concentrated loads to their feet.

4.1.5 Spinal Elongation Study Results

To test the suit's effects on spinal elongation, height measurements were taken at 15 minute intervals over 4 hours of supine rest, in both suited and unsuited conditions. The height measurements for each subject can be seen in figure 4-7. The height measurements were normalized by subtracting the initial supine height measurement, to track the changes in height over the period of unloading.

From these measurements, no clear trend emerges for all subjects. There was high interpersonal differences in the data, and the height measurement data was noisy, which makes any strong conclusions difficult to defend based on the data. The noise in the data was most likely due to inconsistencies in subject posture during the supine

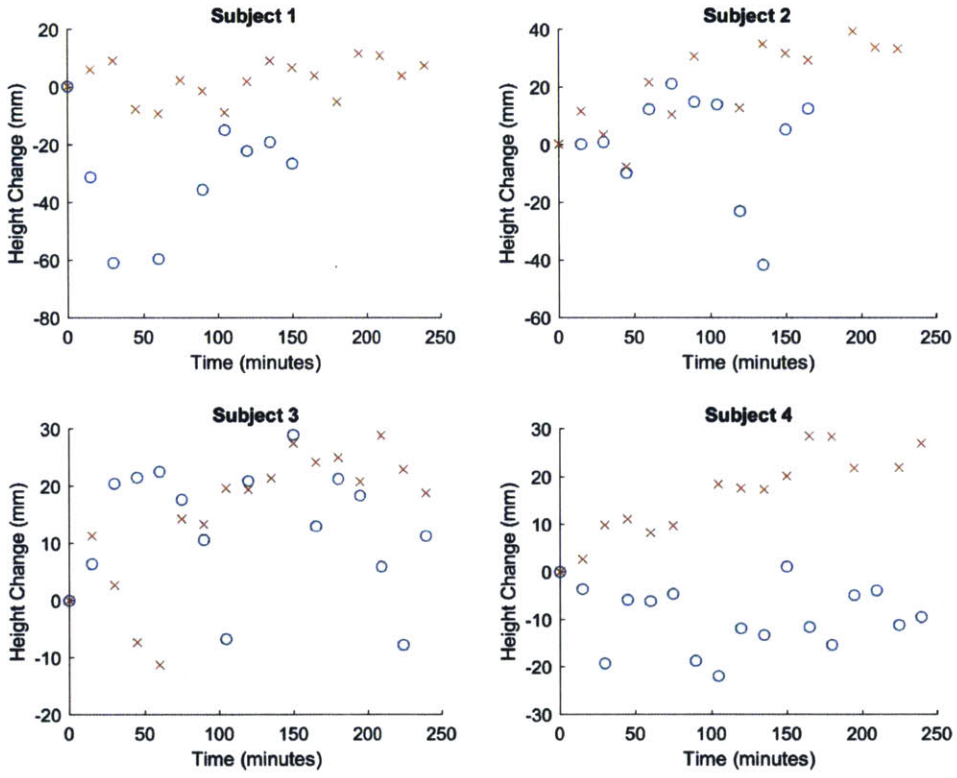

Figure 4-7: Subject height during bed rest ('x' are unsuited measurements and 'o' are suited measurements)

height measurements. While the subjects were instructed to maintain a consistent pose for each measurement, small changes in posture could contribute to changes in the height measurement. These height changes due to postural inconsistencies may have been large enough to mask any actual changes in height due to spinal elongation.

4.2 Vertical Treadmill Testing

4.2.1 Testing Protocol

In order to assess the how the suit affects exercise and integrates with existing countermeasures used by astronauts, subjects performed testing on the enhanced Zero-Gravity Locomotion simulator (eZLS) at NASA Glenn Research Center. The eZLS consists of a treadmill oriented vertically, and a suspension system that suspends the subject in a supine position to simulate the microgravity exercise environment in space. The eZLS loads the subject using a pneumatic Subject Load Device (SLD). The SLD system uses a single pneumatic cylinder to provide nearly constant force through cables that attach to the subject's harness. This force pulls the subjects onto the treadmill, allowing them to run, and can be set to produce a variety of different forces.

The eZLS, with a subject suspended, can be seen in figure 4-8

Subjects performed two exercise trials: one while wearing the GLCS, the other unsuited. During the unsuited trial, the subjects still wore the spandex bodysuit. Subjects were loaded to 75% bodyweight using the eZLS harness system and pneumatic SLD. This loading level was chosen on the advice of the expert operators at NASA Glenn Research Center, as 75% loading had anecdotally produced the most natural locomotion in tests subjects. Each trial included: subject suspension, warm-up, exercise, cool-down and subject dismounting:

- Suspension consisted of donning the harness, a helmet, and eight limb supports (two on each limb), followed by lying in a supine position on a suspension cradle, being raised by an overhead lift system and being suspended by limb supports to suspension cables.

Figure 4-8: eZLS and suspended subject

- Warm-up consisted of 3 minutes of walking at 3 miles per hour.
- Exercise consisted of 3 minutes of jogging at 5 miles per hour
- Cool-down consisted of 3 minutes of walking at 3mph.
- Dismounting consists of lowering and disconnecting the subject from the subject supports system and removing all the harness and limb supports.

For three of the four subjects, both suited and unsuited trials occurred over the course of approximately three hours, with a minimum of 45 minutes separating the two trials. For subject 1, however, difficulties in setting up equipment and various equipment malfunctions caused him to be suspended for 2 full hours before his first trial began.

4.2.2 Data Collection

During each trial, a variety of data was collected:

Motion Capture: A 12 camera Smart-D system [BTS Bioengineering, Milan, IT] collected the motion capture data at 100 Hz. The motion capture system tracked the x, y, and z position of reflective markers approximately 10 mm in diameter and placed at key anatomical sites on the subject. Desired marker placements are shown in figure 4-9.

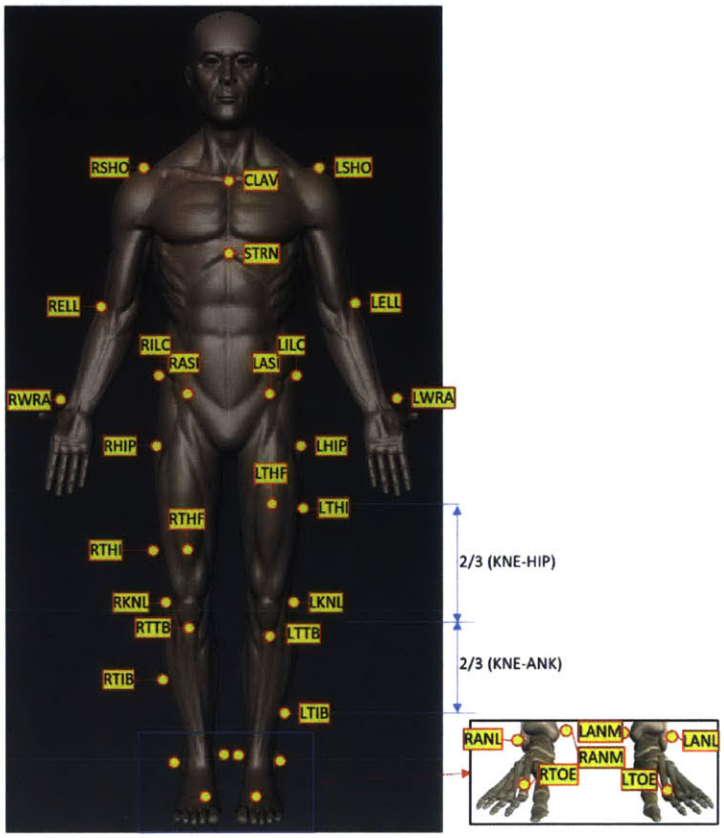

Figure 4-9: Motion capture marker placements

Due to the wearing of the eZLS harnessing system, and the GLCS in the suited trial, it was not possible to place all of the markers on the subjects exactly as shown in figure 4-9. The marker set was adapted for each individual subject to optimize the

capture of subject kinematics during exercise. An image of one subject with markers placed on the body can be seen in figure 4-10.

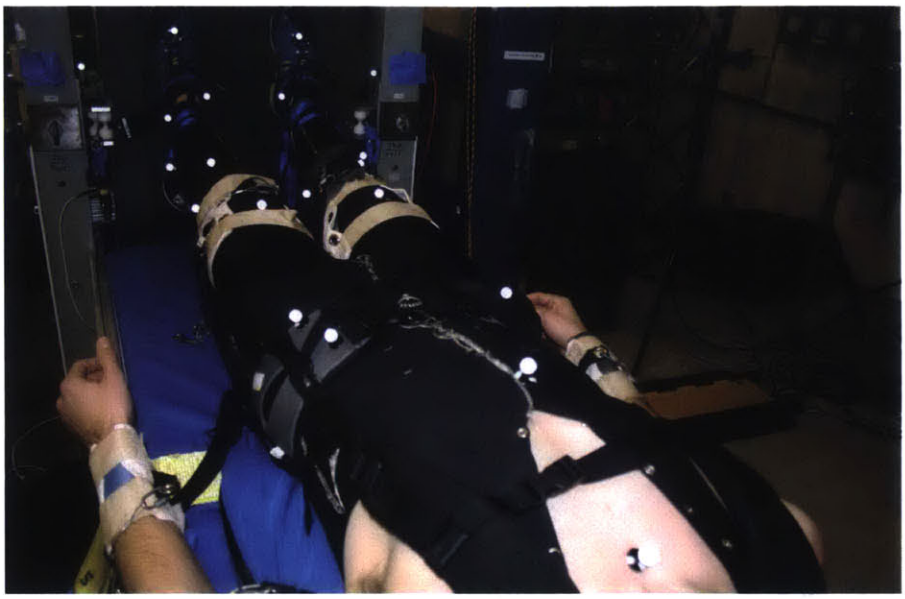

Figure 4-10: Suit testing subject with marker placements

Prior to data collection the cameras were calibrated with an activity volume encompassing the subject and device according to the manufacturer's specifications and procedures. Post-processing of the motion history data was performed using BTS Smart Track software, which removed erroneous marker trajectories and any false light reflections in the room that mimicked markers.

Ground reaction forces: Ground reaction forces (GRF) were measured at 100 Hz using two 40x60cm quartz crystal piezoelectric force plates [Model 9261, Kistler Instruments AG]. A Labview interface program synchronized the GRF data with the motion history data.

Treadmill speed and Heart rate data: The Labview interface also measured the treadmill speed, in order to verify that the trials were conducted accurately. A Zephyr HxM Bluetooth Wireless Heart Rate Sensor [Medtronic, Minneapolis, MN] transmitted heart rate data. Heart rates above 85% of age-predicted maximum heart rate would result in immediate test termination.

Foot Force Data: Foot force data was also collected using the Novel Pliance system with pressure sensing insoles to capture the suit contributions to loading.

Prior to subject suspension they would don the harness system, lay down in the suspension cradle, and reflective markers were placed on the body in areas that would be visible to the motion capture cameras. They were then suspended and attached to the eZLS loading system. This process would take anywhere from 30-45 minutes. Once they were suspended, subjects were given a brief period of time to acquaint themselves with all aspects of the system, and were able to walk and run for a short period to acclimate themselves to moving in this novel environment. After this learning period, the trial would begin. As in the bed rest study, the order of either wearing the suit first or going unsuited first was counterbalanced between the subjects. The subject ordering can be seen in table 4.6.

Table 4.6: Testing order for vertical treamill testing

Subject	Test Session 1	Test Session 2
1	Unsuited	Suited
2	Unsuited	Suited
3	Suited	Unsuited
4	Suited	Unsuited

After completion of the testing on the eZLS, reflective markers were again placed on the subjects at various key landmarks, and motion capture data was collected while they stood in a static, standing pose. This pose was taken for use in OpenSim, to scale the musculoskeletal models in order to perform inverse kinematics and dynamics analyses using the motion capture and ground reaction force data from the exercise trials. An example of a subject in the static standing pose can be seen in figure 4-11.

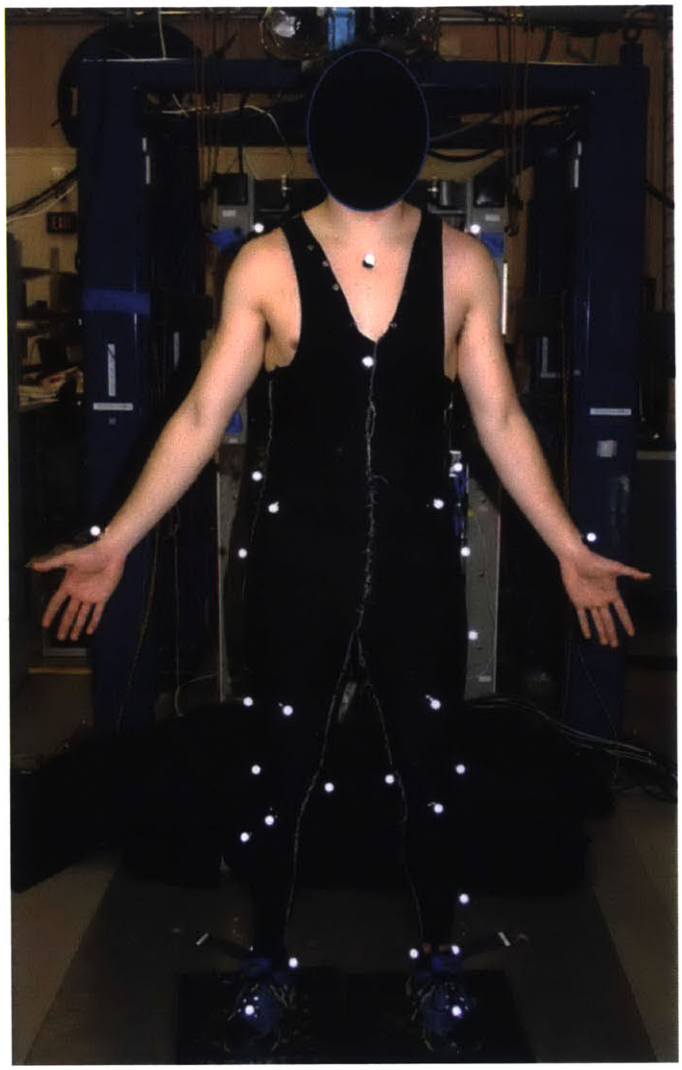

Figure 4-11: Marker placement on static pose

4.2.3 Data Analysis

Raw data from suit testing was analyzed using a combination of Matlab [Mathworks, Natick, MA] and Microsoft Excel [Microsoft, Redmond, WA]. All statistical analyses were performed in Systat [Systat Software, Inc]. Motion capture data were analyzed using OpenSim musculoskeletal modeling software. The dependent measures of interest were heart rate, subjective comfort and mobility, ground reaction forces during walking and running, and subject kinematics.

4.2.4 Vertical Treadmill Testing Results

Heart Rate Data

Heart rate data was taken to compare subject workload across the suited vs. unsuited and walking vs running conditions. The heart rate measurements across the total time spent walking and running can be seen for each subject in figures 4-12 and 4-13.

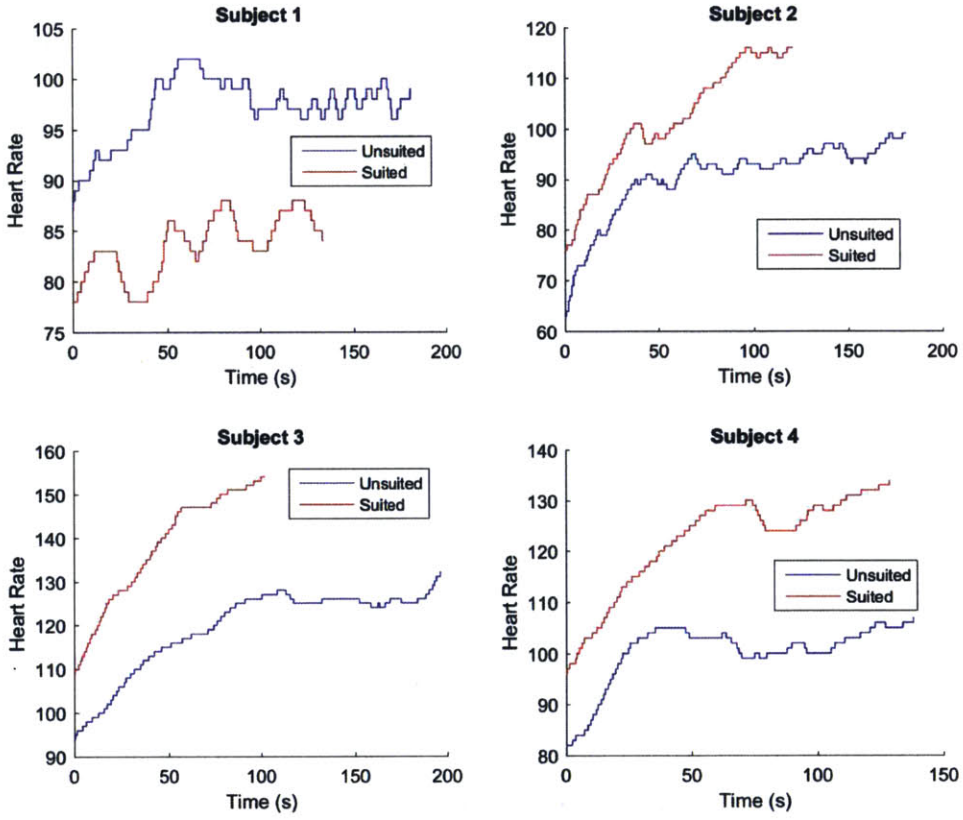

Figure 4-12: Subject heart rate during walking

For subjects 2, 3, and 4 the heart rate in the suited condition was higher for both walking and running than during unsuited testing. Subject 1 was the only subject who had a higher heart rate during the unsuited condition. This was most likely due to the testing circumstances for subject 1. During his initial unsuited testing period, various

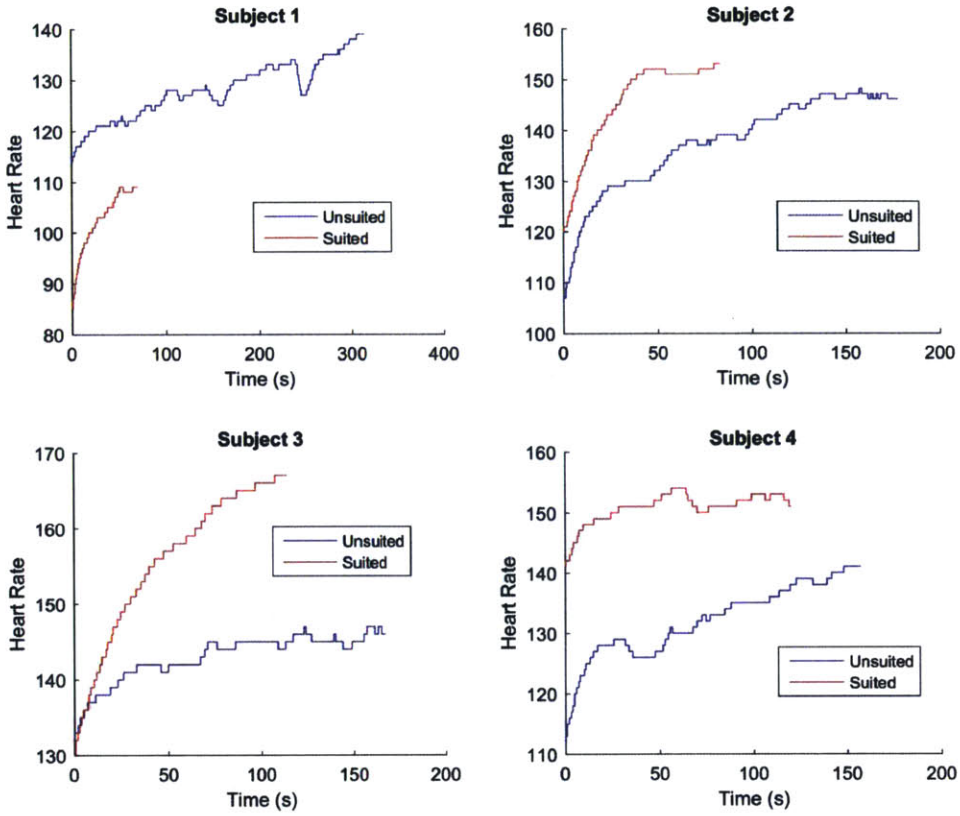

Figure 4-13: Subject heart rate during running

equipment malfunctions and testing aberrations led to subject 1 being suspended in the supine position for at least 2 hours before he began his successful unsuited test session. For the other subjects, the time spent supine before beginning testing ranged from 20-45 minutes. This extended period in the supine pose most likely altered the dynamics of subject 1's cardiovascular system, leading to the difference in results between subject 1 and the other subjects. All subjects gave subjective feedback that they felt more fatigued after the suited test session, which, coupled with the results of the heart rate data, show that the suits did increase the subjects' physiological workload during exercise on the eZLS.

Subjective Measures

Subjective data for discomfort and mobility hindrance ratings were taken immediately following both the suited and unsuited test sessions. The results of the subjective feedback are shown in figure 4-14.

Rating	Discomfort
1	Nude Comfort
2	Pyjamas, casual clothes
3	Formal Attire
4	Minor discomfort if worn all day (16 hrs)
5	Too uncomfortable to wear all day
6	Too uncomfortable for 8 h
7	Too uncomfrtable for 4 h
8	Too uncomfortable for 2 h
9	Too uncomfortable for 1 h
10	Too uncomfortable for 10 min

	Body Control (Mobility)
1	Unrestricted
2	Negligible deficiencies
3	Minimal compensation required
4	Minor but annoying deficiencies
5	Moderately objectionalbe deficiencies
6	Tolerable deficiencies
7	Maximum tolerable compensation required
8	Considerable compensation required
9	Intesnse compensation required
10	Body control lost

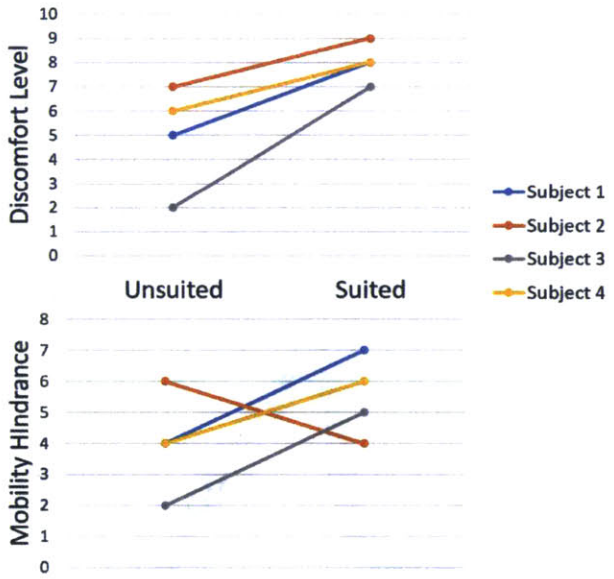

Figure 4-14: Subjective discomfort and mobility hindrance rating during treadmill testing

For all subjects, subjective discomfort increased for all subjects in the suited condition. However, for most subjects, their discomfort level during the unsuited test session was already elevated due to the eZLS harnessing and loading system. As both the suit and harness system were loading the subjects at their shoulders and hips, there was an additive effect of the suit and harness system in increasing subject discomfort.

Three of four subjects felt that wearing the suit led to a decrease in mobility, except for subject 2, who noted that he felt the suit stabilized his movements. None of the subjects felt that the moving while wearing the suit required drastic compensation.

Ground Reaction Force and Stride Time

Ground reaction forces during walking and running were collected for each subject, and the force profiles were analyzed to determine gait factors during suited and unsuited conditions. Data was analyzed for the second minute of locomotion in a particular condition, to allow the subjects to reach steady state, and eliminate any learning effects as the subjects became accustomed to moving in the novel environment of the eZLS. For each subject 100 steps were extracted for both suited and unsuited walking and running. For each of these steps, the force profile was normalized by subject bodyweight and stride time. Plots showing these extracted steps for both walking and running for one suited subject are shown in figure 4-15.

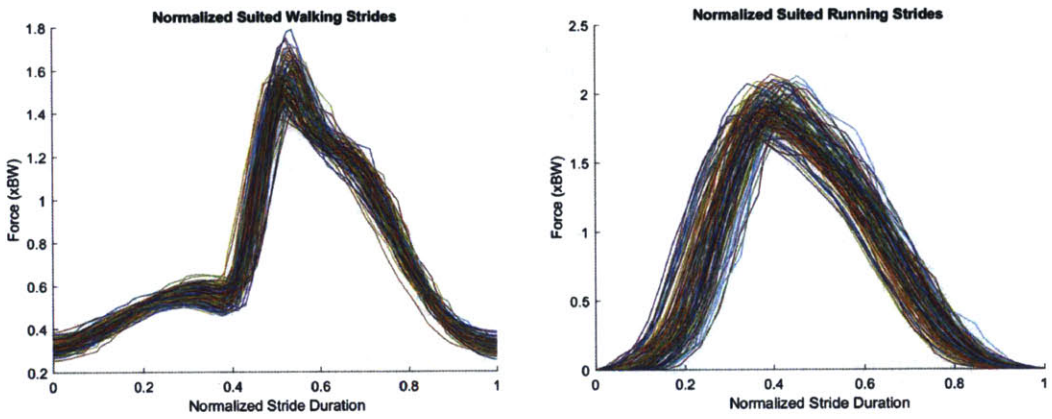

Figure 4-15: Normalized ground readction forces for one subject for (l) walking and (r) running

Using these normalized step force profiles, the average step force profile was calculated. For all subjects, the average force profiles of walking and running in the suited and unsuited conditions, with shaded regions representing the standard deviation of force during the step duration, are shown in figures 4-16 and 4-17. While the force profiles differed between subjects, the profiles were consistent within subjects, as evidenced by the narrow bands of the standard deviation. For all subjects these force profiles for walking and running were consistent with previously measured ground reaction force profiles [36]. During the 3mph treadmill phase, the GRF profile for

subject 3 did not exhibit the double peak force shown by the other subjects. This was because subject 3 was slowly jogging rather than walking, as his run-walk transition occurred at a lower speed than other subjects, due to his shorter leg length.

For most subjects, the force profiles for the suited an unsuited cases were similar, with slightly elevated maximum ground reaction forces in the suited condition during walking, and subject specific differences in max ground reaction force when suited while running, with some subjects exhibiting higher and some exhibiting lower max ground reaction forces. Apart from subject 4's walking ground reaction force profiles, the ground reaction forces during walking and running in the suited and unsuited conditions followed similar patterns, which suggests that the suit was not dramatically affecting how the subjects' feet impacted the ground while running and walking.

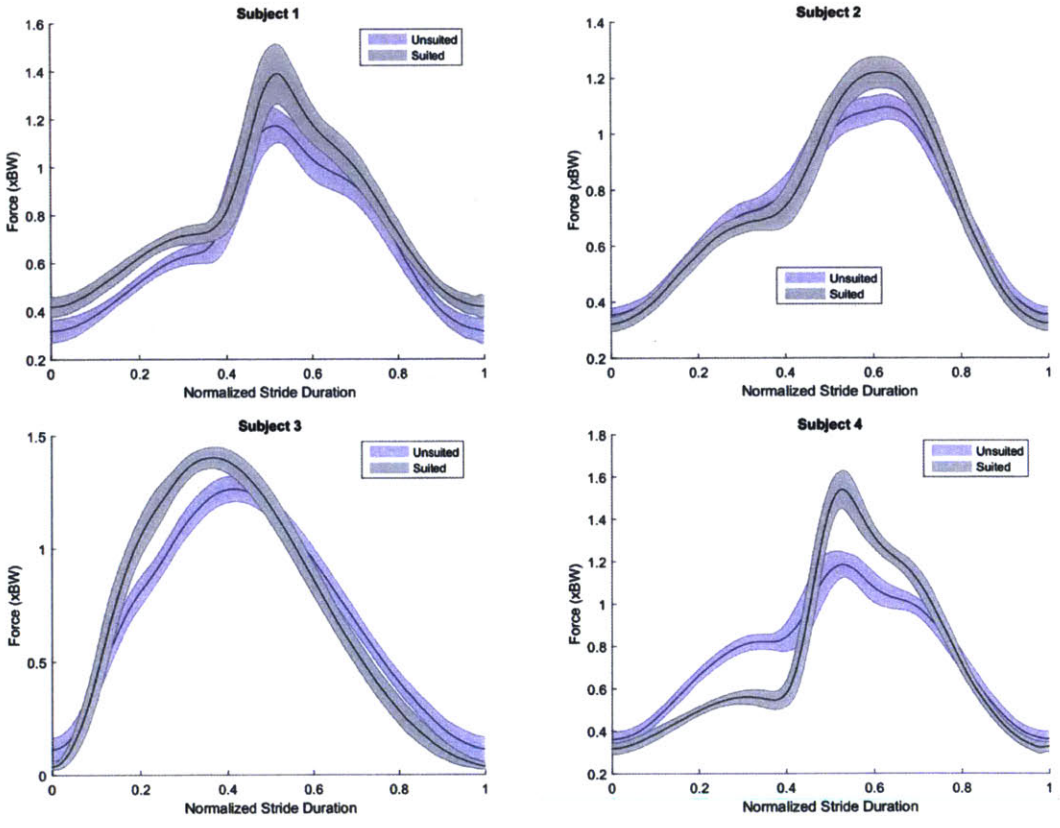

Figure 4-16: Average GRF profiles for all subjects for walking

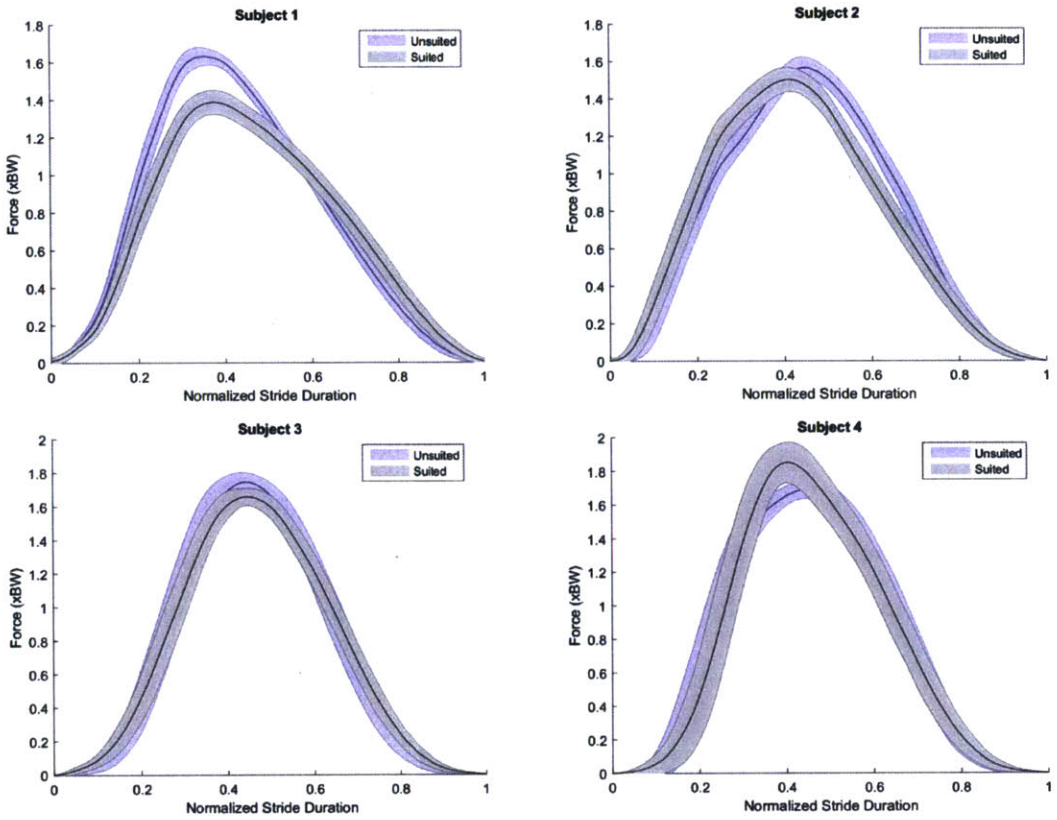

Figure 4-17: Average GRF profiles for all subjects for running

From the ground reaction force data, maximum force and step time data were extracted for each individual step. The mean and standard deviations of each variable for the different testing conditions are shown in the box plots in figures 4-18 and 4-19.

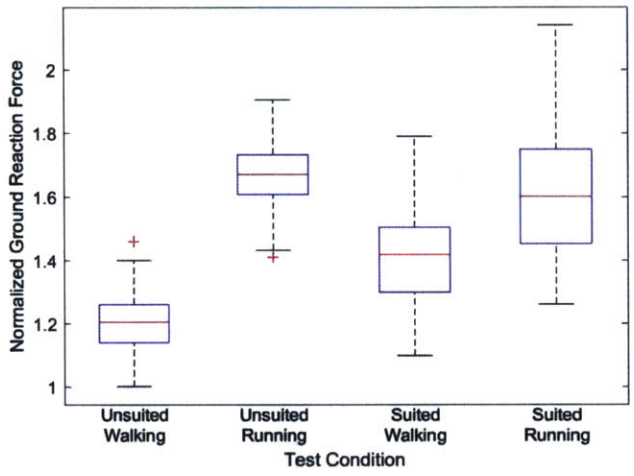

Figure 4-18: Box plots for Ground Reaction Force data for all subjects

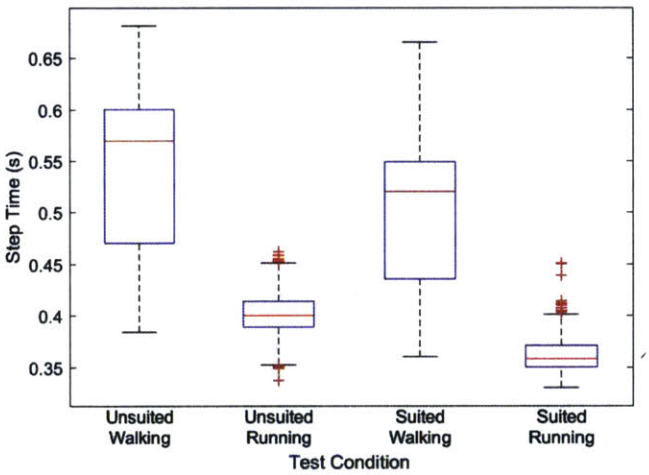

Figure 4-19: Box plots for Step Time data for all subjects

In order to analyze the effects of the testing parameters as well as subject characteristics on these variables, mixed hierarchical regressions were used to fit the data. To fit the model, we down-sampled the step data by selecting 10 random steps from each group of 100, as the strides for each subject were not independent measures, and fit the models to this sub-sample for both max ground reaction force and step time. The final models with their variables and respective coefficients are shown in tables 4.7 and 4.8 below.

Table 4.7: Variables of mixed hierarchical regression model for max ground reaction force data

Variable	Estimate	Standard Error	Z	p-Value
Intercept	1.428	0.0417	34.246	<0.0005
Suited	0.036377	0.0076	4.78972	<0.0005
Running	0.1667	0.0076	21.825	<0.0005
Stride Number	0.0007	.00028	2.681	0.0073
Suited*Running	-0.0775	0.0076	-10.18	<0.0005

Table 4.8: Variables of mixed hierarchical regression model for step time data

Variable	Estimate	Standard Error	Z	p-Value
Intercept	-0.881	0.142	-6.219	<0.0005
Suited	-0.0169	0.0032	-5.263	<0.0005
Running	-0.069	0.0032	-21.488	<0.0005
Leg Length	1.792	0.218	8.22	<0.0005
Leg Length*Weight	-0.0018	0.0004	-4.51	<0.0005

For the maximum ground reaction forces, statistically significant effects were found for suited vs. unsuited, walking vs. running, the interaction effects of the suited/unsuited condition and locomotion speed, and an effect of stride number. Max force increased if the subject was suited, if they were running, and also increased slightly as step number increased. For step time, significant effects were found for suited vs. unsuited, walking vs. running, leg length, and the interaction effect of leg length with subject weight. Step time decreased if the subject was suited, if they were running, and if the subject was heavier. Step time increased with subject leg length.

For each model, the residuals were tested for normality using a one sample Kruskal-Wallis test and homoscedasticity using Levene's Test of multiple variances. For both

models the distribution of residuals was not significantly different than a normal distribution (p = 0.688 for max ground reaction force and p = 0.787 for step time), and there were no statistically significant differences in the variance of the residuals over the range of predicted values (p = 0.1389 for max ground reaction force and p = 0.108 for step time).

While being suited had statistically significant effects on both peak GRF and step time, the differences were quite small (3% of bodyweight and 16 hundredths of a second, respectively). This shows that the suit did not have a dramatic effect on these gait parameters.

Foot Force Data

Measurements were taken using the novel pressure sensing insoles to extract the suit contributions to loading. For each subject, data was analyzed for 60 seconds for walking and running in both the suited and unsuited conditions. Maximum foot forces were extracted from the data, and normalized by subject bodyweight. Box plots of the maximum force recorded at the feet are included in figure 4-20.

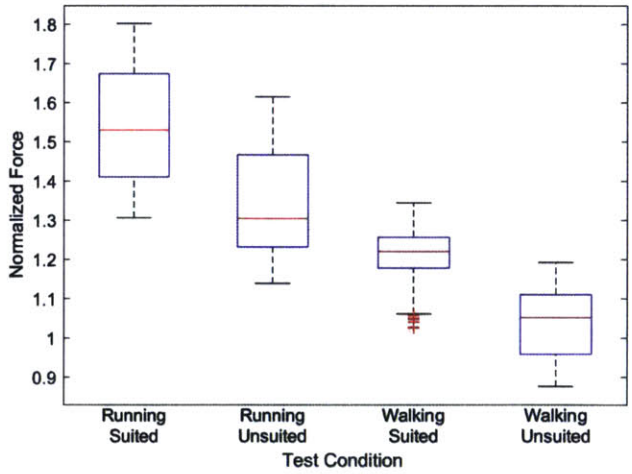

Figure 4-20: Maximum force data from novel sensors for all subjects

Kruskal Wallis non-parametric testing was performed to test for differences between the different treatments. For the maximum force there were significant differences between suited and unsuited running ($p < 0.0005$), suited and unsuited walking ($p < 0.0005$), suited running and suited walking ($p < 0.0005$) and unsuited running and unsuited walking ($p < 0.0005$). These differences were significant even after performing a Bonferroni correction for multiple comparisons.

These results were expected, given that the suit was providing loads to the body in addition to the impact forces from locomotion. These data show that the suit is increasing the loading to the subject while exercising compared to unsuited exercise.

Inverse Kinematics

To test how the suit affected running kinematics, motion capture data was analyzed using OpenSim. Data was analyzed for subjects 2, 3 and 4. Subject 1 had insufficient marker coverage to be used in determining joint angles. First, the Gait2392 model was scaled for each subject based on the static pose recorded during testing. Then, inverse kinematic analyses were run using those models and the motion capture data from the suited and unsuited trials. For each trial, 10 seconds of motion capture data was analyzed, resulting in 12-14 strides per leg for each subject. Comparisons between the joint angles in suited and unsuited conditions were performed using t-tests. A picture of the model with both virtual and experimental markers can be seen in figure 4-21. An example of knee angle over time is shown in figure 4-22.

For each subject, average right knee range of motion and average minimum and maximum flexion angles for the suited and unsuited conditions are shown in table 4.9. In this case, the knee flexion angle is defined as 0 when the leg is straight.

For subjects 2 and 3, knee range of motion decreased in the suited condition ($p < 0.001$ for both), while for subject 4 the range of motion increased in the suited case ($p < 0.001$). For all subjects, there were small changes in the minimum knee angles, seen

Figure 4-21: Subject-scaled model with virtual and experimental markers

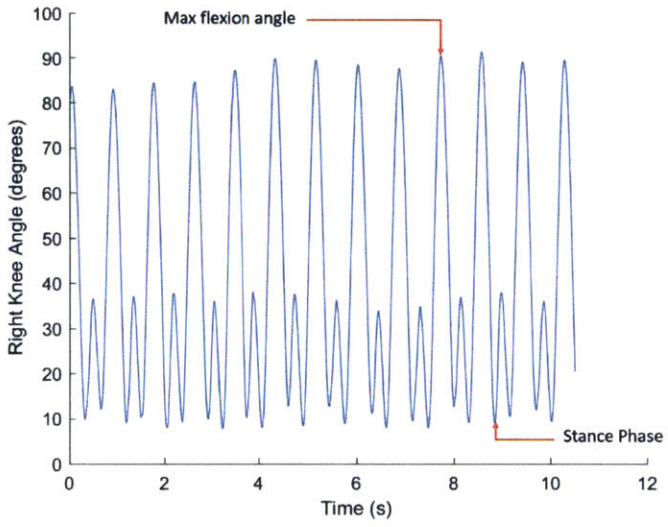

Figure 4-22: Inverse Kinematics results for the knee for one subject

during the stance phase of running. Subject 2 showed no change in minimum knee angle ($p = 0.6786$), and while subjects 3 and 4 had statistically significant differences in minimum knee angle ($p < 0.001$ for both), the differences were between 2 and 5

Table 4.9: Knee range of motion and minimum and maximum angles during running

	Suited (degrees)			Unsuited (degrees)		
Subject	Range of Motion	Minimum	Maximum	Range of Motion	Minimum	Maximum
2	62.68	28.10	90.78	73.18	28.87	102.01
3	65.60	28.09	93.82	72.48	33.30	105.78
4	86.61	12.99	99.59	77.51	10.50	88.01

degrees of flexion. The suit appeared to have a more drastic effect on the maximum knee flexion angle. For subjects 2 and 3 this angle decreased ($p < 0.001$ for both), resulting in a smaller range of motion, while for subject 4 it increased ($p < 0.001$).

Similar analyses were performed for the right hip range of motion for each subject, the results of which can be seen in table 4.10. For the hip, an angle of 0 indicated a straight leg, while positive angles indicate flexion, and negative values indicate extension. For subject 2, the range of motion decreased in the suited condition ($p < 0.001$), for subject 3 the range of motion stayed relatively unchanged ($p = 0.1057$), and for subject 4 the range of motion increased in the suited condition ($p < 0.001$).

Table 4.10: Hip range of motion and minimum and maximum angles during running

	Suited (degrees)			Unsuited (degrees)		
Subject	Range of Motion	Minimum	Maximum	Range of Motion	Minimum	Maximum
2	55.21	-30.34	24.87	63.23	-16.04	47.19
3	53.13	-7.09	46.16	54.67	-4.82	49.85
4	50.30	-10.54	39.76	36.61	-14.51	22.10

While the suit did have effects on subject kinematics while running, it was subject specific, with no clear trends between subjects. The subject joint angles measured with inverse kinematics fit in the range of joint angles measured in previous biomechanics testing [58]. Overall, based on gait parameters extracted from ground reaction force data and subject kinematic data from motion capture, we see that the suit did not drastically change how the subjects were performing locomotion on the eZLS. These results give confidence that that suit will not increase the subjects' risk of injury while using the suit by changing their movement patterns, and that the subjects will be using similar muscle groups during locomotion in the suited and unsuited cases.

Inverse Dynamics, Static Optimization, and Joint Reaction Force Analysis

In order to elucidate how the suit affects muscle and joint loading during running, inverse dynamics, static optimization and joint reaction force analysis were conducted for subject 4. Subject 4 was chosen because the most complete marker data was available for analyzing movements. To measure suit effects, a GLCS model was implemented in the same manner as in chapter 2, using subject 4's anthropometry. For all simulations, gravity was removed, as the data was taken in a simulated unloading environment. Inverse dynamics analyses were completed for both the suited and unsuited case. Inverse dynamics takes subject kinematics and external forces, in this case, ground reaction forces, and computes the net forces and torques required to create the given movements. Figures 4-23 and 4-24 show the average torque profiles over the knee and hip. For the knee, the joint torque magnitude is decreased during the stance phase, while being increased during the swing phase. This suggests that the suit creates a stabilizing force at the knee during impact, and increases the necessary torques around the knee as it straightens during the swing phase, as the knee muscles have to overcome the tension in the suit pulling the knee straight. For the hip, the torque magnitude is roughly equal between the suited and unsuited cases during the stance phase, while the suit imparts increased torques during the swing phase, as the suit stretches over the hips during movement.

In order to isolate the difference in muscle force activation between suited and unsuited conditions, Static optimization was performed over a single stride for the suited and unsuited cases. The forces produced by four muscle groups are shown below in figure 4-25: knee flexors, knee extensors, hip flexors, and hip extensors.

The knee flexor forces in the suited case are lower during the stance phase, when compared to the unsuited case, then increase during the beginning of the swing phase as the knee bends. As the knee straightens, the knee flexor forces in the suited case are greatly increased compared to the unsuited case, given that they are slowing the limbs inertia as well as overcoming the pull of the suit springs. In the knee extensors,

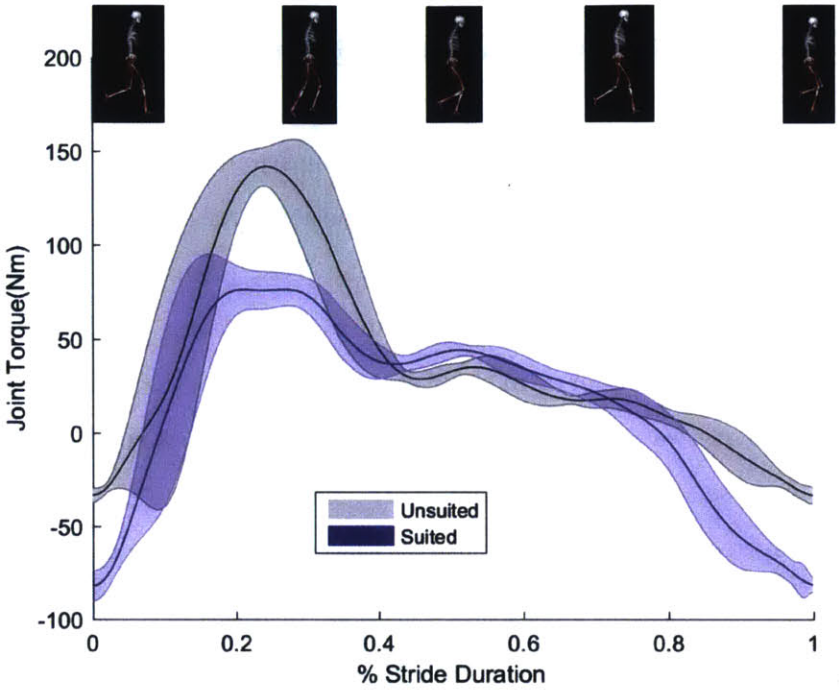

Figure 4-23: Knee torque profile during running

similarly to the knee flexor forces, the muscle forces for the suited case are lower than the unsuited case during the stance phase. This is consistent with the results of the inverse dynamics analysis.

The hip flexor and extensor forces are similar between the suited and usuited cases during the stance phase, which is also consistent with the results of the inverse dynamics analysis. The hip flexor forces are slightly higher during the swing phase in the suited condition, as the suit springs are stretched. The hip extensor forces are greatly elevated in the suited case compared to the unsuited case at the end of the swing phase of the leg.

These results show that the suit helps stabilize the knee joint during impact while running, and increases the work the muscles perform during the rest of the running stride, as the muscles work to overcome the added forces imposed on them by the suit loading materials.

Using the measured kinematics and ground reaction forces, in conjunction with the

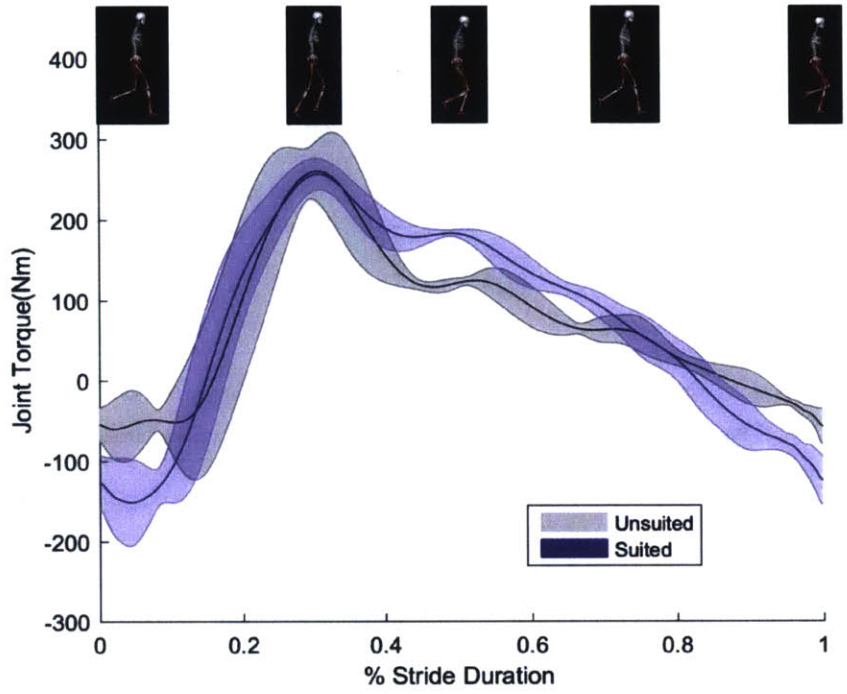

Figure 4-24: Hip torque profile during running

muscle forces computed in static optimization, joint reaction force analysis was completed over the single stride in suited and unsuited conditions. The magnitude of the joint forces for the knee and hip are shown in figures 4-26 and 4-27.

For the knee, the joint reaction force magnitude was greater in the unsuited case during the stance phase, but the joint reaction forces were higher in the suited case during the rest of the stride duration. The hip joint forces in the suited case were elevated over the entire stride duration. Over the complete duration of the stride, the area under the curve was greater in the suited condition for both the knee (2.73 vs 2.20) and the hip (2.90 vs 2.58). This shows that the cumulative load to the joints is greater while wearing the suit. The suit can greatly increase the load to the joints during exercise, which could increase the effectiveness of exercise in helping to mitigate bone loss during spaceflight.

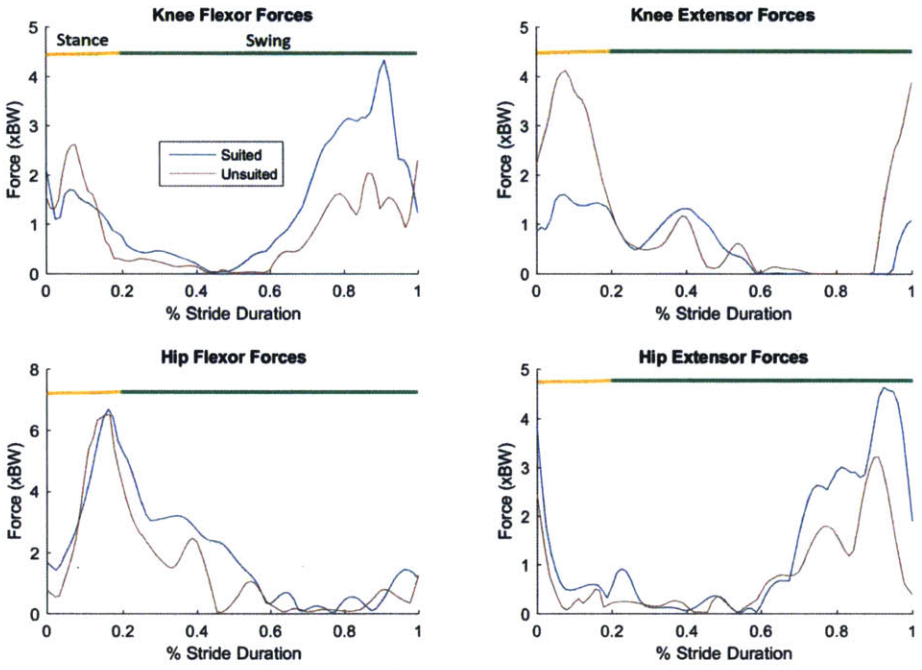

Figure 4-25: Muscle forces during running

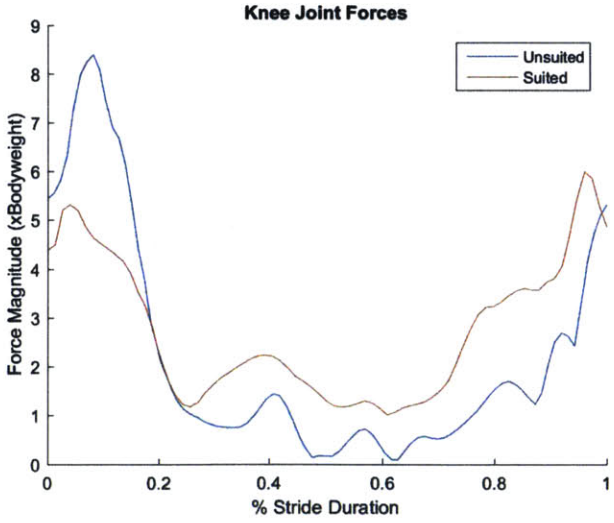

Figure 4-26: Knee joint forces during running

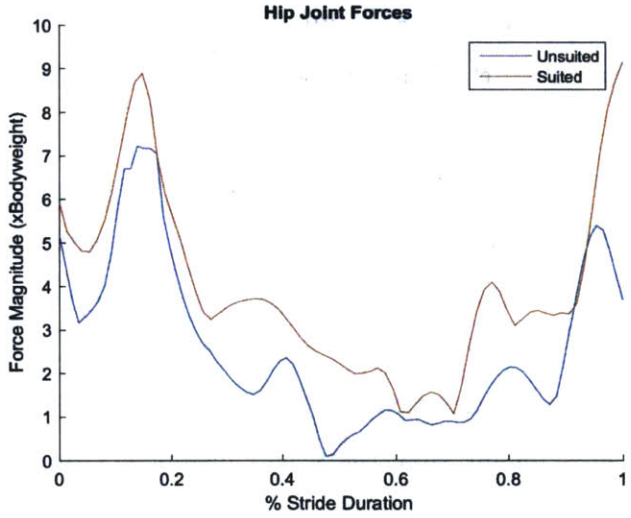

Figure 4-27: Hip joint forces during running

4.3 Summary of Suit Testing Results

Suit testing was performed on four Gravity Loading Countermeasure Skinsuits to characterize the suits and gain understanding into suit loading and its effects on the body. The suits were tested in two different analogs of unloading: bed rest and a vertical treadmill. Suit characterization showed that the suits were constructed with a high degree of accuracy, as measurements of suit loading segment lengths while the suit was unworn showed minimal differences from the desired design lengths. Once worn, the suits were able to impart 67-84% of the subjects' bodyweight to the soles of the feet. While this did not meet the design goal of 100% bodyweight loading, these totals were much higher than the loading levels achieved in previous suit prototypes. Shoulder loading was also measured, with the measured loads being significantly higher than design loads for most subjects. This overloading at the shoulder and under-loading at the feet is directly related to the suit over-stretching over the torso, and under-stretching over the legs. These inaccuracies in suit stretch are the result of insufficient suit-body anchoring. During wear, the Dual Lock strips on the skinsuit that were serving as the anchor points for the loading stages on the loading exoskeleton were breaking off. This meant that there was insufficient anchoring between the bodysuit and loading exoskeleton, which lead to the suit slipping. This was confirmed by showing that if the leg was effectively a single loading stage, it would have produced forces similar to what was actually measured by the suit. In effect, this means that the suit was essentially a two stage loading garment, with upper and lower body loading stages. During testing, comfort issues arose at both the shoulders and the feet, which is consistent with the overloading seen at the shoulders, and the concentration of the load at the feet over a smaller area. Analysis of suited and standing loading distributions showed that over 80% of suit loading was concentrated on the back of the foot, while during normal standing the load was more evenly distributed, with approximately 50-75% of the load concentrated on the back of the foot.

These tests allowed us to examine the suits' effects on the body during unloading and evaluate our initial research questions.

How does the suit affect spinal elongation during unloading?

During the bed rest testing, no clear conclusions could be made about whether the suit had any effect on spinal elongation. This is partly due to limitations in the study and how the heights were measured using the motion capture system. The four hour test duration was chosen because it was hypothesized that the suits would be comfortable enough to wear for that duration. However, previous suit testing on the suit effects on height change was conducted over an eight hour period, and it is possible that a longer test time would have shown more drastic differences between the suited and unsuited conditions. Also, the consistency of height measurements in the supine position was difficult to maintain. Small changes in subject posture could dramatically affect the height measurement, and lead to the noise seen in the height measurements for most subjects.

How does the suit affect the physiological cost of exercise?

During exercise testing on the eZLS, three of four subjects showed elevated heart rates in the suited condition for both walking and running when compared to the unsuited condition. This suggests that for those subjects their physiological workload was increased by the suit. This was corroborated by subjective feedback from subjects that they felt fatigued much more quickly in the suited trials. For subject 1, however these trends were reversed. One reason for why this may have occurred is the subject 1 was suspended for over 2 hours before he began his completed unsuited trial, and had multiple trials aborted due to equipment malfunctions. This meant that he was already fatigued when beginning the unsuited trial, and the extended period of supine suspension may have affected the dynamics of his cardiovascular system. Other subjects were supine for a far shorter period of time before beginning their trials.

How does the suit affect gait during exercise?

The suit had an effect of various gait parameters. Mixed hierarchical regression models showed the suit had effects on peak ground reaction forces and stride times. Inverse kinematic analyses in OpenSim also showed that the suit affected joint range of motion at the hip and knee for the three subjects for which the motion capture data was of sufficient quality. However, these differences were not consistent between subjects. While the suit did have measurable effects on subject gait, these effects were not drastic, and overall, the subjects were able to exercise in the suits with no trouble. However, as in the bed rest study, there were comfort issues with the suit. These issues were exacerbated by the fact that the eZLS subject loading device harness loaded the subjects at their hips and shoulders, which are two areas where the GLCS exerts the most force apart from the soles of the feet. It is possible that the suit would be better suited for use with resistive exercise, such as exercise on the ARED.

How does the suit affect joint and muscle loading during exercise?

Using data collected during exercise trials as inputs to OpenSim allowed for calculation of joint torques, muscle forces and joint reaction forces. The suit appears to act as a stabilizing force, reducing the joint torques at the knee during the stance phase. This aligned with subjective feedback from subjects who said that they felt more stable running in the suit in the novel environment of the simulated microgravity provided by the eZLS. This manifested itself in a reduction in the knee flexor and extensor muscle forces during the stance phase of running in the suited condition as compared to the unsuited case. For both the hip and knee, the torque magnitude at the joint, and consequently the muscle forces in the flexor muscles, were elevated in the suited condition during the swing phase of running, as the leg muscles had to overcome the restoring forces of the suit loading elements as they stretched around the joint. These increases lead to significantly higher overall loading in the joints, which suggests that the suit could increase the loading to the skeleton if worn in envi-

ronments where the wearer is otherwise unloaded, and therefore help to mitigate the effects of unloading on musculoskeletal deconditioning. While analyzing the relative differences in loading is a more accurate use of OpenSim than focusing on the absolute values produced by the simulations, the magnitude of the hip forces produced while wearing the suit are within the range of force measured during various activities using instrumented hip prostheses [75, 7], which suggests that the suit would not increase the subjects' risk of injury while using the suit in high impact environments.

Chapter 5

Conclusion

This thesis described work in developing and testing new GLCS prototypes, to evaluate their potential as a countermeasure to musculoskeletal deconditioning seen during long duration spaceflight. Previous suit prototypes had not been able to provide full bodyweight loading to the subjects. In order to inform suit design, and obtain insights into the loads the GLCS places on the body, a model of the GLCS was developed in OpenSim musculoskeletal modeling software and used in simulations of dynamic movement. Using lessons learned from previous suit prototypes and modeling results, prototype countermeasure suits were designed and constructed with new loading materials to provide higher loads. The suits were tested in analogs of unloading, including bed rest and on a vertical treadmill, in order to determine the suits' loading characteristics, wearability, and effects on the body during unloading and exercise.

5.1 Discussion of Key Findings

This following sections describes the key findings from the modeling efforts, suit design and construction, and suit testing.

5.1.1 Summary of Modeling Findings

In chapter 2, we described the development of a suit-body model in OpenSim. Simulations performed in OpenSim showed that wearing the GLCS could require muscle forces during simple movements that were similar to those seen during unsuited motion in earth gravity. It showed that suit material stiffness ranging from 500 to 2000 N/m was sufficient to provide this loading during movements, and that different levels of stiffness were required for different joints to replicate bodyweight loading. These results give a target stiffness range to attempt to replicate in suit design and construction. Joint reaction forces calculated for suited movement were also elevated in the suited cases, which shows that the suit is providing loads on top of the muscle forces it is imposing. The GLCS, if constructed properly, can fulfill its goal of providing bodyweight-type loading to the wearer.

5.1.2 Summary of Suit Design and Characterization

Chapter 3 presented the suit design process, including the selection of new loading materials, and development of improved anchoring techniques. The major design change between the suit prototypes constructed for this work and previous prototypes are the addition of additional loading elements, and the subsequent decoupling of the spandex skinsuit and the loading exoskeleton. These new loading elements included narrow elastics and resistive exercise bands. The introduction of these new loading elements necessitated the introduction of more non-stretch structural elements to add strength to combat the increased force produced by the suit. The spandex skinsuit acted as an interface between the body and the loading exoskeleton, with siliconized tape on the inside of the skinsuit to increase suit-body anchoring, and strips of Dual Lock fastener on the outside of the suit to improve skinsuit-exoskeleton anchoring. Suit were constructed for four subjects in collaboration with students in the Wearable

Technology Lab at the University of Minnesota.

5.1.3 Summary of Suit Testing Results

In chapter 4, we presented suit testing protocols and the results of the evaluations. Suit loading and construction accuracy was characterized. There was measured under-stretching over the leg loading segments, and over-stretching over the torso, which lead to the suit providing less than 100% of bodyweight loading to the subjects, while still imposing high loads on the shoulder, which led to comfort issues. These loading inaccuracies were the results of failures in the suit anchoring techniques, which lead to suit slip. Despite these discrepancies, the loading achieved by these suit prototypes was significantly higher than that achieved by any of the previous suit prototypes.

Bed rest testing was performed to determine the suit effects on spinal elongation. While no clear conclusions could be drawn from the noisy height data, unloading testing performed with previous suit prototypes has shown that the suits mitigated the height change seen during unloading, and this data was acquired with suits that were imposing around 20% of the loading that the current prototypes provide.

Exercise testing was also performed in the simulated microgravity environment of the eZLS at NASA Glenn Research Center. For both subjective measures and heart rate, the suit increased the workload of the subjects. The suit did affect parameters of gait during exercise, however, the changes imposed by the suit were small, and subjects were able to run and walk normally in the suit. The suit model was implemented for one subject, and was used to analyze the suit's effects on muscle and joint loading during running. The suit acted as a stabilizing force at the knee during the stance phase, and increased the muscle forces needed during rest of the stride. The suit increased the loading in the joints, which suggests that the suit can integrate with existing countermeasures to increase the musculoskeletal loading that astronauts receive.

5.2 Recommendations for Suit Design and Use

5.2.1 Suit Design Recommendations

The process of designing, constructing, and testing suit prototypes has offered many lessons and insights that can be used in future suit prototypes. Three major areas of deficiency in the current suit design are insufficient suit anchoring, shoulder comfort, and foot comfort. These comfort issues are partially tied to the insufficient suit anchoring. The suit anchoring failed, in part, due to insufficient bonding of the Dual Lock strips to the spandex fabric of the body suit. If this bonding were improved in future iterations of the suit, the issue might be solved. However, regardless of anchoring technique, anchoring along the legs will always be difficult, as the circumference of the leg tends to decrease moving from the crotch to the ankle, which is also the direction of increasing force. This means that the circumferential bands will tend to slip in that direction, which will cause under-loading at the feet. Anchoring can be achieved with sufficiently tight circumferential anchoring bands, however, the level of circumferential pressure necessary to hold the suit in place may cause subject discomfort. Because of this, it is necessary to make the most out of the anchoring opportunities that present themselves. Such areas include the hips and top of the shank where the calf diameter tends to decrease as you approach the knee. Putting padding under the circumferential bands to decrease pressure at the point of contact may also aid subject comfort. Making the circumferential belt at the waist more robust, such as making it similar to a backpacking backpack hip belt, or other harnessing belt designed to carry loads, may improve anchoring and subject comfort. Increasing the padding at the shoulder straps, and looking to backpack straps for inspiration, could help with subject comfort at the shoulders.

Many of the design decisions made for this prototype were directly tied to the decision

to provide 100% bodyweight loading to the subject. If the applied load were decreased, subject comfort would go up independent of any other design changes. Suit anchoring would also become easier, as the forces go down. As static loading has been shown to be less effective in preventing bone loss compared to dynamic loads, the static loading component of the suit is less important than the dynamic loads it imposes during movement, so full bodyweight loading might not be necessary. Modeling showed that even when the static loading level of the suit was reduced, it could still provide high loads to the muscles and joints, and loading material stiffness plays a larger role in creating the resistance provided by the suit to the muscles than the static loading level. Previous suit testing has shown that much lower load may reduce spinal elongation during unloading. It is possible that for the suit to reduce spinal elongation and offer resistive exercise to the muscles, you may only need around 50% bodyweight loading [40], as that is the normal load experience by the lumbar spine in upright posture. Further work is necessary to determine what forces are needed to reduce spinal elongation. Desired loading goals for the suit need to be well defined before design and construction, as the loading level will influence many design decisions.

Regardless of desired loading, work needs to be done to distribute the load over the sole of the foot to reduce comfort issues at the feet. Incorporating a rigid insole into the stirrups may help to distribute the load, but other designs should be considered. Additionally, reducing the size of the non-stretch elements is beneficial, especially around the joints, as it will improve subject comfort and mobility. Removing the resistive exercise bands as a loading element would help, given the difficulty in integrating them into the suit, and without their high point loads, the amount of non-stretch elements could be reduced.

The modeling work that informed suit loading material selection was based on the anthropometry of a 50^{th} percentile male astronaut, and the ideal loading material characteristics will most likely vary over the range of different subject body sizes. Smaller subjects would most likely require loading materials with smaller stiffness coefficients to mimic bodyweight loading, while larger subjects would require stiffer

materials to provide adequate loads. There are trade-offs between having stiffer or less stiff materials. Specifically, stiffer materials would not have to stretch as far to achieve the desired loading, which would increase their durability, but the loads they provide when stretching during locomotion or other body movements might be higher than desirable. Less stiff materials might be less durable to repeated loading cycles, but would be easier to move in. Further work is required in determining these relationships.

Additionally, the lines of action of the loading materials could be modified, based on postural specifications. In studying astronaut adaptation to spaceflight, it has been found that their Neutral Body Posture (NBP) deviates from upright during spaceflight [25, 54]. The loading materials of the GLCS could be constructed in order to load the Astronauts more effectively in their preferred NBP, rather than the erect, upright posture in which the suit is currently designed to provide optimal loading. Also, the loading elements could be configured to provide imbalanced loading around certain joints, in order to force the muscles to perform work to maintain a specific posture. For instance, the loading on the front of the torso could be made greater than the loading on the back of the torso, to require the erector spinae muscles to contract to maintain a straight-back posture.

5.2.2 Recommendations for Use

While suit testing conducted for this thesis centered on wearing the suit for an extended period of time, there is evidence in the literature that intermittent use of the suit might prove more beneficial. As previously stated, periods of rest from loading increases the effectiveness of skeletal loading in preserving bone mineral density [26, 43], so wearing the suit for long periods of time may have diminishing effects on bone health. Cyclical wearing of the suit would offer periods of loading and rest that may increase the effectiveness of the countermeasure.

During normal activity on earth, the spine undergoes periods of loading and unloading, resulting in height changes throughout a 24 hour period [74]. This cyclical loading benefits intervertebral disc health by maintaining their mechanical and metabolic properties [3]. Additionally, around 70% of the reduction in spinal height due to loading occurs within the first hour of loading [74], and loading effects on the spine are magnified during the initial period of loading [2]. Taken together, this evidence suggests that cyclical wearing of the suit for shorter periods of time could have significant benefits for spinal health, while also improving subject comfort, as subject comfort tended to decrease over time while wearing the suit.

5.2.3 Earth-based Applications

The Russian Penguin suit has been adapted for use in medical scenarios, specifically in treating patients with cerebral palsy [64, 4]. The GLCS could be similarly employed, with modifications, to provide external stabilization to patients and improve their gross motor function. The suit could also be leveraged in athletic training, to provide additional loads to the subjects and increase their workload during exercise.

5.3 Summary of Contributions

1. *Development of Suit-Body Model*: Development of a musculoskeletal model of the GLCS that was used to elucidate joint and muscle forces imposed by the suit during dynamic motions. This is the first time a soft loading suit was modeled in OpenSim. Future studies can utilize the suit to analyze a variety of different motions and suit parameters. The model was used to calculate forces for simple motions, and later to analyze loading during exercise testing.

2. *Construction and characterization of prototypes suits*: Design and construction

of prototype countermeasure suits that provided the highest loads ever achieved in a GLCS prototype.

3. *Suit exercise testing*: The GLCS has been previously used in cycle ergometer testing, but hasn't been tested in treadmill exercise. This testing showed that the GLCS could be used with treadmill exercise on the International Space Station to increase the loads to the joints and muscles.

5.4 Limitations

There are several limitations to the work presented in this thesis that need to be discussed. One major limitation of this work is the low subject number in suit testing. This number of subjects makes it difficult to make generalizable conclusions about some of the results in suit testing. It is possible that with more subjects, clearer patterns in the testing data would have emerged.

In our modeling efforts, there are limitations in using the Gait2392 model, specifically, that results may be inaccurate for motions with high degrees of knee flexion. However, the model has previously been used and validated in analysis of running kinematics and dynamics, so the model was not being used outside of its intended uses in our analyses. Additionally, an assumption made when implementing the model was that there was perfect anchoring between stages, which was shown to be inaccurate during suit testing. This may have affected the results of the simulation, however, the loading to the joint and surrounding muscles is directly tied to the stretch of the suit over the joint, which is independent of suit anchoring.

There were also limitations involved with using analogs of unloading for suit testing. While suspending the subject supine in the eZLS changes the gravity vector with respect to locomotion, the inertial properties of the limbs are still influenced by the earth gravity level. The harnessing and suspension system could also impose changes

on subject gait. During the bed rest test, the subjects were in contact with the air mattress, and not floating as they would be in space. This contact force may have affected the results of the spinal elongation testing.

5.5 Future Work

There are many avenues for future work on the GLCS. Suit design can be further refined, as specified in the recommendations for suit design. Additionally, finding or creating other loading materials would be beneficial. Ideally, the loading material would also be the material against the body, similar to how previous prototypes were constructed. This would greatly simplify suit construction. Further work could be done to identify how much loading is required to prevent spinal elongation, as this could be a useful set point for the static loading level of the suit. This could be done through empirical testing, or by adapting the current GLCS model in OpenSim. There are available models of the spine that could be used for this analysis [11]. Finally, further testing could be conducted to gain more insight into the suit's effects on the musculoskeletal system. Larger subject number bed rest trials could be conducted to see the long term effects of wearing the suit on bone and muscle loss. More refined testing could be conducted to determine the suit's effects on spinal elongation. Testing could also be performed to assess how the suit interacts with other forms of exercise, such as the resistive exercise provided by the ARED.

Appendix A

Subjective Comfort Survey

Subject: Study:

Please indicate your comfort and mobility rankings by circling the appropriate number:

Rating	Discomfort
1	Nude Comfort
2	Pajamas, casual clothes
3	Formal Attire
4	Minor discomfort if worn all day (16 hrs)
5	Too uncomfortable to wear all day
6	Too uncomfortable for 8 h
7	Too uncomfortable for 4 h
8	Too uncomfortable for 2 h
9	Too uncomfortable for 1 h
10	Too uncomfortable for 10 min

	Body Control (Mobility)
1	Unrestricted
2	Negligible deficiencies
3	Minimal compensation required
4	Minor but annoying deficiencies
5	Moderately objectionable deficiencies
6	Tolerable deficiencies
7	Maximum tolerable compensation required
8	Considerable compensation required
9	Intense compensation required
10	Body control lost

Appendix B

Ground Reaction Force Analysis Code

```
%%Script to analyze and graph Ground Reaction Force Data from Kistler
%%Force plates

clear all
close all

%Load Labview Data
labviewUnsuited = load('SUB4_UNSUITED.csv');
labviewSuited = load('SUB4_SUITED.csv');

%Unsuited
indexUnsuitedWalk = labviewUnsuited(10000:16000,8);
timeUnsuitedWalk = labviewUnsuited(10000:16000,1);
forceUnsuitedWalk = labviewUnsuited(10000:16000, 5);
indexUnsuitedRun = labviewUnsuited(26700:32848,8);
timeUnsuitedRun = labviewUnsuited(26700:32848,1);
forceUnsuitedRun = labviewUnsuited(26700:32848, 5);

%Suited
indexSuitedWalk = labviewSuited(10000:16000,8);
timeSuitedWalk = labviewSuited(10000:16000,1);
forceSuitedWalk = labviewSuited(10000:16000, 5);
indexSuitedRun = labviewSuited(24600:30600,8);
timeSuitedRun = labviewSuited(24600:30600,1);
forceSuitedRun = labviewSuited(24600:30600, 5);

%Subject Weight for normalization
weight = 190.0;

%smooth the force data to eliminate noise peaks
unsuitedForceSmoothWalk = smooth(forceUnsuitedWalk);
suitedForceSmoothWalk = smooth(forceSuitedWalk);
```

```
unsuitedForceSmoothRun = smooth(forceUnsuitedRun,7);
suitedForceSmoothRun = smooth(forceSuitedRun,7);

plotForces = false;
if plotForces
    figure(1)
    hold on
    title('Unsuited Running Forces')
    plot(timeUnsuitedRun, unsuitedForceSmoothRun)
    hold off
    figure(2)
    hold on
    title('Suited Running Forces')
    plot(timeSuitedRun, suitedForceSmoothRun)
    hold off
end

%% Find GRF Minimums to separate individual strides
%Unsuited
%Walk
invData = 1.01*max(unsuitedForceSmoothWalk) - unsuitedForceSmoothWalk;
[mins, unsuitedminlocWalk] = findpeaks(invData, 'MinPeakProminence', 30);
unsuitedmintimesWalk = zeros(length(unsuitedminlocWalk),1);
unsuitedminforcesWalk = zeros(length(unsuitedminlocWalk),1);
unsuitedminindexWalk = zeros(length(unsuitedminlocWalk),1);
for i = 1:length(unsuitedminlocWalk)
    unsuitedminindexWalk(i) = indexUnsuitedWalk(unsuitedminlocWalk(i));
    unsuitedmintimesWalk(i) = timeUnsuitedWalk(unsuitedminlocWalk(i));
    unsuitedminforcesWalk(i) = unsuitedForceSmoothWalk(unsuitedminlocWalk(i));
end

%Run
invData = 1.01*max(unsuitedForceSmoothRun) - unsuitedForceSmoothRun;
[mins, unsuitedminlocRun] = findpeaks(invData, 'MinPeakProminence', 30);
unsuitedmintimesRun = zeros(length(unsuitedminlocRun),1);
unsuitedminforcesRun = zeros(length(unsuitedminlocRun),1);
unsuitedminindexRun = zeros(length(unsuitedminlocRun),1);
for i = 1:length(unsuitedminlocRun)
    unsuitedminindexRun(i) = indexUnsuitedRun(unsuitedminlocRun(i));
    unsuitedmintimesRun(i) = timeUnsuitedRun(unsuitedminlocRun(i));
    unsuitedminforcesRun(i) = unsuitedForceSmoothRun(unsuitedminlocRun(i));
end

%Suited
%Walk
invData = 1.01*max(suitedForceSmoothWalk) - suitedForceSmoothWalk;
[suitedmins, suitedminlocWalk] = findpeaks(invData, 'MinPeakProminence', 20);
suitedmintimesWalk = zeros(length(suitedminlocWalk),1);
suitedminforcesWalk = zeros(length(suitedminlocWalk),1);
suitedminindexWalk = zeros(length(suitedminlocWalk),1);
for i = 1:length(suitedminlocWalk)
    suitedminindexWalk(i) = indexSuitedWalk(suitedminlocWalk(i));
    suitedmintimesWalk(i) = timeSuitedWalk(suitedminlocWalk(i));
    suitedminforcesWalk(i) = suitedForceSmoothWalk(suitedminlocWalk(i));
end
%Run
invData = 1.01*max(suitedForceSmoothRun) - suitedForceSmoothRun;
[suitedmins, suitedminlocRun] = findpeaks(invData, 'MinPeakProminence', 20);
suitedmintimesRun = zeros(length(suitedminlocRun),1);
suitedminforcesRun = zeros(length(suitedminlocRun),1);
suitedminindexRun = zeros(length(suitedminlocRun),1);
```

```
for i = 1:length(suitedminlocRun)
    suitedminindexRun(i) = indexSuitedRun(suitedminlocRun(i));
    suitedmintimesRun(i) = timeSuitedRun(suitedminlocRun(i));
    suitedminforcesRun(i) = suitedForceSmoothRun(suitedminlocRun(i));
end
%% Remove Drift from running forces
%Unsuited
pUnsuited = polyfit(unsuitedminindexRun, unsuitedminforcesRun, 1);
fUnsuited = polyval(pUnsuited, unsuitedminindexRun);

for i = 1:length(unsuitedForceSmoothRun)
    unsuitedForceSmoothRun(i) = unsuitedForceSmoothRun(i)- polyval(pUnsuited, indexUnsuitedRun(i));
    if unsuitedForceSmoothRun(i) < 0
        unsuitedForceSmoothRun(i) = 0;
    end
end

%Suited
pSuited = polyfit(suitedminindexRun, suitedminforcesRun, 1);
fSuited = polyval(pSuited, suitedminindexRun);

normForces = zeros(length(suitedForceSmoothRun));
for i = 1:length(suitedForceSmoothRun)
    suitedForceSmoothRun(i) = suitedForceSmoothRun(i)- polyval(pSuited, indexSuitedRun(i));
    if suitedForceSmoothRun(i) < 0
        suitedForceSmoothRun(i) = 0;
    end
end

plotCorrection = true;
if plotCorrection
   figure(3)
    hold on
    title('Unsuited Running Corrections')
    plot(unsuitedminindexRun, fUnsuited);
    plot(unsuitedminindexRun, unsuitedminforcesRun);
    hold off
    figure(4)
    hold on
    title('Suited Running Corrections')
    plot(suitedminindexRun, fSuited);
    plot(suitedminindexRun, suitedminforcesRun);
    hold off
    figure(5)
    hold on
    title('Corrected Unsuited Running Forces')
    plot(timeUnsuitedRun, unsuitedForceSmoothRun);
    hold off
    figure(6)
    hold on
    title('Corrected Suited Running Forces')
    plot(timeSuitedRun, suitedForceSmoothRun);
    hold off
end

%% Separate Strides and Normalize by Stride Time

%Separate strides and normalize by stride time
stridesRun = 100;
stridesWalk = 95;
```

```
%Unsuited
%Walk
indivTimesUnsuitedWalk = cell(stridesWalk,1);
indivForcesUnsuitedWalk = cell(stridesWalk, 1);

StrideTimesUnsuitedWalk = zeros(stridesWalk,1);
maxForceUnsuitedWalk = zeros(stridesWalk,1);
minStrideTimeUnsuitedWalk = timeUnsuitedWalk(unsuitedminlocWalk(2))-timeUnsuitedWalk(unsuitedminlocWalk(1));

for i = 1:stridesWalk
    times = timeUnsuitedWalk(unsuitedminlocWalk(i):unsuitedminlocWalk(i+1));
    firsttime = timeUnsuitedWalk(unsuitedminlocWalk(i));
    StrideTimesUnsuitedWalk(i) = timeUnsuitedWalk(unsuitedminlocWalk(i+1))-timeUnsuitedWalk(unsuitedminlocWalk(i));
    if StrideTimesUnsuitedWalk(i) < minStrideTimeUnsuitedWalk
        minStrideTimeUnsuitedWalk = StrideTimesUnsuitedWalk(i);
    end
    indivTimesUnsuitedWalk{i} = (times - firsttime)./StrideTimesUnsuitedWalk(i);
    indivForcesUnsuitedWalk{i} = unsuitedForceSmoothWalk(unsuitedminlocWalk(i):unsuitedminlocWalk(i+1));
    [maxForceUnsuitedWalk(i), loc] = findpeaks(indivForcesUnsuitedWalk{i}, 'MinPeakProminence', 30);
end

%Run
indivTimesUnsuitedRun = cell(stridesRun,1);
indivForcesUnsuitedRun = cell(stridesRun, 1);

StrideTimesUnsuitedRun = zeros(stridesRun,1);
maxForceUnsuitedRun = zeros(stridesRun,1);
minStrideTimeUnsuitedRun = timeUnsuitedRun(unsuitedminlocRun(2))-timeUnsuitedRun(unsuitedminlocRun(1));

for i = 1:stridesRun
    times = timeUnsuitedRun(unsuitedminlocRun(i):unsuitedminlocRun(i+1));
    firsttime = timeUnsuitedRun(unsuitedminlocRun(i));
    StrideTimesUnsuitedRun(i) = timeUnsuitedRun(unsuitedminlocRun(i+1))-timeUnsuitedRun(unsuitedminlocRun(i));
    if StrideTimesUnsuitedRun(i) < minStrideTimeUnsuitedRun
        minStrideTimeUnsuitedRun = StrideTimesUnsuitedRun(i);
    end
    indivTimesUnsuitedRun{i} = (times - firsttime)./StrideTimesUnsuitedRun(i);
    indivForcesUnsuitedRun{i} = unsuitedForceSmoothRun(unsuitedminlocRun(i):unsuitedminlocRun(i+1));
    [maxForceUnsuitedRun(i), loc] = findpeaks(indivForcesUnsuitedRun{i}, 'MinPeakProminence', 30);
end

%Suited
%Walk
indivTimesSuitedWalk = cell(stridesWalk, 1);
indivForcesSuitedWalk = cell(stridesWalk,1);

StrideTimesSuitedWalk = zeros(stridesWalk,1);
maxForceSuitedWalk = zeros(stridesWalk,1);
minStrideTimeSuitedWalk = timeSuitedWalk(suitedminlocWalk(2))-timeSuitedWalk(suitedminlocWalk(1));

for i = 1:stridesWalk
    times = timeSuitedWalk(suitedminlocWalk(i):suitedminlocWalk(i+1));
    firsttime = timeSuitedWalk(suitedminlocWalk(i));
    StrideTimesSuitedWalk(i) = timeSuitedWalk(suitedminlocWalk(i+1))-timeSuitedWalk(suitedminlocWalk(i));
    if StrideTimesSuitedWalk(i) < minStrideTimeSuitedWalk
        minStrideTimeSuitedWalk = StrideTimesSuitedWalk(i);
    end
    indivTimesSuitedWalk{i} = (times - firsttime)./StrideTimesSuitedWalk(i);
    indivForcesSuitedWalk{i} = suitedForceSmoothWalk(suitedminlocWalk(i):suitedminlocWalk(i+1));
    [maxForceSuitedWalk(i), loc] = findpeaks(indivForcesSuitedWalk{i}, 'MinPeakProminence', 30);
end
```

```
%Run
indivTimesSuitedRun = cell(stridesRun, 1);
indivForcesSuitedRun = cell(stridesRun,1);

StrideTimesSuitedRun = zeros(stridesRun,1);
maxForceSuitedRun = zeros(stridesRun,1);
minStrideTimeSuitedRun = timeSuitedRun(suitedminlocRun(2))-timeSuitedRun(suitedminlocRun(1));

for i = 1:stridesRun
    times = timeSuitedRun(suitedminlocRun(i):suitedminlocRun(i+1));
    firsttime = timeSuitedRun(suitedminlocRun(i));
    StrideTimesSuitedRun(i) = timeSuitedRun(suitedminlocRun(i+1))-timeSuitedRun(suitedminlocRun(i));
    if StrideTimesSuitedRun(i) < minStrideTimeSuitedRun
       minStrideTimeSuitedRun = StrideTimesSuitedRun(i);
    end
    indivTimesSuitedRun{i} = (times - firsttime)./StrideTimesSuitedRun(i);
    indivForcesSuitedRun{i} = suitedForceSmoothRun(suitedminlocRun(i):suitedminlocRun(i+1));
    [maxForceSuitedRun(i), loc] = findpeaks(indivForcesSuitedRun{i}, 'MinPeakProminence', 30);
end
%% Plot foot forces
plotForces = true;
if plotForces
    %Walk
    figure(7)
    title('Unsuited Walking Strides')
    hold on
    for i = 1:stridesWalk
        plot(indivTimesUnsuitedWalk{i}, indivForcesUnsuitedWalk{i})
    end
    hold off
    figure(8)
    title('Suited Walking Strides')
    hold on
    for i = 1:stridesWalk
        plot(indivTimesSuitedWalk{i}, indivForcesSuitedWalk{i});
    end
    %Run
    figure(9)
    title('Unsuited Running Strides');
    hold on
    for i = 1:stridesRun
        plot(indivTimesUnsuitedRun{i}, indivForcesUnsuitedRun{i})
    end
    hold off
    figure(10)
    title('Suited Running Strides');
    hold on
    for i = 1:stridesRun
        plot(indivTimesSuitedRun{i}, indivForcesSuitedRun{i});
    end

end
%% Normalize the GRF by subject weight

%Calculate mean and std deviation for suited and unsuited
%Walk
meanStrideTimeUnsuitedWalk = mean(StrideTimesUnsuitedWalk)
stdUnsuitedWalk = std(StrideTimesUnsuitedWalk)
meanStrideTimeSuitedWalk = mean(StrideTimesSuitedWalk)
stdSuitedWalk = std(StrideTimesSuitedWalk)
%Run
```

```
meanStrideTimeUnsuitedRun = mean(StrideTimesUnsuitedRun)
stdUnsuitedRun = std(StrideTimesUnsuitedRun)
meanStrideTimeSuitedRun = mean(StrideTimesSuitedRun)
stdSuitedRun = std(StrideTimesSuitedRun)

%Normalize force by weight
bwForcesSuitedWalk = cell(stridesWalk, 1);
bwForcesUnsuitedWalk = cell(stridesWalk, 1);
bwForcesSuitedRun = cell(stridesRun, 1);
bwForcesUnsuitedRun = cell(stridesRun, 1);

%Walk
for i = 1:stridesWalk
   bwForcesSuitedWalk{i} = indivForcesSuitedWalk{i}./weight;
   bwForcesUnsuitedWalk{i} = indivForcesUnsuitedWalk{i}./weight;
end
%Run
for i = 1:stridesRun
   bwForcesSuitedRun{i} = indivForcesSuitedRun{i}./weight;
   bwForcesUnsuitedRun{i} = indivForcesUnsuitedRun{i}./weight;
end

plotNormalizedForces = true;
if plotNormalizedForces
   figure(11)
   title('Normalized Unsuited Walking Strides')
   hold on
   for i = 1:stridesWalk
      plot(indivTimesUnsuitedWalk{i}, bwForcesUnsuitedWalk{i});
   end
   xlabel('Normalized Stride Duration')
   ylabel('Force (xBW)')
   hold off
   figure(12)
   title('Normalized Suited Walking Strides')
   hold on
   for i = 1:stridesWalk
      plot(indivTimesSuitedWalk{i}, bwForcesSuitedWalk{i});
   end
   xlabel('Normalized Stride Duration')
   ylabel('Force (xBW)')
   figure(13)
   title('Normalized Unsuited Running Strides')
   hold on
   for i = 1:stridesRun
      plot(indivTimesUnsuitedRun{i}, bwForcesUnsuitedRun{i});
   end
   xlabel('Normalized Stride Duration')
   ylabel('Force (xBW)')
   hold off
   figure(14)
   title('Normalized Suited Running Strides')
   hold on
   for i = 1:stridesRun
      plot(indivTimesSuitedRun{i}, bwForcesSuitedRun{i});
   end
   xlabel('Normalized Stride Duration')
   ylabel('Force (xBW)')
end
%% Prepare matrices for plotting using shadedErrorBar
%Resample data to make each vector the same length
```

```
Fs = 1001;
unsuitedErrorTimeWalk = zeros(stridesWalk, Fs);
unsuitedErrorForceWalk = zeros(stridesWalk,Fs);
unsuitedErrorTimeRun = zeros(stridesRun, Fs);
unsuitedErrorForceRun = zeros(stridesRun,Fs);
suitedErrorTimeWalk = zeros(stridesWalk, Fs);
suitedErrorForceWalk = zeros(stridesWalk,Fs);
suitedErrorTimeRun = zeros(stridesRun, Fs);
suitedErrorForceRun = zeros(stridesRun,Fs);

for i = 1:stridesWalk
    min = bwForcesUnsuitedWalk{i}(1);
    [Y, Ty] = resample(bwForcesUnsuitedWalk{i}-min, indivTimesUnsuitedWalk{i}, Fs);
    unsuitedErrorForceWalk(i,:) = Y(1:1001)+min;
    unsuitedErrorTimeWalk(i,:) = Ty(1:1001);
    min = bwForcesSuitedWalk{i}(1);
    [Y, Ty] = resample(bwForcesSuitedWalk{i}-min, indivTimesSuitedWalk{i}, Fs);
    suitedErrorForceWalk(i,:) = Y(1:1001)+min;
    suitedErrorTimeWalk(i,:) = Ty(1:1001);
end

for i = 1:stridesRun
    [Y, Ty] = resample(bwForcesUnsuitedRun{i}, indivTimesUnsuitedRun{i}, Fs);
    unsuitedErrorForceRun(i,:) = Y(1:1001);
    unsuitedErrorTimeRun(i,:) = Ty(1:1001);
    [Y, Ty] = resample(bwForcesSuitedRun{i}, indivTimesSuitedRun{i}, Fs);
    suitedErrorForceRun(i,:) = Y(1:1001);
    suitedErrorTimeRun(i,:) = Ty(1:1001);
end

figure(15)
title('Subject 4')
hold on
hunsuit = shadedErrorBar(unsuitedErrorTimeWalk(1,:), unsuitedErrorForceWalk, {@mean,@std},'-b',1);
hsuit = shadedErrorBar(suitedErrorTimeWalk(1,:), suitedErrorForceWalk, {@mean,@std});
%legend('Unsuited Std Dev','Unsuited Average','Suited Std Dev','Suited Average')
legend([hunsuit.patch hsuit.patch], 'Unsuited', 'Suited','Location','Best')
xlabel('Normalized Stride Duration')
ylabel('Force (xBW)')
hold off
figure(16)
title('Subject 4')
hold on
hunsuit = shadedErrorBar(unsuitedErrorTimeRun(2,:), unsuitedErrorForceRun, {@mean,@std},'-b',1);
hsuit = shadedErrorBar(suitedErrorTimeRun(2,:), suitedErrorForceRun, {@mean,@std});
%legend('Unsuited Std Dev','Unsuited Average','Suited Std Dev','Suited Average')
legend([hunsuit.patch hsuit.patch], 'Unsuited', 'Suited','Location','Best')
xlabel('Normalized Stride Duration')
ylabel('Force (xBW)')
axis([0 1 0 2])
hold off

%% Divide running foot forces for use in OpenSim and save to files

%Unsuited
unsuitedminindexRun = unsuitedminindexRun - indexUnsuitedRun(1);
foot1forcesUnsuited = zeros(length(unsuitedForceSmoothRun),1);
foot2forcesUnsuited = zeros(length(unsuitedForceSmoothRun),1);
for i = 1:length(unsuitedminlocRun)
    if i == 1
```

```
        foot1forcesUnsuited(1:unsuitedminindexRun(1)) = unsuitedForceSmoothRun(1:unsuitedminindexRun(1));
    else
        if mod(i,2) == 1
            foot1forcesUnsuited(unsuitedminindexRun(i-1):unsuitedminindexRun(i)) = unsuitedForceSmoothRun(unsuitedminind
        else
            foot2forcesUnsuited(unsuitedminindexRun(i-1):unsuitedminindexRun(i)) = unsuitedForceSmoothRun(unsuitedminind
        end
    end
end

suitedminindexRun = suitedminindexRun - indexSuitedRun(1);
foot1forcesSuited = zeros(length(suitedForceSmoothRun),1);
foot2forcesSuited = zeros(length(suitedForceSmoothRun),1);
for i = 1:length(suitedminlocRun)
    if i == 1
        foot1forcesSuited(1:suitedminindexRun(1)) = suitedForceSmoothRun(1:suitedminindexRun(1));
    else
        if mod(i,2) == 1
            foot1forcesSuited(suitedminindexRun(i-1):suitedminindexRun(i)) = suitedForceSmoothRun(suitedminindexRun(i-1
        else
            foot2forcesSuited(suitedminindexRun(i-1):suitedminindexRun(i)) = suitedForceSmoothRun(suitedminindexRun(i-1
        end
    end
end

figure(17)
title('Unsuited Running Forces Divided')
hold on
plot(indexUnsuitedRun(1:1000), foot1forcesUnsuited(1:1000))
plot(indexUnsuitedRun(1:1000), foot2forcesUnsuited(1:1000))
hold off

figure(18)
title('Suited Running Forces Divided')
hold on
plot(indexSuitedRun(1:1000), foot1forcesSuited(1:1000))
plot(indexSuitedRun(1:1000), foot2forcesSuited(1:1000))
hold off

writetofile = false;
if writetofile
    %Unsuited
    footforcesUnsuited = [foot1forcesUnsuited;foot2forcesUnsuited];
    fileIDunsuited = fopen('Subject4_UnsuitedRun_FootForces.txt', 'w');
    for i = 1:length(unsuitedForceSmoothRun)
        fprintf(fileIDunsuited, '%f ', foot1forcesUnsuited(i));
        fprintf(fileIDunsuited, '%f\n', foot2forcesUnsuited(i));
    end
    fclose(fileIDunsuited);

    %Suited
    footforcesSuited = [foot1forcesSuited;foot2forcesSuited];
    fileIDsuited = fopen('Subject4_SuitedRun_FootForces.txt', 'w');
    for i = 1:length(suitedForceSmoothRun)
        fprintf(fileIDsuited, '%f ', foot1forcesSuited(i));
        fprintf(fileIDsuited, '%f\n', foot2forcesSuited(i));
    end
    fclose(fileIDsuited);

    %For Statistical Analysis
    subjectNumber = 4;
```

```
    suited = 1;
    unsuited = 0;
    walking = 0;
    running = 1;
    fIDstats = fopen('Subject4_Systat.txt', 'w');
    for i = 1:stridesWalk
        fprintf(fIDstats, '%f ', subjectNumber);
        fprintf(fIDstats, '%f ', unsuited);
        fprintf(fIDstats, '%f ', walking);
        fprintf(fIDstats, '%f ', StrideTimesUnsuitedWalk(i));
        fprintf(fIDstats, '%f\n', maxForceUnsuitedWalk(i)/weight);
    end
    for i = 1:stridesWalk
        fprintf(fIDstats, '%f ', subjectNumber);
        fprintf(fIDstats, '%f ', suited);
        fprintf(fIDstats, '%f ', walking);
        fprintf(fIDstats, '%f ', StrideTimesSuitedWalk(i));
        fprintf(fIDstats, '%f\n', maxForceSuitedWalk(i)/weight);
    end
    for i = 1:stridesRun
        fprintf(fIDstats, '%f ', subjectNumber);
        fprintf(fIDstats, '%f ', unsuited);
        fprintf(fIDstats, '%f ', running);
        fprintf(fIDstats, '%f ', StrideTimesUnsuitedRun(i));
        fprintf(fIDstats, '%f\n', maxForceUnsuitedRun(i)/weight);
    end
    for i = 1:stridesRun
        fprintf(fIDstats, '%f ', subjectNumber);
        fprintf(fIDstats, '%f ', suited);
        fprintf(fIDstats, '%f ', running);
        fprintf(fIDstats, '%f ', StrideTimesSuitedRun(i));
        fprintf(fIDstats, '%f\n', maxForceSuitedRun(i)/weight);
    end
    fclose(fIDstats);
end
```

Appendix C

Institutional Review Board Approvals

MIT Committee On the Use of Humans as Experimental Subjects

MASSACHUSETTS INSTITUTE OF TECHNOLOGY
77 Massachusetts Avenue
Cambridge, Massachusetts 02139
Building E 25-143B
(617) 253-6787

To:	Leia Stirling 33-311
From:	Leigh Firn, Chair COUHES
Date:	11/19/2015
Committee Action:	**Approval**
Committee Action Date	11/19/2015
COUHES Protocol #	1510282671
Study Title	Evaluating the Gravity Loading Countermeasure Skinsuit
Expiration Date	11/18/2016

The above-referenced protocol has been APPROVED following Full Board Review by the Committee on the Use of Humans as Experimental Subjects (COUHES).

If the research involves collaboration with another institution then the research cannot commence until COUHES receives written notification of approval from the collaborating institution's IRB.

It is the Principal Investigator's responsibility to obtain review and continued approval before the expiration date. Please allow sufficient time for continued approval. You may not continue any research activity beyond the expiration date without COUHES approval. Failure to receive approval for continuation before the expiration date will result in the automatic suspension of the approval of this protocol.

Information collected following suspension is unapproved research and cannot be reported or published as research data. If you do not wish continued approval, please notify the Committee of the study termination.

Adverse Events: Any serious or unexpected adverse event must be reported to COUHES within 48 hours. All other adverse events should be reported in writing within 10 working days.

Amendments: Any changes to the protocol that impact human subjects, including changes in experimental design, equipment, personnel or funding, must be approved by COUHES before they can be initiated.

Prospective new study personnel must, where applicable, complete training in human subjects research and in the HIPAA Privacy Rule before participating in the study.

You must maintain a research file for at least 3 years after completion of the study. This file should include all correspondence with COUHES, original signed consent forms, and study data.

National Aeronautics and
Space Aministration
Lyndon B. Johnson Space Center
2101 Nasa Parkway
Houston, Texas 77058-3696

NOTIFICATION OF APPROVAL
December 16, 2015

Leia Stirling

To:
Gail Perusek
Dustin Kendrick

From: SA/Chair, Institutional Review Board

Title: Evaluating the Gravity Loading Countermeasure Skinsuit

Protocol Number: Pro1970
Method of Review: Full IRB Review
Type of Review: Initial/Actions
IRB Disposition: Approved
Approval Validity: November 19, 2015 to November 30, 2016
Risk Level: Greater than Minimal Risk
Medical Monitor: Level III

NASA MPA Number: NASA 7116301606HR
FWA Number: 00019876

IRB approval is valid for a period of 1 year from the time of the Initial Review and/or Protocol Renewal. Changes, including action item responses or modifications, do not extend the initial review and/or protocol renewal date. There is no grace period beyond one year from the last approval date. In order to avoid lapses in approval of your research and the possible suspension of subject enrollment, please submit your continuation request at least six (6) weeks before the protocol's expiration date. It is your responsibility to submit your research protocol for continuing review.

The Investigator must report any adverse reactions or unexpected problems resulting from this study to the JSC IRB Chair, JSC Human Research Program (and/or funding personnel), and the JSC Safety Office (if applicable).

The proposal was reviewed and approved by the IRB in accordance with the requirements of the Code of Federal Regulations on the Protection of Human Subjects (45 CFR 46 and 21 CFR 50 and 56), including its relevant Subparts.

Charles Lloyd, Pharm.D.
Chair, JSC IRB

Bibliography

[1] Carvil Phil A, Julia Attias, Simon Evetts, James Waldie, and David A Green. The effect of the gravity loading countermeasure skinsuit upon movement and strength. *The Journal of Strength and Conditioning Research*, 2016.

[2] MA Adams, P Dolan, and WC Hutton. Diurnal variations in the stresses on the lumbar spine. *Spine*, 12(2):130–137, 1987.

[3] MA Adams and WC Hutton. The effect of posture on the fluid content of lumbar intervertebral discs. *Spine*, 8(6):665–671, 1983.

[4] Jagatheesan Alagesan and Angelina Shetty. Effect of modified suit therapy in spastic diplegic cerebral palsy-a single blinded randomized controlled trial. *Online Journal of Health and Allied Sciences*, 9(4), 2011.

[5] Frank C Anderson and Marcus G Pandy. A dynamic optimization solution for vertical jumping in three dimensions. *Computer methods in biomechanics and biomedical engineering*, 2(3):201–231, 1999.

[6] Frank C Anderson and Marcus G Pandy. Dynamic optimization of human walking. *Journal of biomechanical engineering*, 123(5):381–390, 2001.

[7] Graichen Bergmann, F Graichen, and A Rohlmann. Hip joint loading during walking and running, measured in two patients. *Journal of biomechanics*, 26(8):969–990, 1993.

[8] Wendy C Bevier, Robert A Wiswell, Gisela Pyka, Kathryn C Kozak, Katherine M Newhall, and Robert Marcus. Relationship of body composition, muscle strength, and aerobic capacity to bone mineral density in older men and women. *Journal of bone and mineral research*, 4(3):421–432, 1989.

[9] F Biering-Sørensen, H Bohr, and O Schaadt. Bone mineral content of the lumbar spine and lower extremities years after spinal cord lesion. *Spinal Cord*, 26(5):293–301, 1988.

[10] Daniel D Bikle, Takeshi Sakata, and Bernard P Halloran. The impact of skeletal unloading on bone formation. *Gravitational and Space Research*, 16(2), 2007.

[11] Alexander G Bruno, Mary L Bouxsein, and Dennis E Anderson. Development and validation of a musculoskeletal model of the fully articulated thoracolumbar spine and rib cage. *Journal of biomechanical engineering*, 137(8):081003, 2015.

[12] Jay C Buckey. *Space physiology.* Oxford University Press, 2006.

[13] DR Carter, DP Fyhrie, and RT Whalen. Trabecular bone density and loading history: regulation of connective tissue biology by mechanical energy. *Journal of biomechanics*, 20(8):785–794, 1987.

[14] Peter R Cavanagh, Angelo A Licata, and Andrea J Rice. Exercise and pharmacological countermeasures for bone loss during longduration space flight. *Gravitational and Space Research*, 18(2), 2007.

[15] Peter R Cavanagh and Andrea J Rice. *Bone loss during spaceflight: etiology, countermeasures, and implications for bone health on Earth.* Cleveland Clinic Press, 2007.

[16] E Churchill, LL Laubach, JT McConville, and I Tebbetts. Anthropometric source book. *Volume*, 1:7–78, 1978.

[17] Ramzi S Cotran, Vinay Kumar, Tucker Collins, and Stanley Leonard Robbins. Robbins pathologic basis of disease. 1999.

[18] Scott L Delp, Frank C Anderson, Allison S Arnold, Peter Loan, Ayman Habib, Chand T John, Eran Guendelman, and Darryl G Thelen. Opensim: open-source software to create and analyze dynamic simulations of movement. *Biomedical Engineering, IEEE Transactions on*, 54(11):1940–1950, 2007.

[19] RH Fitts, SW Trappe, DL Costill, Philip M Gallagher, Andrew C Creer, PA Colloton, Jim R Peters, JG Romatowski, JL Bain, and Danny A Riley. Prolonged space flight-induced alterations in the structure and function of human skeletal muscle fibres. *The Journal of physiology*, 588(18):3567–3592, 2010.

[20] Tamar Flash and Neville Hogan. The coordination of arm movements: an experimentally confirmed mathematical model. *The journal of Neuroscience*, 5(7):1688–1703, 1985.

[21] Harold M Frost. Bone âĂIJmassâĂİ and the âĂIJmechanostatâĂİ: a proposal. *The anatomical record*, 219(1):1–9, 1987.

[22] Kerim O Genc, Brad T Humphreys, and Peter R Cavanagh. Enhanced daily load stimulus to bone in spaceflight and on earth. *Aviation, space, and environmental medicine*, 80(11):919–926, 2009.

[23] Rahul Goel, Justin Kaderka, and Dava Newman. Modeling the benefits of an artificial gravity countermeasure coupled with exercise and vibration. *Acta Astronautica*, 70:43–51, 2012.

[24] Raghavan Gopalakrishnan, Kerim O Genc, Andrea J Rice, Stuart Lee, Harlan J Evans, Christian C Maender, Hakan Ilaslan, and Peter R Cavanagh. Muscle volume, strength, endurance, and exercise loads during 6-month missions in space. *Aviation, space, and environmental medicine*, 81(2):91–104, 2010.

[25] Brand Norman Griffin. Design guide: the influence of zero-g and acceleration on the human factors of spacecraft design. *NASA Johnson Space Centre*, 1978.

[26] Ted S Gross, Sandra L Poliachik, Brandon J Ausk, David A Sanford, Blair A Becker, and Sundar Srinivasan. Why rest stimulates bone formation: a hypothesis based on complex adaptive phenomenon. *Exercise and sport sciences reviews*, 32(1):9, 2004.

[27] Douglas R Hamilton, Ashot E Sargsyan, Kathleen Garcia, Douglas J Ebert, Peggy A Whitson, Alan H Feiveson, Irina V Alferova, Scott A Dulchavsky, Vladimir P Matveev, Valery V Bogomolov, et al. Cardiac and vascular responses to thigh cuffs and respiratory maneuvers on crewmembers of the international space station. *Journal of Applied Physiology*, 112(3):454–462, 2012.

[28] Samuel R Hamner and Scott L Delp. Muscle contributions to fore-aft and vertical body mass center accelerations over a range of running speeds. *Journal of biomechanics*, 46(4):780–787, 2013.

[29] Samuel R Hamner, Ajay Seth, and Scott L Delp. Muscle contributions to propulsion and support during running. *Journal of biomechanics*, 43(14):2709–2716, 2010.

[30] Jennifer L Hicks, Thomas K Uchida, Ajay Seth, Apoorva Rajagopal, and Scott L Delp. Is my model good enough? best practices for verification and validation of musculoskeletal models and simulations of movement. *Journal of biomechanical engineering*, 137(2):020905, 2015.

[31] Rik Huiskes, Ronald Ruimerman, G Harry Van Lenthe, and Jan D Janssen. Effects of mechanical forces on maintenance and adaptation of form in trabecular bone. *Nature*, 405(6787):704–706, 2000.

[32] International Society of Gravitational Physiology. *The Gravity-loading Countermeasure Skinsuit Attenuates Spinal Elongation and Back Pain during 8 hours of Human Spinal Unloading*, All ACM Conferences, Ljubljana, Slovenia, June 2015.

[33] B Issekutz, JJ Blizzard, NC Birkhead, and K Rodahl. Effect of prolonged bed rest on urinary calcium output. *Journal of Applied Physiology*, 21(3):1013–1020, 1966.

[34] Chand T John, Ajay Seth, Michael H Schwartz, and Scott L Delp. Contributions of muscles to mediolateral ground reaction force over a range of walking speeds. *Journal of biomechanics*, 45(14):2438–2443, 2012.

[35] Smith L Johnston, Mark R Campbell, Rick Scheuring, and Alan H Feiveson. Risk of herniated nucleus pulposus among us astronauts. *Aviation, space, and environmental medicine*, 81(6):566–574, 2010.

[36] TS Keller, AM Weisberger, JL Ray, SS Hasan, RG Shiavi, and DM Spengler. Relationship between vertical ground reaction force and speed during walking, slow jogging, and running. *Clinical Biomechanics*, 11(5):253–259, 1996.

[37] Eric L Kerstman, Richard A Scheuring, Matt G Barnes, Tyson B DeKorse, and Lynn G Saile. Space adaptation back pain: a retrospective study. *Aviation, space, and environmental medicine*, 83(1):2–7, 2012.

[38] JH Keyak, AK Koyama, A LeBlanc, Y Lu, and TF Lang. Reduction in proximal femoral strength due to long-duration spaceflight. *Bone*, 44(3):449–453, 2009.

[39] Si-Hyun Kim, Oh-Yun Kwon, Kyue-Nam Park, In-Cheol Jeon, and Jong-Hyuck Weon. Lower extremity strength and the range of motion in relation to squat depth. *Journal of human kinetics*, 45(1):59–69, 2015.

[40] Shinji Kimura, Gregory C Steinbach, Donald E Watenpaugh, and Alan R Hargens. Lumbar spine disc height and curvature responses to an axial load generated by a compression device compatible with magnetic resonance imaging. *Spine*, 26(23):2596–2600, 2001.

[41] Inessa B Kozlovskaya and Anatoly I Grigoriev. Russian system of countermeasures on board of the international space station (iss): the first results. *Acta Astronautica*, 55(3):233–237, 2004.

[42] David E Krebs, Claire E Robbins, Leroy Lavine, and Robert W Mann. Hip biomechanics during gait. *Journal of Orthopaedic & Sports Physical Therapy*, 28(1):51–59, 1998.

[43] Jeremy M LaMothe and Ronald F Zernicke. Rest insertion combined with high-frequency loading enhances osteogenesis. *Journal of Applied Physiology*, 96(5):1788–1793, 2004.

[44] Thomas Lang, Adrian LeBlanc, Harlan Evans, Ying Lu, Harry Genant, and Alice Yu. Cortical and trabecular bone mineral loss from the spine and hip in long-duration spaceflight. *Journal of bone and mineral research*, 19(6):1006–1012, 2004.

[45] Thomas F Lang, Adrian D Leblanc, Harlan J Evans, and Ying Lu. Adaptation of the proximal femur to skeletal reloading after long-duration spaceflight. *Journal of Bone and Mineral Research*, 21(8):1224–1230, 2006.

[46] Lance E Lanyon and CT Rubin. Static vs dynamic loads as an influence on bone remodelling. *Journal of biomechanics*, 17(12):897–905, 1984.

[47] A LeBlanc, V Schneider, E Spector, H Evans, R Rowe, H Lane, L Demers, and A Lipton. Calcium absorption, endogenous excretion, and endocrine changes during and after long-term bed rest. *Bone*, 16(4):S301–S304, 1995.

[48] Adrian LeBlanc, Toshio Matsumoto, Jeffrey A Jones, Jay Shapiro, Thomas F Lang, Scott M Smith, Linda C Shackelford, Jean Sibonga, Harlan Evans, Elisabeth Spector, et al. Bisphosphonates as a countermeasure to space flight induced bone loss. 2009.

[49] Adrian D LeBlanc, Theda B Driscol, Linda C Shackelford, Harlan J Evans, Nahid J Rianon, Scott M Smith, and Dejian Lai. Alendronate as an effective countermeasure to disuse induced bone loss. 2002.

[50] Adrian D LeBlanc, Harlan J Evans, Victor S Schneider, Richard E Wendt III, and Thomas D Hedrick. Changes in intervertebral disc cross-sectional area with bed rest and space flight. *Spine*, 19(7):812–817, 1994.

[51] Adrian D LeBlanc, Elisabeth R Spector, Harlan J Evans, and Jean D Sibonga. Skeletal responses to space flight and the bed rest analog: a review. *Journal of Musculoskeletal and Neuronal Interactions*, 7(1):33, 2007.

[52] Thomas H Mader, C Robert Gibson, Anastas F Pass, Larry A Kramer, Andrew G Lee, Jennifer Fogarty, William J Tarver, Joseph P Dervay, Douglas R Hamilton, Ashot Sargsyan, et al. Optic disc edema, globe flattening, choroidal folds, and hyperopic shifts observed in astronauts after long-duration space flight. *Ophthalmology*, 118(10):2058–2069, 2011.

[53] *NASA-STD-3000: Man-Systems Integration Standards.*

[54] Frances E Mount, Mihriban Whitmore, and Sheryl L Stealey. Evaluation of neutral body posture on shuttle mission sts-57 (spacehab-1). *NASA technical memorandum*, pages 2003–104805, 2003.

[55] Dava J Newman, Amir R Amir, and Sherwin M Beck. Astronaut-induced disturbances to the microgravity environment of the mir space station. *Journal of spacecraft and rockets*, 38(4):578–583, 2001.

[56] Bo E Nilsson and Nils E Westlin. Bone density in athletes. *Clinical orthopaedics and related research*, 77:179–182, 1971.

[57] TF Novacheck. Running injuries: a biomechanical approach. *Instructional course lectures*, 47:397–406, 1998.

[58] Tom F Novacheck. The biomechanics of running. *Gait & posture*, 7(1):77–95, 1998.

[59] Y Ohira, T Yoshinaga, M Ohara, I Nonaka, T Yoshioka, K Yamashita-Goto, BS Shenkman, IB Kozlovskaya, RR Roy, and VR Edgerton. Myonuclear domain

and myosin phenotype in human soleus after bed rest with or without loading. *Journal of Applied Physiology*, 87(5):1776–1785, 1999.

[60] Stanley Plagenhoef, F Gaynor Evans, and Thomas Abdelnour. Anatomical data for analyzing human motion. *Research quarterly for exercise and sport*, 54(2):169–178, 1983.

[61] Jojo V Sayson, Jeffrey Lotz, Scott Parazynski, and Alan R Hargens. Back pain in space and post-flight spine injury: Mechanisms and countermeasure development. *Acta Astronautica*, 86:24–38, 2013.

[62] RA Scheuring, CH Mathers, JA Jones, ML Wear, and B Djojonegoro. In-flight musculoskeletal injuries and minor trauma in the us space program: a comprehensive summary of occurrence and injury mechanism. *AVIATION SPACE AND ENVIRONMENTAL MEDICINE*, 79(3):422, 2008.

[63] Lex Schultheis. The mechanical control system of bone in weightless spaceflight and in aging. *Experimental gerontology*, 26(2):203–214, 1991.

[64] KA Semenova. Basis for a method of dynamic proprioceptive correction in the restorative treatment of patients with residual-stage infantile cerebral palsy. *Neuroscience and behavioral physiology*, 27(6):639–643, 1997.

[65] LC Shackelford, AD LeBlanc, TB Driscoll, HJ Evans, NJ Rianon, SM Smith, E Spector, DL Feeback, and D Lai. Resistance exercise as a countermeasure to disuse-induced bone loss. *Journal of Applied Physiology*, 97(1):119–129, 2004.

[66] Amy Silder, Thor Besier, and Scott L Delp. Predicting the metabolic cost of incline walking from muscle activity and walking mechanics. *Journal of biomechanics*, 45(10):1842–1849, 2012.

[67] Scott M Smith, Martina A Heer, Linda C Shackelford, Jean D Sibonga, Lori Ploutz-Snyder, and Sara R Zwart. Benefits for bone from resistance exercise and nutrition in long-duration spaceflight: evidence from biochemistry and densitometry. *Journal of Bone and Mineral Research*, 27(9):1896–1906, 2012.

[68] Scott M Smith, Jeannie L Nillen, Adrian LeBlanc, Allan Lipton, Laurence M Demers, Helen W Lane, and Carolyn S Leach. Collagen cross-link excretion during space flight and bed rest 1. *The Journal of Clinical Endocrinology & Metabolism*, 83(10):3584–3591, 1998.

[69] Scott M Smith, Meryl E Wastney, Kimberly O O'Brien, Boris V Morukov, Irina M Larina, Steven A Abrams, Janis E Davis-Street, Victor Oganov, and Linda C Shackelford. Bone markers, calcium metabolism, and calcium kinetics during extended-duration space flight on the mir space station. *Journal of Bone and Mineral Research*, 20(2):208–218, 2005.

[70] Ellen M Strickland, Magda Fares, David E Krebs, Patrick O Riley, Deborah L Givens-Heiss, W Andrew Hodge, and Robert W Mann. In vivo acetabular contact pressures during rehabilitation, part i: acute phase. *Physical Therapy*, 72(10):691–699, 1992.

[71] Dennis R Taaffe, Tracey L Robinson, Christine M Snow, and Robert Marcus. High-impact exercise promotes bone gain in well-trained female athletes. *Journal of bone and mineral research*, 12(2):255–260, 1997.

[72] Ben H Thacker. Asme standards committee on verification and validation in computational solid mechanics. *Report, The American Society of Mechanical Engineers (ASME) Council on Codes and Standards (Sep 2001)*, 2001.

[73] William K Thompson, Christopher A Gallo, Lawton Crentsil, Beth E Lewandowski, Brad T Humphreys, John K DeWitt, Renita S Fincke, and Lealem Mulugeta. Digital astronaut project biomechanical models: Biomechanical modeling of squat, single-leg squat and heel raise exercises on the hybrid ultimate lifting kit (hulk). 2015.

[74] AR Tyrrell, T Reilly, and JDG Troup. Circadian variation in stature and the effects of spinal loading. *Spine*, 10(2):161–164, 1985.

[75] ANTON J van den Bogert, Lynda Read, and Benno M Nigg. An analysis of hip joint loading during walking, running, and skiing. *Medicine and science in sports and exercise*, 31(1):131–142, 1999.

[76] J Vernikos, DA Ludwig, AC Ertl, CE Wade, L Keil, and D O'Hara. Effect of standing or walking on physiological changes induced by head down bed rest: implications for spaceflight. *Aviation, space, and environmental medicine*, 67(11):1069–1079, 1996.

[77] Geraldo Magela Vieira, Hildeamo Bonifácio Oliveira, Daniel Tavares de Andrade, Martim Bottaro, and Robert Ritch. Intraocular pressure variation during weight lifting. *Archives of ophthalmology*, 124(9):1251–1254, 2006.

[78] James M Waldie and Dava J Newman. A gravity loading countermeasure skinsuit. *Acta Astronautica*, 68(7):722–730, 2011.

[79] PC Wing, IK Tsang, L Susak, F Gagnon, R Gagnon, and JE Potts. Back pain and spinal changes in microgravity. *The Orthopedic Clinics of North America*, 22(2):255–262, 1991.

[80] Peter Wing, Ian Tsang, Faith Gagnon, Lark Susak, and Roy Gagnon. Diurnal changes in the profile shape and range of motion of the back. *Spine*, 17(7):761–766, 1992.

[81] Julius Wolff. Das gesetz der transformation der knochen. *DMW-Deutsche Medi-*

zinische Wochenschrift, 19(47):1222–1224, 1893.

[82] Katsumasa Yamashita-Goto, Ryoko Okuyama, Masanori Honda, Kensuke Kawasaki, Kazuhiko Fujita, Takahiro Yamada, Ikuya Nonaka, Yoshinobu Ohira, and Toshitada Yoshioka. Maximal and submaximal forces of slow fibers in human soleus after bed rest. *Journal of Applied Physiology*, 91(1):417–424, 2001.

[83] KS Young and S Rajulu. The effects of microgravity on seated height (spinal elongation). 2011.